NOVEL METHODS FOR MANIPULATING AND COMBINING LIGHT FIELDS

A DISSERTATION
SUBMITTED TO THE DEPARTMENT OF COMPUTER SCIENCE
AND THE COMMITTEE ON GRADUATE STUDIES
OF STANFORD UNIVERSITY
IN PARTIAL FULFILLMENT OF THE REQUIREMENTS
FOR THE DEGREE OF
DOCTOR OF PHILOSOPHY

Billy Chen

September 2006

Abstract

Image-based modeling is a family of techniques that uses images, rather than 3D geometric models, to represent a scene. A light field is a common image-based model used for rendering the appearance of objects with a high-degree of realism. Light fields are used in a variety of applications. For example, they are used to capture the appearance of real-world objects with complex geometry, like human bodies, furry teddy bears, or bonsai trees. They are also used to represent intricate distributions of light, like the illumination from a flash light. However, despite the increasing popularity of using light fields, sufficient tools do not exist for editing and manipulating them. A second limitation is that those tools that have been developed have not been integrated into toolkits, making it difficult to combine light fields.

This dissertation presents two contributions towards light field manipulation. The first is an interactive tool for deformation of a light field. Animators could use this tool to deform the shape of captured objects. The second contribution is a system, called *LightShop*, for manipulating and combining light fields. Operations such as deforming, compositing, and focusing within light fields can be combined together in a single system. Such operations are specified independent of how that light field is captured or parameterized, allowing a user to simultaneously manipulate and combine multiple light fields of varying parameterizations. This dissertation first demonstrates light field deformation for animating captured objects. Then, LightShop is demonstrated in three applications: 1) animating captured objects in a composite scene containing multiple light fields, 2) focusing on multiple depths in an image, for emphasizing different layers in sports photography and 3) integrating captured objects into interactive games.

Acknowledgments

My success in graduate school would not have been possible if not for the support and guidance of many people. First I would like to thank my advisor, Marc Levoy, for his enduring patience and advice throughout my graduate career. There have been multiple times when Marc went above and beyond the call of duty to edit paper drafts, finalize submissions, and review talks. His guidance played a critical role in my success. I would also like to thank Hendrik Lensch for his practical advice and support. Hendrik has an excellent intuition for building acquisition systems; his advice on such matters was invaluable. In the course of conducting research together, Hendrik became not only my mentor but also my good friend. I would also like to thank the other members of my committee, Pat Hanrahan, Leo Guibas, and Bernd Girod for their discussions on this dissertation. Their insights greatly improved this thesis.

I would also like to thank my friends and family for their recreational and emotional support. In particular, my colleagues in room 360 have become my life-long friends: Vaibhav Vaish, Gaurav Garg, Doantam Phan, and Leslie Ikemoto. When I look back at our graduate years, I will remember our experiences the most. I am also honored to have the opportunity to share my Ph.D. adventure with other friends in the department. Most notably, those notorious *gslackers*, with which I have had many mind-altering conversations and experiences, greatly enhanced my time at Stanford. I am also deeply indebted to my family for believing in me and for giving me the inspiration to apply and complete a doctoral degree.

Last but not least, I would like to thank my girl friend, Elizabeth, who was my pillar of support throughout my graduate career. During times of stress, she listened.

After paper deadlines, she celebrated. When research hit a dead-end, she inspired. When research felt like it was spiraling out of control, she brought serenity. It should be no surprise that this dissertation would be impossible without her. I dedicate this thesis to her.

Contents

List of Tables

List of Figures

Chapter 1

Introduction

A long-term goal in computer graphics has been rendering photo-realistic imagery. One approach for increasing realism is image-based modeling, which uses images to represent appearance. In recent years, the light field [LH96], a particular image-based model, has been used to increase realism in a variety of applications. For example, light fields capture the appearance of real-world objects with complex geometry, like furry teddy bears [COSL05], or bonsai trees [MPN$^+$02]. Incident light fields capture the local illumination impinging on an object, whether it is a flash light with intricate light patterns [GGH03], or general 4D illumination [MPDW03, SCG$^+$05, CL05]. In the film industry, light fields have found their use in creating "bullet-time" effects in production films like *The Matrix* or national sports broadcasts like the Superbowl of 2001. Light fields are useful in representing objects that are challenging for traditional model-based graphics[1].

However, light fields have their limitations, compared to traditional modeling. Light fields are typically represented using images, so it is not obvious how to manipulate them as we do with traditional models. This difficulty explains why only a handful of editing tools exist for light fields. However, if one could deform, composite or segment light fields, this would enable a user to interact with the object, rather than just to view it from different viewpoints.

[1] "traditional model" refers to the use of models to represent the geometry, lighting and surface appearance in a scene.

Another challenge is that the existing tools found in the literature, like view-interpolation [LH96], focusing [VWJL04], or morphing [ZWGS02], were not designed for general light field editing. Consequently, the ability to combine tools, similar to how images are edited in Adobe Photoshop, is simply not offered by these research systems..

To address the two problems of interacting with a light field and combining such interactions, this dissertation presents two contributions toward manipulating and combining light fields:

1. a novel way to manipulate a light field by approximating the appearance of object deformation
2. a system that enables a user to apply and combine operations on light fields, regardless of how each dataset is parameterized or captured

In the first contribution, a technique is presented that enables an animator to deform an object represented by a light field. Object deformation is a common operation for traditional, mesh-based objects. Deformation is performed by moving the vertices of the underlying mesh. The goal is to apply this operation to light fields. However, light fields do not have an explicit geometry, so it is not immediately clear how to simulate a deformation of the represented object. Furthermore, we require the deformation to be intuitive so that it is accessible by animators.

The key insight that enables light field deformation is the use of *free-form deformation* [SP86] to specify a transformation on the rays in a light field. Free-form deformation is a common animation tool for specifying a deformation for mesh-based objects. We modify this deformation technique to induce a transformation on rays. The ray transformation approximates a deformation of the underlying geometry represented by the light field. This operation enables a user to deform real, captured objects for use in animation or interactive games.

In the second contribution, we introduce a system that incorporates deformation, along with a host of other tools, into a unified framework for light field manipulation. We call this system *LightShop*. Previous work for manipulating light fields are systems designed for a single task, like view interpolation. A system that incorporates multiple operations faces additional challenges. First, operations can manipulate light fields in a variety of ways, so the system must expose different functionality for each operation. Some examples include summing over multiple pixels in each image (like focusing), or shifting pixels across images (like deformation). Second, light fields may be captured and parameterized differently, so the system must abstract the light field representation from the user. These challenges indicate that careful thought must be given to how to specify operations.

There are two key insights that drive the design of LightShop. The first insight is to leverage the conceptual model of existing 3D modeling packages for manipulating traditional 3D objects. In systems like RenderMan [Ups92] or OpenGL [BSW$^+$05], a user first defines a scene made up of polygons, lights, and cameras. Then, the user manipulates the scene by transforming vertices, and adjusting light and camera properties. Finally, the user renders a 2D image using the defined cameras and the scene. We call this conceptual model, *model, manipulate, render.* LightShop is designed in the same way, except that the scene contains only light fields and cameras. LightShop exports functions in an API to model (e.g. define) a scene. The light fields are then manipulated and an image is rendered from the scene. The problem of manipulating and rendering a light field is solved using the second key insight.

The second key insight is to specify light field operations as operations on rays. Ray operations can be defined independent of the light field parameterization. Furthermore, we define these operations using a *ray-shading language* that enables a programmer to freely combine operations. In a ray-shading program, by composing multiple function calls, a user can combine multiple operations on light fields. To render an image from this manipulated scene, we map the ray-shading program to a pixel shading language that runs on the graphics hardware. The same ray-shading program is executed for every pixel location of the image. When the program has finished execution for all pixels, the final image is returned. Rendering an image using the programmable graphics hardware allows LightShop to produce images at interactive rates and makes it more amenable for integration into video games.

A system like LightShop can be used in a variety of applications. In this dissertation, three applications are prototyped: 1) a light field compositing program that allows a user to rapidly compose and deform a scene, 2) a novel post-focusing program that allows for simultaneously focusing at multiple depths, and 3) an integration of a captured light field into a popular OpenGL space-flight simulator.

The dissertation is organized in the following way. Chapter 2 describes background material related to light fields. This chapter also motivates the need to manipulate light fields by describing the increasing number of acquisition systems and their decreasing cost and complexity in acquiring a dataset. Chapter 3 describes the first contribution of this thesis: a novel way to manipulate light fields through deformation. Chapter 4 describes the second contribution: LightShop, a system for manipulating and combining light fields. In this chapter, results are shown for applications in digital photography, and interactive games. Many of these results are time-varying, so the reader is invited to peruse the webpage, `http://graphics.stanford.edu/papers/bchen_thesis`. Chapter 5 concludes with a summary of the contributions and future improvements.

Chapter 2

Background

In this chapter, image-based models are reviewed. In particular, the physics-based notion of a light field is discussed, and its approximation, by a set of images, is reviewed. Next, the need to manipulate and combine light fields is motivated by a discussion of the progression of light field acquisition systems. In this discussion, it is shown that these systems are becoming easier to use, cheaper to build, and more commonplace. These factors lead to the result that light fields are becoming akin to images and traditional 3D models. Consequently, there is an increasing need to manipulate and interact with such datasets, beyond just rendering from novel viewpoints.

2.1 Image-based Models and Light Fields

An image-based model (IBM) uses images to represent an object's appearance, without explicitly modeling geometry, surface properties or illumination. The key idea is that an object's appearance is fully captured by the continuous distribution of radiance eminating from that object. This distribution of radiance is called the *plenoptic function* [AB91]. In practice, one can not fully capture an object's continuous plenoptic function and must therefore capture restrictions of it. The *light field* [LH96, GGSC96] is one such restriction that allows for convenient acquisition of real-world objects and efficient rendering. In the following, the notion of the plenoptic function is briefly reviewed, followed by a discussion of the light field.

2.1.1 The Plenoptic Function

The plenoptic function [AB91, MB95a] is a seven dimensional function that describes the radiance along a ray at time t, wavelength λ:

$$P = P(x, y, z, \theta, \phi, \lambda, t) \tag{2.1}$$

x, y, z, θ, ϕ describe the ray incident to the point (x, y, z) with direction (θ, ϕ) in spherical coordinates. The interesting point about Equation 2.1 is that it fully describes the appearance of an object under fixed lighting. An object's appearance depends on the incident illumination, surface properties, and geometry [Kaj86]. The plenoptic function captures this appearance parameterized as radiance along each point and direction pair in the scene. When an image needs to be rendered from the plenoptic function, the radiance along a ray is computed by evaluating the plenoptic function.

In practice, measuring an object's entire continuous plenoptic function is impossible, so it is approximated by discretization and restricted by dimension reduction. The 4D light field is one such approximation/restriction.

2.1.2 The Light Field

First, assume that the plenoptic function is static and does not vary over time. Next, based on the tristimulus theory of color perception [FvDFH97], the locus of spectral colors is approximated by a basis of three primaries: red, green and blue. This converts Equation 2.1 to the following vector-valued equation:

$$P_{rgb} = P_{rgb}(x, y, z, \theta, \phi) \tag{2.2}$$

where P_{rgb} is a 3-vector corresponding to the weights for each red, green, and blue primary.

One more reduction can be performed, which assumes that the radiance along a ray is constant. This assumption is true when the plenoptic function is defined in free space. The redundancy in Equation 2.2 is removed by parameterizing the light field in terms of rays instead of a (x, y, z) point and (θ, ϕ) direction [LH96, Mag05]. Hence, a light field is a four dimensional function mapping rays in free space to radiance:

$$L = L(u, v, s, t) \tag{2.3}$$

The input, a ray in free space, takes 4 coordinates u, v, s, t to represent [LH96]. The output, radiance, is approximated by a three-component RGB vector. The input coordinates can represent spatial positions or directions depending on the parameterization. For example, in the two-plane parameterization [LH96], u, v and s, t are the ray-intersections with the $UV-$ and ST-planes. The next section describes the two light field parameterizations used in this thesis. However, the light field operations, as described in Chapter 4, are independent of the parameterization.

2.1.3 Parameterizations

Throughout this thesis, light fields use one of two parameterizations, two-plane and sphere-plane. A third, the circular parameterization, is a special case of the latter for 3D light fields. These parameterizations are not defined on any surface in the scene. This property allows the representation of objects with complex geometry, like hair, or fur (since the parameterization need not lie on the hair or fur geometry). However, the disadvantage is that more samples need to be captured in order to avoid ghosting when rendering [CTCS00]. For light field parameterizations that make use of surface geometry, the reader is referred to surface light fields [WAA+00], and view-dependent texture maps [DTM96].

Two-plane

$$L = L(u, v, s, t) \tag{2.4}$$

In a two-plane parameterization, two planes, a UV- and ST-plane, are defined. A ray is described by four coordinates, (u, v, s, t) which describe the two intersections with the UV- and ST-plane. This is a natural parameterization for datasets acquired from an array of cameras. The UV-plane is defined as the plane on which the cameras lie. The ST-plane is the plane on which all camera images are rectified. Images are rectified by capturing a light field of a planar calibration target and computing homographies to a user-selected camera image [VWJL04].

Sphere-plane

$$L = L(\phi, \theta, s, t) \tag{2.5}$$

The sphere-plane light field parameterization (SLF) uses a different set of four coordinates. A sphere with radius R surrounds the object represented by the light field. A ray is parameterized by two intersections, (ϕ, θ) and (s, t). The first is the closest intersection with the sphere. This is parameterized using spherical coordinates; ϕ is the angle from the vertical axis of the sphere and θ is the rotation angle around the vertical axis. The second intersection, parameterized by $(s,\ t)$, is on a plane that is incident to the center of the sphere, with normal N. Figure 2.1 illustrates this parameterization.

A special case of the SLF for 3D light fields is the *circular parameterization*, which fixes ϕ to 90°. The fish, teddy bear and toy warrior light fields listed in Table A.1 use this parameterization.

2.1.4 A Discrete Approximation to the Continuous Light Field

Given the two parameterizations described above, acquisition systems discretely sample the continuous light field with ray samples. In practice, these discrete samples are acquired from captured photographs. Assuming that cameras are pinhole devices, each photograph measures the radiance along a bundle of rays converging to the center of projection of the camera. If multiple photographs are captured from different viewpoints, these images approximate the continuous light field.

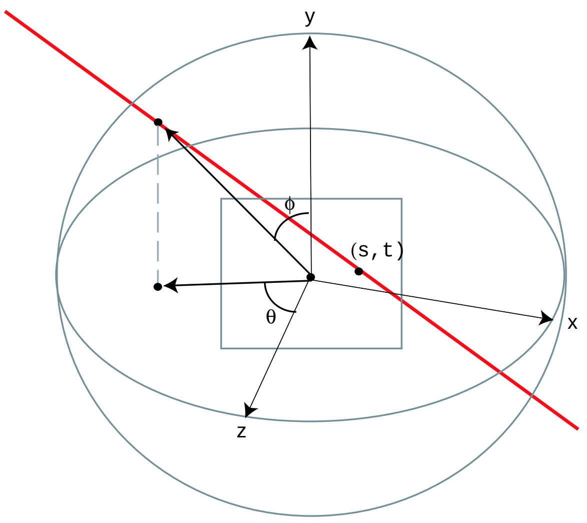

Figure 2.1: Ray parameterization for a sphere-plane light field. (ϕ, θ, s, t) are the four coordinates defining a ray. The ray is shown in red.

Using discrete ray samples requires calculating a sampling pattern and the number of samples to acquire. Assuming no knowledge about the geometry of the underlying object, a good sampling strategy for the two-plane and sphere-plane parameterizations is to pick uniformly-spaced samples [LH96, CLF98]. For the two-plane parameterization, this means picking samples on a grid in the UV- and ST-planes. For the sphere-plane parameterization, this means picking ϕ and θ so that the samples are equally spaced on the surface of the sphere. Ideally, s and t on the plane are chosen so that their projection to the rear-surface of the sphere form equally spaced samples[1].

2.1.5 Rendering an Image from a Light Field

Once a discrete approximation of a light field has been captured, a common task is to render a virtual view of the light field. Naturally, if the virtual view coincides with a captured viewpoint, then the relevant image can be returned. More interestingly, if the virtual view is a novel view, an image can be rendered by sampling nearest rays from the captured light field. Rendering a novel view from a light field is discussed in

[1]In practice, the sampling distribution on this ST-plane is determined by the pixel grid pattern on the camera sensor, which creates a non-uniform pattern when projected onto the rear surface of the sphere. However, in our datasets the samples are dense enough that few artifacts are visible.

more detail in [LH96, GGSC96, BBM+01]. This process of rendering an image from a light field has numerous names, including "light field sampling," "rendering from a light field," "novel view synthesis," and "extracting a 2D slice".

2.2 Acquisition Systems

Historically, a major hurdle in the use of light fields is acquiring dense samples to approximate the continuous function shown in Equation 2.3. Fortunately, recent advances in camera technology combined with novel uses of optics have made acquisition not only a practical task, but also a cheap and potentially common one as well. As light fields become more common, users will want to interact with them as they do with images and traditional 3D models.

Early acquisition systems made use of mechanical gantries to acquire light fields. A camera is attached to the end of the gantry arm and the arm is moved to multiple positions. Two useful gantry configurations are the planar and spherical ones. In a planar configuration, the end effector of the gantry arm moves within a plane, enabling acquisition of two-plane parameterized light fields. One example is the gantry [Lev04a] used to acquire 3D scans of Michelangelo's David [LPC+00] and a light field of the statue of Night. This gantry is used to acquire several two-plane light fields listed in Table A.1. In a spherical configuration, the end-effector travels on the surface of a sphere, enabling acquisition of circular and spherical light fields. The Stanford Spherical Gantry [Lev04b] is one example. This gantry is also used to acquire the sphere-plane and circular light fields in Table A.1. While these gantries can capture a dense sampling of a light field, they assume a static scene, are bulky, and are costly. The Stanford Spherical Gantry costs $130,000.

To capture dynamic scenes, researchers have built arrays of cameras. The ability to acquire dynamic scenes enables the acquisition of complex objects like human actors. Manex Entertainment first popularized this technique in the movie, *The Matrix*. During one scene, the actress appears to freeze while the camera moves around her. This effect, now coined the "Matrix effect" or "bullet-time," was created by simultaneously triggering an array of cameras, and rendering images from the captured photographs.

Other camera arrays include the video camera array in the Virtualized Reality Project at CMU [RNK97] , the 8x8 webcam array at MIT [YEBM02], the 48 pan-translation camera array [ZC04], and the Stanford Multi-camera Array [WJV+05, WSLH02]. This thesis uses several datasets captured using the Stanford Multi-camera Array. With the exception of the webcam array, each system is costly and makes use of specialized hardware. Furthermore, arrays like the Stanford Multi-camera Array generally span a large area (3 x 2 meters), which makes it challenging to move. These acquisition devices are useful in a laboratory setting, but have limited use in everyday settings.

To build mobile and cheap acquisition devices, researchers have exploited optics to trade off the spatial resolution of a single camera for multiple viewpoints of a scene. One of the first techniques is integral photography, in which a fly's-eye lens sheet is placed in front of a sensor array, thereby allowing the array to capture the scene from many viewpoints [Oko76]. The total image is composed of tiny images, each with a different viewpoint. Today, such images are created by embedding lenses within a camera body [NLB+05] or a lens encasement [GZN+06]. This thesis contains light fields captured from the hand-held light field camera built by Ng et al. In [GZN+06], they construct a lens encasement containing 20 lenses. Each lens provides a different viewpoint of the scene. The lens encasement is attachable to any conventional SLR camera. A light field is captured simply by pressing the shutter button. Acquisition devices such as this are mobile, cheap, and easy to use. As such devices become common, light fields will become abundant and users will want to manipulate this data type as they do with images and 3D objects. The first contribution of this thesis is a novel way to manipulate these light fields, described in Chapter 3.

Chapter 3

Light Field Deformation

The first contribution of this thesis is a novel way to manipulate light fields, by approximating object deformation. An animator can then “breathe life” into objects represented by light fields. Our goal is similar to cartoon animation; the final result is a deformed object, but the object need not be physically plausible, volume-preserving, or “water-tight”. Figure 3.1 illustrates a deformation that twists a light field of a toy Terra Cotta Warrior.

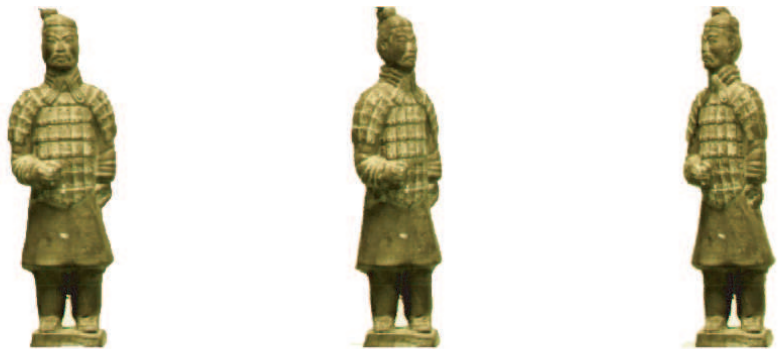

Figure 3.1: Light field deformation enables an animator to interactively deform photo-realistic objects. The left figure is an image from a light field of a toy Terra Cotta Warrior. The middle image shows a view of the light field after applying a deformation, in this case, a twist to the left. Notice that his feet remain fixed and his right ear now becomes visible. The right image shows the warrior turning to his right. Animating the light field in this way makes it appear alive and dynamic, properties not commonly associated with light fields.

In order to deform a light field there are two core problems that need to be solved. The first is specifying a transformation on the rays of the light field so that it approximates a change in shape. The second is ensuring that the illumination conditions after deformation remain consistent.

For the first problem, recall from Chapter 2 that a light field is a 4D function mapping rays to RGB colors. In practice, this 4D function is approximated by a set of images. In other words, a light field can be thought of as a set of rays, or a set of pixels. An object represented by a light field is composed of these rays. The goal is to specify a transformation that maps rays in the original light field to rays in a deformed light field. Many ray-transformations exist, but we seek a mapping that approximates a change in the shape of the represented object. For example, a simple ray-transformation can be constructed by exploiting the linear mapping of 3D points. If we represent this mapping as a 4x4 matrix and represent 3D points in homogeneous coordinates, then to deform the light field we simply take each ray, pick two points along that ray, apply the 4x4 matrix to both points, and form a new ray from the two transformed points. This ray-transformation simulates a homogeneous transformation on the object represented by the light field. In this chapter, we present a ray-transformation that can intuitively express Euclidean, similarity, and affine transformations. This transformation can also simulate the effect of twisting the 3D space in which an object is embedded, an effect that is difficult with a projective transformation.

The second problem to deformation is related to the property that the RGB color along any ray in a light field is a function of the illumination condition. When a ray is transformed, the illumination condition is transformed along with the ray. When multiple rays are transformed, this can produce an overall illumination that is different than the original. For example, consider a light field of a scene with a point light and a flat surface. Consider a ray r that is incident to a point on the surface. The incident illumination makes an angle with respect to r. If we transform r, the illumination angle remains fixed, relative to r. This causes the apparent illumination to differ from the original light direction. The goal is to provide a way to ensure that after deformation, the illumination remains consistent to the original lighting conditions. To solve this problem, a special kind of light field, called a *coaxial light field* is captured.

These two problems are not new. Previous approaches avoid the two problems of specifying a ray-transform and preserving illumination by attempting to reconstruct a 3D model based on the input images[1]. Hence, an accurate 3D model is necessary. The solution presented in this thesis avoids building an explicit model and provides a solution for maintaining a specific form of illumination during deformation.

3.1 Previous Work: 3D Reconstruction for Deformation

Previous approaches reconstruct geometry, surface properties and illumination using the images from the light field. Then the geometry is deformed by displacing mesh vertices. The deformed object can then be re-rendered. However, reconstructing a geometry from images is a difficult problem in computer vision. Nevertheless, several techniques exist, including multi-baseline stereo [KS96] and voxel coloring [SK98].

Assuming that a 3D model can be constructed, reflectance properties are then estimated. In [SK98], they assume the object is diffuse. Meneveaux and Fournier discuss a system that can make use of more complex reflectance properties [MSF02]. The reflectance properties can also be represented in a sampled form, as is shown by Weyrich et al., in which they capture and deform a surface reflectance field [WPG04]. Knowing the surface properties and geometry is sufficient to keep the apparent illumination consistent after object deformation. Once the mesh vertices have been deformed, the appearance of that part of the mesh can be rendered using the local surface normal, incident light direction and view direction.

This approach is successful as long as geometry, surface properties, and illumination can be accurately modeled. Unfortunately, this assumption fails for many interesting objects for which light fields are commonly used, like furry objects. The

[1]One approach, used in light field morphing [ZWGS02], avoids 3D reconstruction and instead induces a ray-transformation between two input light fields by specifying corresponding rays. However, they do not address the problem of inconsistent illumination.

approach presented in this thesis avoids explicit reconstruction and presents a technique for keeping illumination consistent and for specifying a ray-transformation.

3.2 Solving the Illumination Problem

In introducing our technique for light field deformation, we first address the problem of maintaining consistent illumination during a transformation of the rays of a light field. Then, we discuss how a transformation can be specified by an animator in an intuitive, interactive manner.

To understand the illumination problem that arises when transforming the rays of a light field, consider the scene shown in Figure 3.2. A point light is located at infinity, emitting parallel light rays onto a lambertian, checkerboard surface. A light field of this checkerboard is captured. Two rays of this light field are shown as black, vertical arrows. The corresponding light direction for these two rays is shown in yellow. Notice that since both rays of the light field are vertical and the illumination is distant, the angle between the illumination ray and the light field ray is ϕ. The key idea is that no matter how a ray is transformed, the color along that ray direction will be as if the illumination direction had made an angle ϕ to the ray.

Figure 3.3 shows the illumination directions for the two rays of the light field after transforming the upper-right ray. Notice that the illumination direction maintains an angle ϕ with the ray direction. However, the two illumination directions are no longer parallel. The illumination after transforming the rays is different than the original.

Because the color along a ray is a function of the relative angle between the illumination and the ray, after transforming this ray the illumination direction points in a different direction. In most cases, this means that when a light field is deformed (e.g. all its rays are transformed), the apparent illumination will also change. To solve this problem, we capture a new kind of light field, called a *coaxial light field*, which maintains lighting consistency during deformation but still captures interesting shading effects.

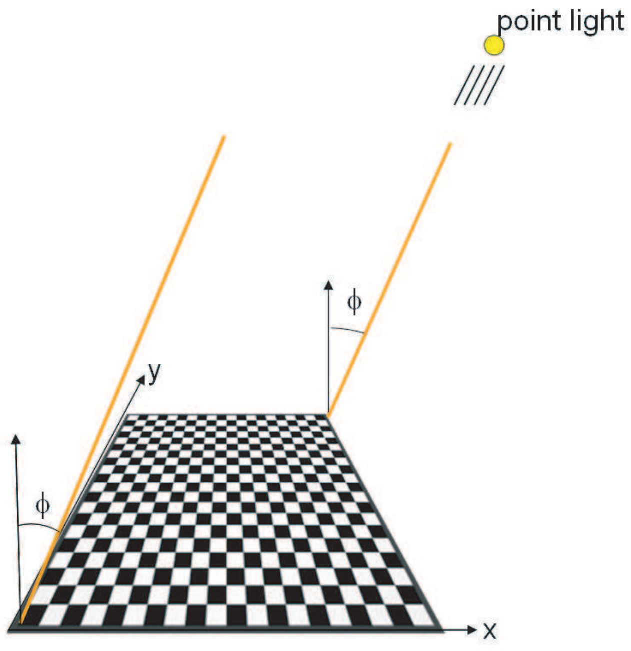

Figure 3.2: A lambertian scene with distant lighting. The checkerboard surface is lit by a point light located at infinity. Two rays of the light field are shown in black. They make an angle ϕ with respect to the illumination direction.

3.2.1 The Coaxial Light Field

Chapter 2 defines the 4D light field as radiance along rays as a function of position and direction in a scene under fixed lighting. Their definitions permit construction of new views of an object, but its illumination cannot be changed. By contrast, [DHT+00] defines the 4D reflectance field as radiance along a particular 2D set of rays, i.e. a fixed view of the world, as a function of (2D) direction to the light source. Their definition permits the relighting of an object, but the observer viewpoint cannot be changed. If one could capture an object under both changing viewpoint and changing illumination, one would have an 8D function (recently captured by [GLL+04]). The light fields of [LH96] and [DHT+00] are 4D slices of this function.

In this section, for the purposes of deformation, we introduce a different 4D slice, which we call the *coaxial light field*. With a coaxial light field, we capture different views of an object, but with the light source fixed to the camera as it moves. In

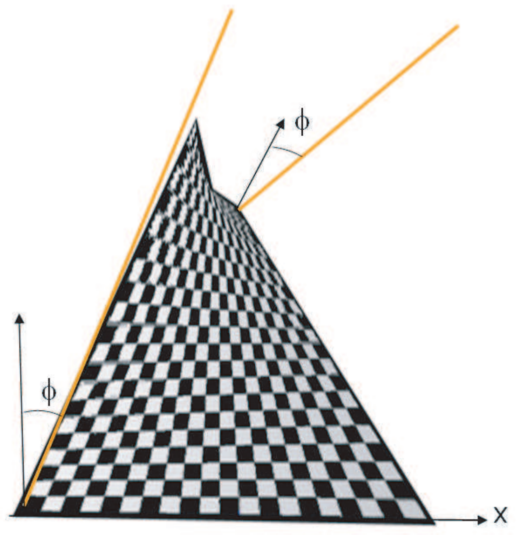

Figure 3.3: The rays representing the checkerboard are now transformed. Notice that the illumination angle ϕ remains fixed, relative to the ray directions. This causes the illumination to differ from the original conditions.

fact, the camera rays and illumination rays coincide. Since perfectly coaxial viewing and illumination is difficult to achieve in practice, we merely place our light source as close to our camera as we can. As an alternative, a ring light source could also be used. Figure 3.4 shows two images from a coaxial light field captured of a lambertian, checkerboard surface. This kind of illumination is analogous to examining an object with a flashlight attached to the observer's head. Given this definition of a coaxial light field, we now show how to use it to solve the illumination consistency problem.

3.2.2 Using Coaxial Light Fields to Solve Illumination Inconsistency

What we show is that after deforming a coaxial light field the illumination remains consistent to the original. That is, the lighting remains coincident to the center of the virtual view. One way to study lighting in a scene is to examine the goniometric

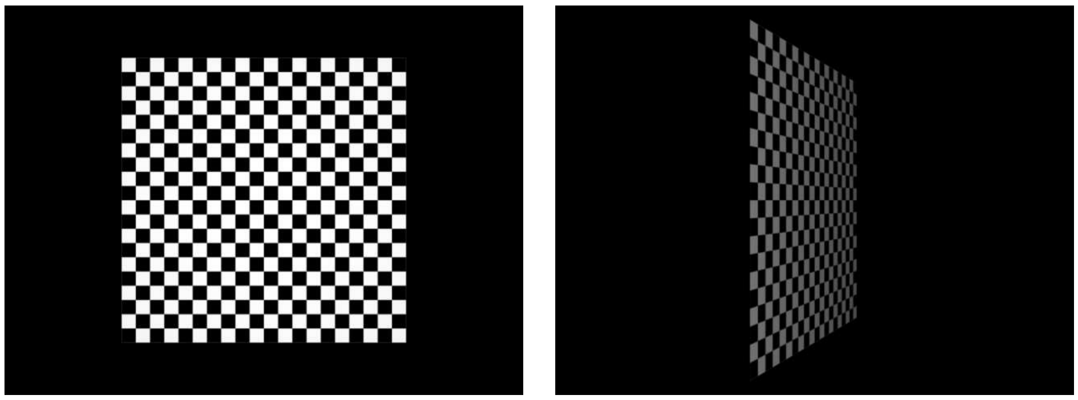

Figure 3.4: Two images from a coaxial light field. The lighting is a point light source placed at the center of projection of the camera. As the camera moves to an oblique position (right), the checkerboard is dimmed due to the irradiance falling off with the angle between the lighting direction and the surface normal.

diagram at a differential patch on a lambertian surface. A goniometric diagram plots the distribution of reflected radiance over the local bundle of rays incident to that patch[2]. In a goniometric diagram, the length of the plotted vectors is proportional to the reflected radiance quantity in that direction. Since the patch is on a lambertian surface, it reflects light equally in all directions (e.g. the diagram is not biased in any direction by the reflectance properties). Thus the shape and size of the diagram gives us insight into the illumination condition. For example, under fixed lighting a goniometric diagram of a patch on a lambertian surface has the shape of a semi-circle. This is because the lambertian surface reflects radiance equally in all directions. Furthermore, the radius of the semi-circle is a function of the angle between the surface normal and the illumination direction.

Now let us examine the goniometric diagram corresponding to coaxial lighting. Let us return to Figure 3.4 which shows a checkerboard captured by a coaxial light field. Consider two differential patches A_1 and A_2 on the checkerboard. Figure 3.5 shows the associated goniometric diagrams. Compared to fixed lighting, the diagrams indicate that reflected radiance is now a function of the reflection angle.

Described mathematically, because the surface is lambertian the radiance R can

[2]Some goniometric diagrams are drawn as a function of radiant intensity. However, we felt that plotting radiance provides a more intuitive notion of the reflected "light energy".

be described as a function of the light direction L and the surface normal N [CW93]:

$$R = \rho E = \rho I \frac{N \bullet L}{r^2} \tag{3.1}$$

where ρ is the BRDF for a diffuse surface, E is irradiance, I the radiant intensity of the point light and r the distance from the light to the patch.

Since the illumination is coaxial, any ray V from the patch has coaxial illumination, e.g. $V = L$. If we substitute this equality into Equation 3.1,

$$R = \rho I \frac{N \bullet V}{r^2} \tag{3.2}$$

we observe that the distribution of radiance from the patch is a function of the viewing direction V. This explains why there is a cosine-falloff shown in the goniometric diagrams.

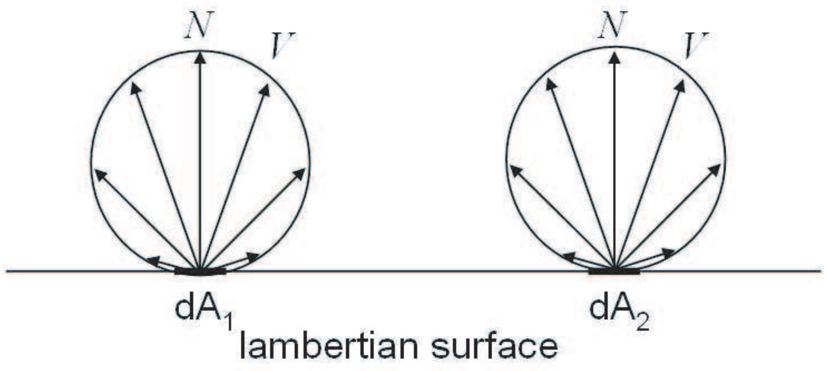

Figure 3.5: Goniometric diagrams of two differential patches, A_1 and A_2. The radiance in the local light field incident to each patch is plotted. The length of the ray is proportional to the radiance in that direction. Notice that the length of ray V has a cosine fall-off with respect to the angle between the ray direction and the surface normal, N

Now let us consider what happens when we deform the local light field about patch A_1 and render a novel view. Figure 3.6 illustrates a rigid-body transformation of the local light field about A_1. When rendering a novel view, we select one ray emanating from A_1 and one ray from A_2. In both rays, the radiance along those directions have coaxial illumination. Only one illumination condition satisfies this constraint: a point light source located at the virtual viewpoint. This illumination is consistent with the initial conditions before deforming the rays.

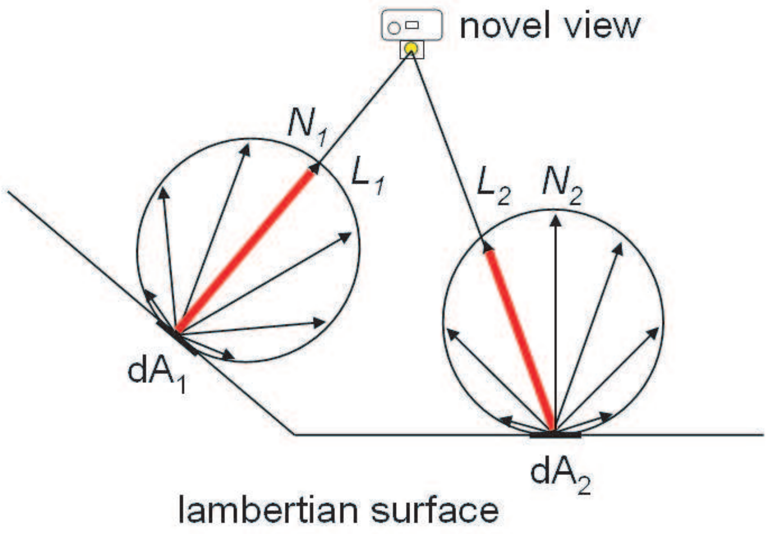

Figure 3.6: Goniometric diagrams of two differential patches, A_1 and A_2, after transforming the rays from A_1. When a novel view is rendered by sampling rays from the two diagrams, notice that the radiance along L_1 has coaxial illumination (shown in red). Similarly, the radiance along L_2 has coaxial illumination. The only plausible illumination condition for these constraints is a point light located at the virtual viewpoint.

For comparison, Figure 3.7 shows novel views after deforming a coaxial and fixed-illumination light field. Only the coaxial light field generates a correct rendering of the deformed checkerboard.

Thus, the advantage of using coaxial light fields is that it ensures the correct appearance of objects under deformation, even though no geometry has been captured. However, coaxial light fields have several limitations. First, the object must be diffuse; specular highlights will look reasonable when deformed, but they will not

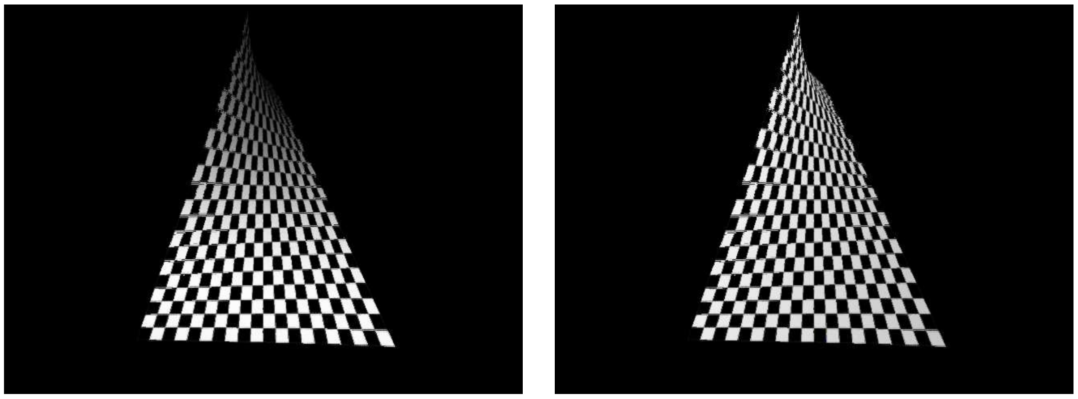

Figure 3.7: Comparing deformation of a coaxial and fixed lighting light field. The left image is a view from the deformed coaxial light field. Notice that the illumination remains consistent; it simulates a point light located at the virtual viewpoint. This is evident because the checkerboard dims at the top as its apparent surface normal deviates away from the lighting direction. The right image is a view from the fixed lighting light field. There is no appearance due to point light illumination; the radiance along each ray has a different illumination direction.

be correct. Second, perfectly coaxial lighting contains no shadows. This makes objects look somewhat flat. In practice, our light source is placed slightly to the side of our camera, thereby introducing some shadowing, at the expense of slightly less consistency in the rendering.

The coaxial light field is one of several solutions for maintaining illumination consistency. In fact, a solution depends on the both the complexity of the lighting and the complexity of the ray-transformation. The next section discusses this trade-off.

3.2.3 Trading-off Ray-transformation and Lighting Complexity

In general, no solution exists for keeping arbitrary illumination consistent under arbitrary ray-transformation. The reason is that under any lighting condition, a ray transformation could cause the illumination direction to differ from the original lighting conditions. The key to maintaining lighting consistency is that the transformed ray must have an associated lighting direction that is consistent with the original illumination[3]. Therefore, the simpler the ray-transform, the more complex the lighting can be, and vice-versa. A trivial example is the identity transform. Under this ray-mapping, the illumination can be arbitrarily complex. The equivalent trivial example for lighting is ambient lighting[4]. In this case the ray-transform can be arbitrary complex. Both these cases maintain lighting consistency. Something between trivial lighting and trivial ray-transformation is if the illumination is distant (and hence has parallel illumination directions). In this case any pure translation will preserve lighting.

Given this trade-off for preserving lighting during ray-transformation, we chose coaxial lighting because it has reasonable illumination properties and preserves coaxial illumination during transformation. The next section discusses the details of the actual ray-transformation.

3.3 Specifying a Ray Transformation

The second problem to light field deformation is specifying a ray transformation. Our goal is to enable an animator to artistically express motion and feeling using light fields.

There are many ways to specify a transformation on rays. For example, in the beginning of this chapter, a 4x4 matrix was used to specify a rigid-body transformation. However, specifying a matrix is not intuitive for an animator. Instead, we borrow a technique from the animation community for specifying transformations on traditional 3D models (e.g. with mesh geometry). We adapt it to transform light fields. The technique is called *free-form deformation* [SP86]. We first introduce the original technique, then adapt it to deform light fields.

[3]Here, we ignore global illumination effects like self-shadowing, and inter-reflection.

[4]In computer graphics, ambient lighting is a constant term added to all lighting calculations for an object. In reality, the ambient lighting is a composition of all indirect illumination. The trivial case being considered is if the object is only lit by ambient lighting, and hence has uniform lighting from all directions.

3.3.1 Free-form Deformation

In a traditional free-form deformation (FFD) [SP86], a deformation box C is defined around a mesh geometry. The animator deforms C to form C_w, a set of eight displaced points defining a deformed box[5]. The free-form deformation D is a 3D function mapping C, the original box, to C_w, the deformed one:

$$D : \Re^3 \to \Re^3 \tag{3.3}$$

More importantly, D is used to warp all points inside the box C.

How is D parameterized? In the original paper by Sederberg and Parry, D is represented by a trivariate tensor product Bernstein polynomial. The details of their formulation of D are unimportant for deforming light fields. The key idea is that we use their method for specifying a deformation. That is, an animator manipulates a deformation box to specify a warp. The difference is that while the original FFD warps 3D points, our formulation warps rays.

To make use of the FFD paradigm, we first define a function that makes use of the deformation box to warp 3D points. We will prove that this function does not preserve straight lines, so we modify it to warp ray parameters instead of 3D points. This modified form will be the final ray warp. Let us begin by introducing the 3D warping function, parameterized by trilinear interpolation.

3.3.2 Trilinear Interpolation

To introduce trilinear interpolation, assume that a deformation box (e.g. a rectangular parallelepiped) is defined with 8 vertices, c_i, $i = 1 \dots 8$. These 8 vertices also define three orthogonal basis vectors, U, V, and W. The origin of these basis vectors is X_0, one of the vertices of the box. Then for any 3D point p, Equation 3.4 defines coordinates, u, v, and w:

$$u = \tfrac{V\times W\cdot(X-X_0)}{V\times W\cdot U} \quad v = \tfrac{U\times W\cdot(X-X_0)}{U\times W\cdot V} \quad w = \tfrac{U\times V\cdot(X-X_0)}{U\times V\cdot W} \tag{3.4}$$

[5]One assumption is that the animator does not move points to form self-intersecting polytopes.

By trilinearly interpolating across the volume, p can be described in terms of the interpolation coordinates and the 8 vertices of the cube:

$$\begin{array}{llll} p = (1-u)(1-v)(1-w)c_1 & + & (u)(1-v)(1-w)c_2 & + \\ (1-u)(v)(1-w)c_3 & + & (u)(v)(1-w)c_4 & + \\ (1-u)(1-v)(w)c_5 & + & (u)(1-v)(w)c_6 & + \\ (1-u)(v)(w)c_7 & + & (u)(v)(w)c_8 & \end{array} \tag{3.5}$$

Given the trilinear coordinates u, v, w for a point p, the transformed point is computed using Equation 3.5 and the points in C_w substituted for c_i. Any 3D point can be warped using this technique.

Unfortunately, this technique does not preserve straight lines. To observe this property, without loss of generality let us examine the bilinear interpolation case and consider the deformation shown in Figure 3.8. Three collinear points a, b and c are transformed. We test for collinearity by forming a line between two points (in this case, a and c) and showing that the third point lies on the line:

$$ax + by + c = 0 \quad \text{(line in standard form)} \tag{3.6}$$

$$-x + y = 0 \quad \text{(line through a and c)} \tag{3.7}$$

$$1 - 1 = 0 \quad \text{(substituting b)} \tag{3.8}$$

We show that after transformation, a', b' and c' are no longer collinear. After bilinear interpolation,

$$a' = \begin{bmatrix} 0 \\ 0 \end{bmatrix} \quad b' = \begin{bmatrix} \frac{2}{3} \\ \frac{10}{9} \end{bmatrix} \quad c' = \begin{bmatrix} 3 \\ 4 \end{bmatrix} \tag{3.9}$$

The line formed from a' and c' is:

$$\frac{4}{3}x - y = 0 \tag{3.10}$$

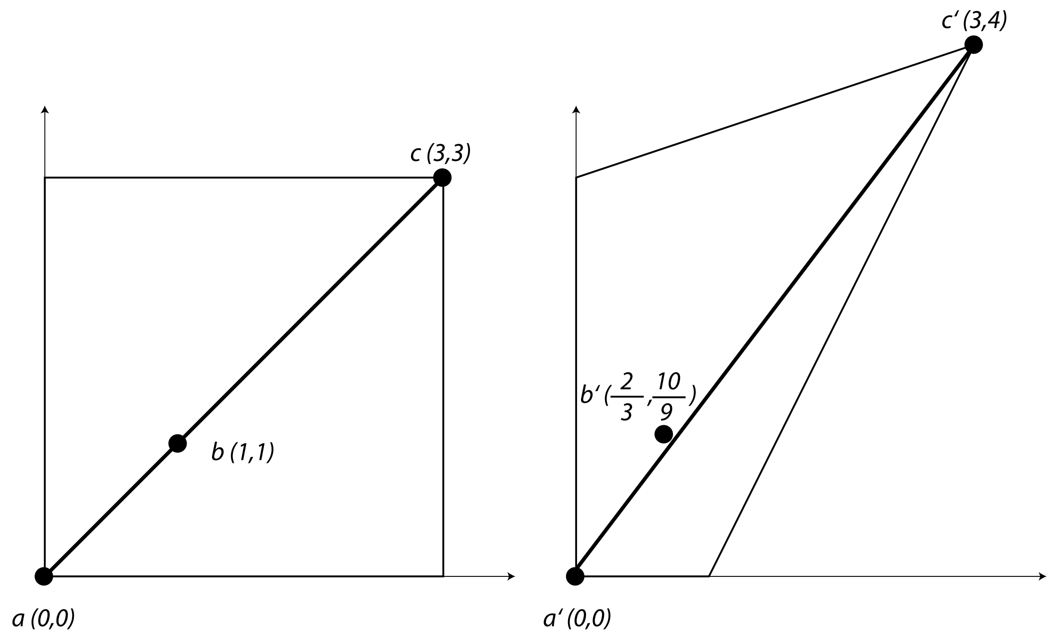

Figure 3.8: A transformation using bilinear interpolation does not preserve collinearity. On left, four control points are initially arranged in a square. On right, the control points are displaced. Three collinear points, a, b, and c are selected. On the right, the line formed by a' and c' is no longer coincident to displaced point b'.

and substituting b' into Equation 3.10 yields the following statement:

$$\left(\frac{4}{3}\right)\left(\frac{2}{3}\right) - \frac{10}{9} = \frac{-2}{9} \neq 0 \tag{3.11}$$

This shows that b' does not lie on the line formed by a' and c'. Therefore straight lines are not preserved.

To preserve the straight rays representing a light field, we define the transformation on its ray parameters instead of the 3D space in which the rays are embedded. In this way, rays in the light field are always mapped to straight rays. Note however, that preserving straight rays in the light field during transformation does not guarantee that straight lines represented by the light field remain straight. We come back to this property after defining the light field ray transformation.

3.3.3 Defining a Ray Transformation

The key idea in defining a ray transformation that preserves the straight rays of the light field is to define the transformation in terms of the ray parameters. In this way, rays are always mapped to straight rays. We use the two-plane parameterization of a ray and factor the trilinear warp into two bilinear warps that displace the (u, v) and (s, t) coordinates in the UV- and ST-plane, respectively.

First, to compute the location of the UV- and ST-planes and the (u, v, s, t) coordinates for a ray, we intersect the ray of the light field[6] with the deformation box C. The two intersection planes define the UV- and ST-planes. The corresponding intersection points define the (u, v, s, t) coordinates. In other words, the two planes define the entrance and exiting plane for the ray as it travels through the deformation box.

Next, a separate bilinear warp is applied to the (u, v) and (s, t) coordinates. Factorizing the trilinear warp into two bilinear warps is advantageous for two reasons. First, bilinearly warping in this way preserves straight rays representing the light field. That is, the new light field is represented by a set of straight rays. Second, two bilinear warps take 18 scalar multiplications of the coefficients. A single trilinear warp takes 42 scalar multiplications. Therefore bilinear warps can be computed quicker.

The bilinear warp is a simplified version of Equation 3.5. The four interpolating points are those defining the UV- or ST-plane. This warp produces a new ray (u', v', s', t') which is then re-parameterized to the original parameterization of the light field. Figure 3.9 summarizes the algorithm for transforming a ray of the light field. Figure 3.10 illustrates how a ray is transformed, pictorially.

3.3.4 Properties of the Ray Transformation

Given the above definition of a ray transformation, it is useful to compare it to other transformations to understand its advantages and disadvantages. A common set of 3D transformations is the specializations of a projective transformation. The projective

[6]The captured light field already has a ray parameterization, but needs to be re-parameterized for ray transformation.

```
TRANSFORM_RAY ($ray$)
1   $r_{uvst} \leftarrow$ REPARAMETERIZE($ray$)
2   $p_{uv} \leftarrow$ BIWARP($r_{uv}$)
3   $p_{st} \leftarrow$ BIWARP($r_{st}$)
4   $q_{uvst} \leftarrow [p_{uv}, p_{st}]$
5   return   REPARAMETERIZE_ORIGINAL($q_{uvst}$)
```

Figure 3.9: Algorithm for using bilinear interpolation to transform rays.

transformation is a group of invertible n x n matrices, related by a scalar multiplier. In the case of transformations on 3D points, $n = 4$.

The projective transformation maps straight lines to straight lines [HZ00]. Therefore, it is useful to compare our ray-transformation to it. We show that our ray-transformation can define Euclidean, similarity, and affine transforms. Unfortunately, as we will show, not all general projective transforms can be produced. However, we show that our ray-transform can perform mappings beyond projective mappings, like twisting.

Euclidean, Similarity, and Affine Transforms

A Euclidean transform models the motion of a rigid object; angles between lines, length and area are preserved. If the object is also allowed to scale uniformly, then this models a similarity transform; angles are still preserved, as well as parallel lines. If an object can undergo non-isotropic scaling and rotation followed by a translation, this transformation models an affine one[7]. Affine transforms preserve parallel lines, ratios of lengths of parallel line segments, and ratios of areas.

Mathematically, these three transforms can be written in matrix form:

$$x' = Tx = \begin{bmatrix} A & t \\ 0 & 1 \end{bmatrix} x \tag{3.12}$$

where x and x' are 4x1 vectors, T a 4x4 matrix, A a 3x3 matrix, t a 3x1 vector and 0 a 1x3 vector. If $A = G$, for orthogonal matrix G, then T is a Euclidean transform.

[7]It can be shown that an affine matrix can be factored into a rotation, a non-isotropic scaling, and another two rotations, followed by a translation [HZ00].

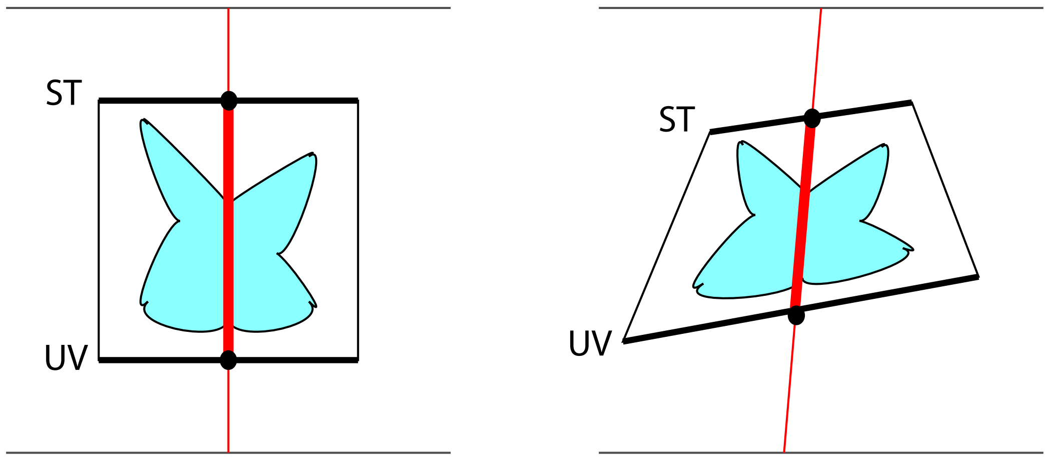

Figure 3.10: An illustration of ray transformation. On the left is a top-down view of the original light field. The parameterization of the light field is shown as two horizontal lines. The deformation box is drawn as a black square; it has its own two-plane parameterization, labeled UV and ST. One ray, shown in bold red, is re-parameterized using the UV and ST two planes of the box. The ray in the original parameterization is shown in light red. The intersection points are shown as black points. These two points are transformed using bilinear interpolation to map to the two black points on the right image. The two new points defining the warped ray are re-parameterized to the original light field. The warped ray is shown in bold red, the repararameterized one, in light red.

If $A = sG$, for scalar s, then T is a similarity transform. If A can be factored as

$$A = R(\theta)R(-\phi)DR(\phi) \tag{3.13}$$

where R is a rotation matrix and D a diagonal matrix, then T is an affine transform. Notice that the Euclidean and similarity transforms are special cases of the affine one.

Given these transforms, we now show how to place 8 control points, which define the two planes for ray-transformation, to produce the equivalent ray-mapping. The two key ideas are 1) the control points are transformed by the affine (or a special case, like Euclidean) mappings and 2) the affine mappings preserve collinearity. A mapping that preserves collinearity ensures that points that lie on a line still lie on a line after the transformation. We will prove by construction, the following theorem:

Theorem 1 *A line transformation defined by an affine map, A, can be produced by*

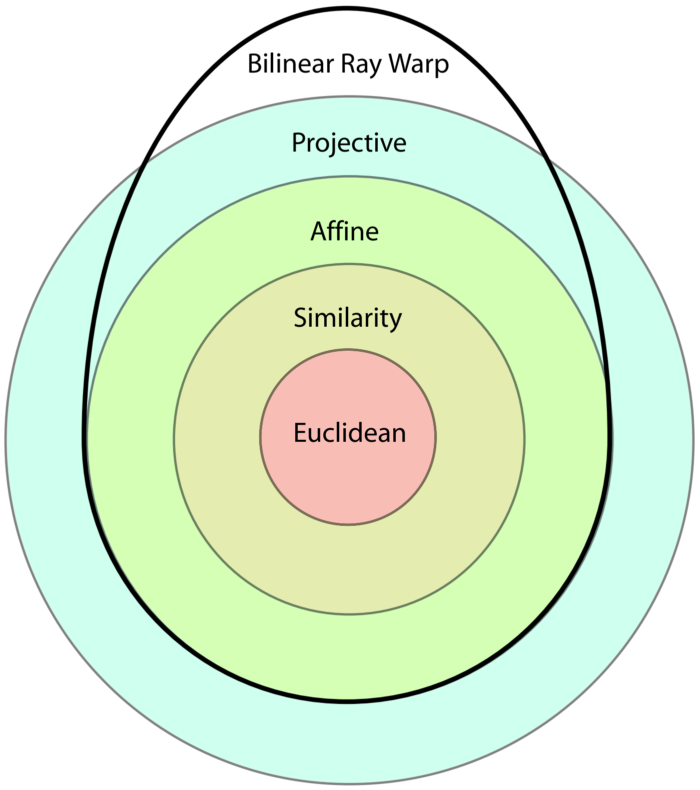

Figure 3.11: A hierarchy of line/ray transformations. The bilinear ray-transformation introduced in Section 3.3.3 can simulate up to affine transforms and a subset of the projective ones. It can also perform line transformations that are impossible with the projective transform, such as twisting.

the ray-transformation described in Section 3.3.3 by applying A to all 8 control points.

The proof is by construction. The ray-transform in Section 3.3.3 is specified by 8 control points, 4 defining the UV-plane and 4 for the ST-plane. We call the control points, which are in homogeneous coordinates, a, b, c, $\ldots$, h. The new control points are defined as follows: $a' = Aa$, $b' = Ab$, $c' = Ac$, $\ldots$, $h' = Ah$. In other words, the new control points are simply the affine mappings of the original control points. These control points will be used for the bilinear warp in the UV- and ST-planes

Given the displaced control points a', $\ldots h'$, we now show that any warped ray is transformed in exactly the same way as the affine mapping. This is done by taking 2 points in the UV- and ST-planes, bilinearly warping them, and showing that these two new points are the same points using an affine warp. Furthermore, since the affine warp preserves collinearity, the line formed by the two affinely warped points is the same as the line made by connecting the bilinearly warped points on the UV- and ST-planes.

Suppose we have a point P_{uv} on the UV-plane:

$$\begin{aligned} P_{uv} = \quad & (1-u)(1-v)a + (u)(1-v)b + \\ & (1-u)(v)c + (u)(v)d \end{aligned} \tag{3.14}$$

where u and v are the interpolation coordinates on the UV-plane. Then using the displaced control points, we can bilinearly interpolate the warped point for P_{uv}:

$$\begin{aligned} P'_{uv} = \quad & (1-u)(1-v)a' + (u)(1-v)b' + \\ & (1-u)(v)c' + (u)(v)d' \end{aligned} \tag{3.15}$$

But recall that $a' = Aa$, $b' = Ab$, $c' = Ac$, $\ldots$, $h' = Ah$. Substituting this in:

$$\begin{aligned} P'_{uv} = \quad & (1-u)(1-v)Aa + (u)(1-v)Ab + \\ & (1-u)(v)Ac + (u)(v)Ad \end{aligned} \tag{3.16}$$

and factoring out A reveals:

$$P'_{uv} = A[(1-u)(1-v)a + (u)(1-v)b + (1-u)(v)c + (u)(v)d] = AP_{uv} \tag{3.17}$$

Equation 3.17 states that the bilinearly warped point P'_{uv} can be computed by applying the affine warp A to P_{uv}. A similar argument can be made for $P'_{st} = AP_{st}$. Since affine warps preserve collinearity of points, the affine warp has mapped any line through P_{uv} and P_{st} to a line through P'_{uv} and P'_{st}. This proves that any affine mapping of lines can be produced by our ray-transform. ∎

Tackling the General Projective Transform

Unfortunately, the proof-by-construction presented above does not apply to general projective transforms. In Equation 3.17, suppose A is a projective transform of the form:

$$x' = Ax = \begin{bmatrix} P & t \\ v^T & s \end{bmatrix} x \tag{3.18}$$

with 3x3 matrix P, 3x1 vector t, 3x1 vector v and scalar s. In this case, A can not be factored out of the equation because there may be a different homogeneous division for each term in the equation. This means that directly applying a projective transform to the control points will not yield the same ray-transform as a projective transform. Note that this was the case with the affine map. Figure 3.12 is a graphical explanation of the projective transform. In this case, the transform is in flatland, e.g. a 2D projective transform. What we've shown so far is that a bilinear ray-warp constructed by projectively mapping the original control points does not produce the same ray-warp. But can a different construction of the control points yield an equivalent ray-warp? Unfortunately, the answer is no. The reason is simple. If the control points are not projectively mapped, then warped rays between control points will never match projectively warped rays. Therefore, for general projective transforms, it is impossible to produce an equivalent bilinear ray warp.

Fundamentally, the 8 control points of the bilinear ray transform need to map to the 8 projectively transformed points. If this is not the case, then rays formed from opposing corners in the undeformed case will map to different rays when using the bilinear and the projective warp. However, as shown in Figure 3.12 for the 2D case, if the 4 control points coincide with the projectively warped points then rays still do not match between bilinear and projective mappings. Therefore, for general projective transforms, it is impossible to produce an equivalent bilinear ray warp.

Beyond Projective Transforms

Although the bilinear ray-transform cannot reproduce all projective transforms, it has two nice properties that make it more useful for an animator. First, bilinear ray-transforms can simulate the effect of twisting (like in Figure 3.1); projective transforms can not. Twisting is a rotation of one of the faces of the deformation box. Bilinear ray-warping handles this case as it normally handles any ray warp. 3D projective transforms, however, cannot map a cube to a twisted one because some

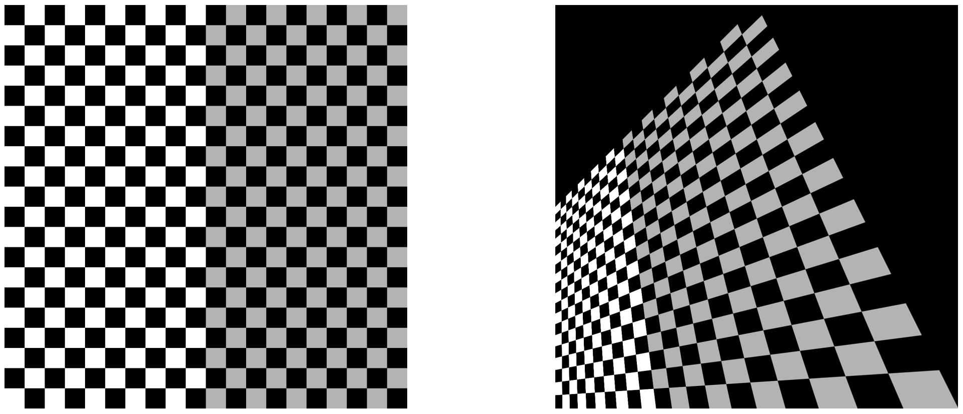

Figure 3.12: A 2D projective transform applied to lines on a checkerboard. On the left, are the checkerboard lines before transformation. The checkerboard is a unit square, with the lower-left corner at the origin. Notice, the lines intersect the borders of the checkerboard in a uniform fashion. On the right, are the checkerboard lines after a projective transform. The projective transformation has translated the top-left corner to $(0, 0.5)$ and the top right corner to $(0.5, 1)$ Notice, that the intersections are no longer uniform along the borders. In our ray-transformation, the uniformly-spaced intersections on the left image map to uniform intersections on the right image (this is also true in the affine case because parallel lines are preserved). However, the projective transform does not preserve this property for the borders, shown on the right.

of the sides of the box are no longer planar. Projective transforms preserve planes: any four points that lie on a plane must lie on the same plane after the transformation[8]. Because of this invariant, projective transforms cannot represent ray warps that involve bending the sides of the deformation box, like twisting. However, this ray transformation is useful for an animator to produce twisting effects on toys or models.

The trade-off is that the bilinear ray-transform no longer preserves straight lines within the scene represented by the light field. Although this transform keeps the rays of the light field straight after warping, lines in the scene represented by the

[8]The proof is a simple extension of the 2D version (that preserves lines), described in Theorem 2.10 of [HZ03].

light field may curve. Figure 3.13 illustrates this idea. The light field is representing a scene containing a single, straight line. This line is shown in bold. Three points are selected on this line, l, p, and q. The light field rays that are incident to these three points are shown in light blue. Now, suppose we induce a deformation of the light field by displacing the points c and d, defining the UV-plane. Since a and b are not displaced, the plane containing points a, b, l and q remains the same after deformation. However, the bilinear transformation of the uv coordinates causes the ray through p to be transformed into the ray going through p' in the deformed case. p' does not lie on the plane containing the original line. This shows that the line through l, p, q is no longer a line after applying this bilinear-transformation on the UV-plane.

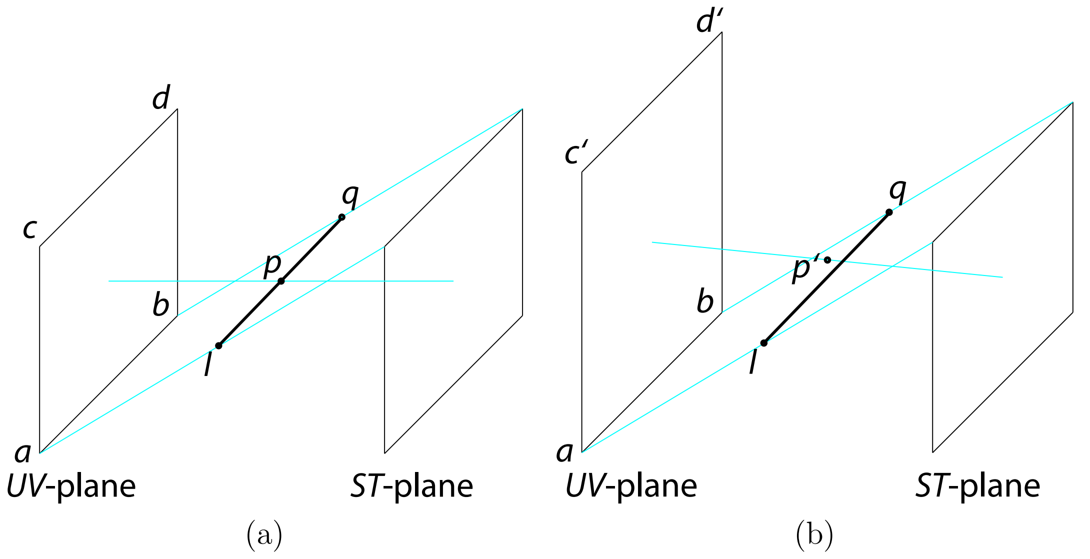

Figure 3.13: A light field of a single straight line is deformed. (a) shows the original light field configuration. The line is shown in bold. Three points on the line are selected. The light field rays through these points are shown in light blue. In (b), the light field is deformed by vertically displacing c and d to c' and d'. The new light field represents a non-straight line, even though the bilinear ray transform preserved straight rays.

The second useful property of the bilinear-transform is that it guarantees that the deformed box always adheres to the animator's specification. In other words, the boundary edges and faces of the resulting deformed box will always be what the animator specifies. In contrast, when using a projective transform the deformed box may not be exactly the same as what the animator specified. This is a useful property when specifying multiple adjacent deformation boxes.

In summary, our analysis of the bilinear ray-transform shows that it can reproduce up to affine mappings of rays. It cannot reproduce all projective mappings, but can produce other effects, like twisting, which are impossible for projective transforms. Furthermore, a bilinear ray-transform is guaranteed to adhere to the eight new control points specified by the animator. This enables an intuitive method for specifying a ray-transformation of the light field. Next we discuss how the bilinear ray transform is implemented to enable interactive light field deformation.

3.4 Implementing the Ray Transformation

The ray transformation discussed so far warps all rays of the light field. The problem is that light fields are dense, so transforming every ray is a time consuming process. A typical light field has over 60 million rays (see Appendix A). Applying a transformation to all 60 million rays prevents interactive deformation. Instead, we exploit the fact that at any given time, an animator only needs to see a 2D view of the deformed light field, e.g. never the entire dataset. This means that we only need to warp the view rays of the virtual camera. In other words, we deform rays "on demand" to produce an image from the desired view point.

How are the warps on the light field and the warps on the view rays related? The two warps are in fact inverses of each other, as shown in [Bar84]. For example, to translate an object to the left, one can either apply a translation to the object, or apply the inverse translation (i.e. translate to the right) to the viewing camera.

Therefore, to render an image from a deformed light field, we apply the inverse ray warp to the view rays of the virtual camera. Given a view ray in the deformed space, we need to find the *pre-image* (e.g. ray) in the undeformed space such that warping the pre-image yields the given view ray. To find the pre-image of a ray, we forward warp many rays, and interpolate amongst nearby rays. Figure 3.14 illustrates this interpolation in ray space.

In the actual implementation, we use texture-mapping to help us forward-warp many ray samples and interpolate amongst them. Recall from Section 3.3.3 that a ray transformation is defined by 8 control points defining a deformation box (e.g. two planes in the $UVST$ parameterization). To forward warp many ray samples, we simply create many samples on the UV- and ST-planes and bilinearly warp them. To interpolate between UV- and ST-samples, we triangulate the points and use barycentric coordinates to shade each triangle. In this way, the texture color codes the original coordinates of each UV and ST point. We used 64 x 64 x 2 textured triangles per plane for our datasets. Figure 3.15 shows the UV-planes (left) and ST-planes (right) for a deformation box.

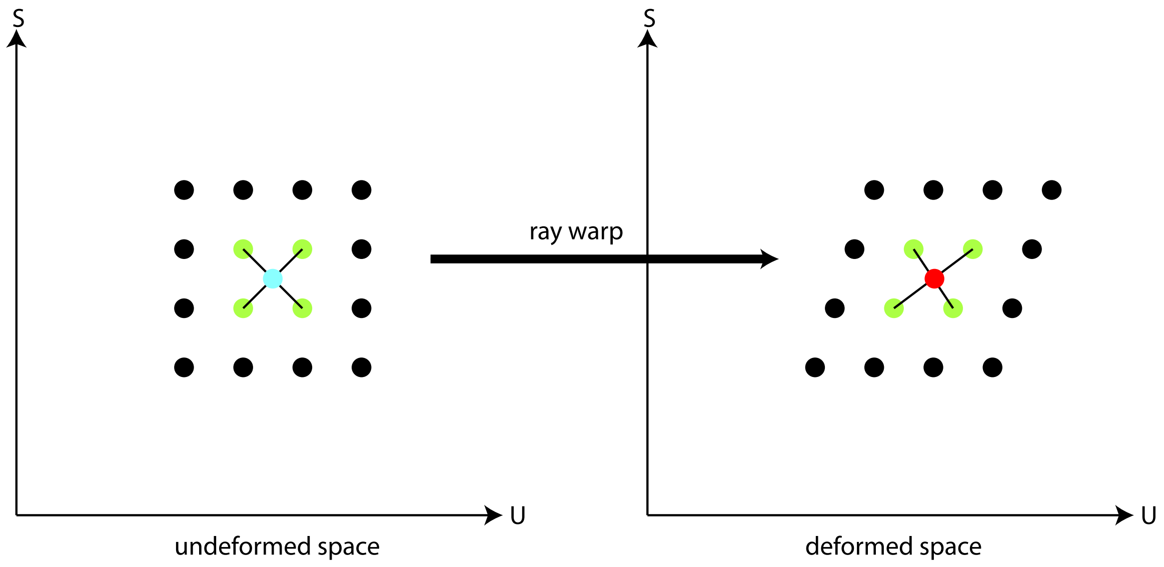

Figure 3.14: A pre-image of a ray is found by computing the forward warp for many sample rays, and interpolating amongst nearest rays. The above two diagrams are 2D ray-space diagrams illustrating the undeformed space (left) and the deformed space (right). Rays in ray-space are represented as points. The pre-image of the ray in the deformed space (shown in red) is found by computing the nearest rays (shown in green), finding their counterparts in the undeformed space, and interpolating the original ray positions. The interpolation is represented by the black lines. The pre-image is shown in blue in the undeformed space.

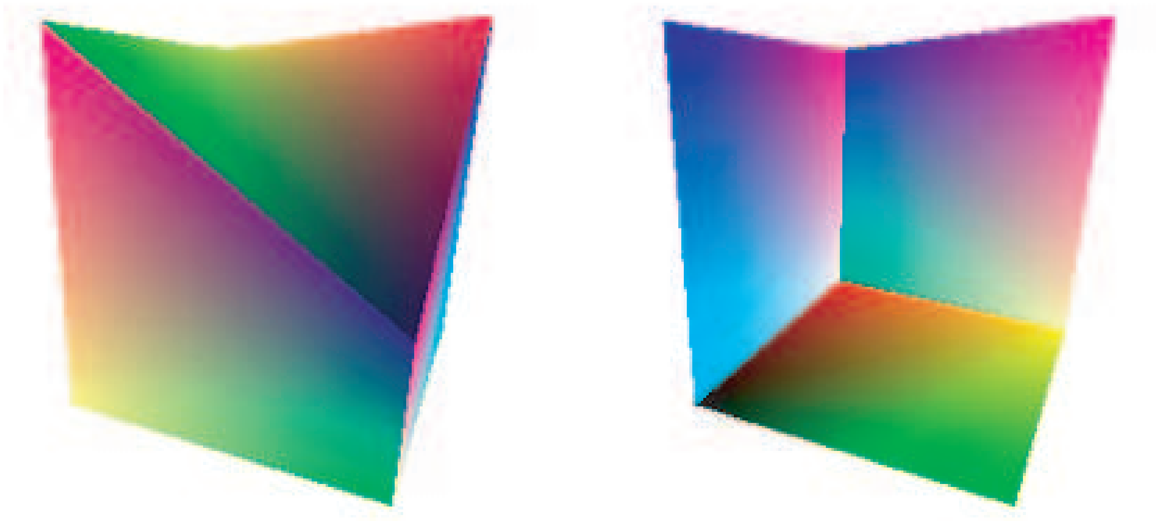

Figure 3.15: An inverse warp is approximated by forward warping many ray samples and then interpolating the results. We use a hardware-accelerated texture-mapping approach to quickly interpolate among the ray samples.

3.5 Results

We now present results illustrating how the bilinear ray-transform is used to intuitively specify a ray-transformation on the light field. This ray-transformation simulates the effect of deforming the object represented by the light field. The animations can be found at the following webpage:
`http://graphics.stanford.edu/papers/bchen_thesis`.

Figure 3.1 at the beginning of this chapter illustrates a twisting effect on the light field. Figure 3.16 shows the associated deformation box for the twisted soldier. The twisting of the deformation box is impossible for a projective transform. Figure 3.17 illustrates a bilinear ray-transform that simulates an affine ray warp. The user supplies a deformation by moving vertices of the box (shown in gray) to a deformed position (shown in red).

In these results so far, the deformation is global and lacks local control. In contrast, an animator typically applies multiple deformations to a single object. In the next section, we introduce a technique for applying multiple, independent ray transforms

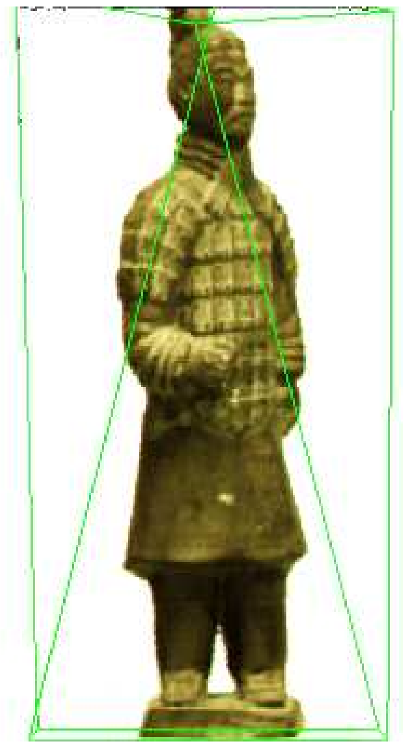

Figure 3.16: Deformation box used to twist the toy Terra Cotta Warrior.

to a single light field, to further increase the expressive power of animating light fields.

3.6 Specifying Multiple Ray Transformations

The deformations shown in the previous section illustrate global effects like twisting. However, such effects are broad; they apply over the entire light field. In contrast, with traditional mesh models the animator may have local control over parts of the mesh, enabling subtle deformations and effects. Local control over a light field is accomplished by segmenting the light field into *layers* and by supplying a different ray transformation to each layer.

A layer is simply a light field, whose input rays are a subset of the original input rays. Recall that light fields are approximated by a set of images. In this representation, a layer is simply a subset of pixels (over all images) corresponding to a particular region of the object. For example, consider Figure 3.18, which shows an image from

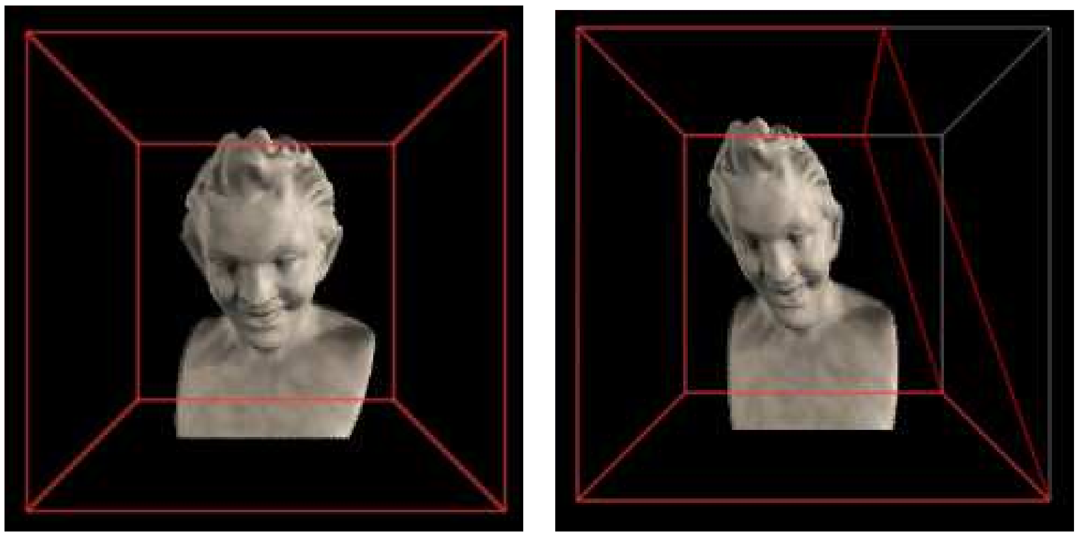

Figure 3.17: Illustration of free-form deformation on a light field. The left image is from a light field of a statue bust. The deformation box has been overlaid in red. Moving vertices of the box induces a ray-transformation on the light field. The visual effect is a deformation on the object represented by the light field, as shown in the image on the right. The red lines show the deformed box, the gray lines show the original box. The user supplies the deformation by dragging vertices with the mouse in a graphical user interface.

a light field captured of a toy teddy bear. The "head" layer of the light field are all pixels (in all images) that "see" the teddy bear's head. Therefore, in segmenting the teddy bear light field, we split the light field into multiple light fields, which we call layers. To compute these layers, we use projector illumination. Appendix B describes this technique in more detail. The important thing is that the output is a set of coaxial layers (e.g. light fields). The animator then supplies deformations to each coaxial layer. Finally, the deformed layers are rendered together with correct visibility. This rendering algorithm is described next.

3.7 Rendering Multiple Deformed Layers

The goal of the rendering algorithm is to produce an image from a given viewpoint, while maintaining correct visibility between deformed layers of the light field. Unlike

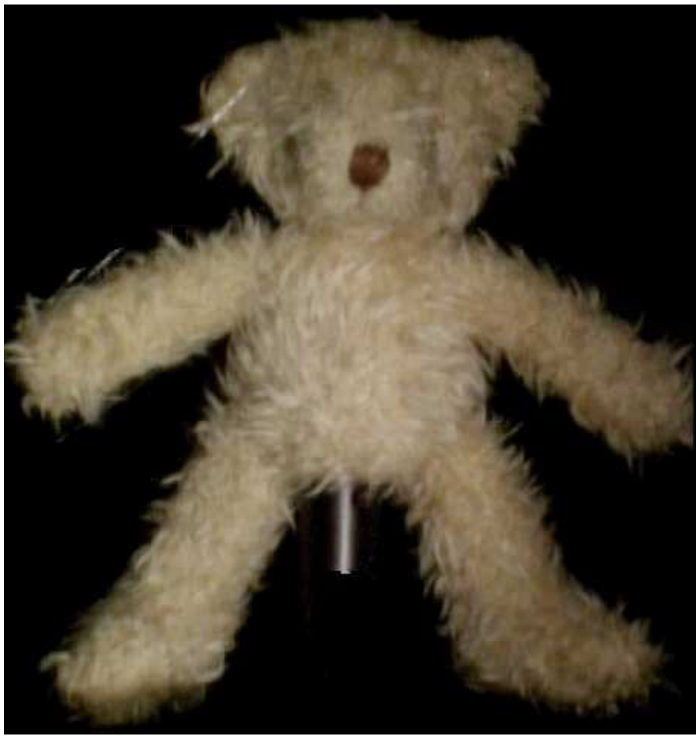

Figure 3.18: Illustrating a "layer" of a light field. An image from a light field of a teddy bear is shown. The head layer of this light field corresponds to every pixel in all images that see the teddy bear's head.

the global deformation case, deforming a layer can cause a visibility change. In other words, deforming a layer may reveal or occlude layers behind it.

In order to render with correct visibility, the algorithm makes two assumptions about the deformed layers: 1) the control points defining the deformation box completely enclose the region represented by that layer and 2) the alpha masks computed from projector-based segmentation accurately describe that object's opacity. We use the first assumption to sort the layers in a front-to-back depth order with respect to each view ray. The second assumption allows us to use alpha to test whether a view ray is incident upon an object represented by a particular layer.

To render an image, a view ray is shot out from each pixel. The idea is that this ray travels through different deformed layers. As it travels through each layer the ray is transformed; we then test if it is incident to an object represented by that layer. If it is not, then the ray continues to the next layer, and the process is repeated. If the ray is incident to an object within the layer, then the color sampled from this layer is returned as the color along the original view ray.

More concretely, for each output pixel of the image form a view ray. Sort the layers in a front-to-back order with respect to the view-ray. The layer locations are defined by their deformation box. The boxes are assumed to be non-intersecting. Traversing each layer, warp the view-ray using the associated ray-transformation (see Section 3.4 for how this is implemented). Use the transformed ray to sample from this layer. If the alpha along this ray is non-zero, this means the ray has "hit" an object in this layer and we return its color[9]. If the alpha is zero, then we proceed to the next layer along the view-ray. Figure 3.19 gives a pictorial example of this rendering algorithm for a single view-ray.

Does this rendering algorithm solve our problem with changes in visibility? For occlusions, yes. For disocclusions, only partially. For occlusions, if a layer is deformed to occlude another layer, when traversing the ray in a front-to-back order, the front layer will be rendered correctly. Disocclusions are more challenging. A layer may deform in a way that reveals parts of background layers that were not captured during acquisition. This problem can be solved by using hole-filling techniques, although our work has not implemented such techniques. Heuristics based on texture structure [EL99, WL01] or a priori knowledge [ZWGS02] could be used to reconstruct the holes in these layers. These algorithms could be applied on the layers of the segmented light field before deformation. Now we show results using the entire deformation process.

3.8 Results with Multiple Deformations

In Figure 3.20 a fish light field is animated by controlling three deformation boxes. The middle box is being warped, while the front box (the head) and the back box (the tail) are rotated according to the bending of the middle box. Notice that visibility is rendered correctly: the head pixels are drawn in front of the body and tail pixels.

[9]Recall that the alpha values in each layer are determined using the projector-base segmentation technique described in Appendix B.

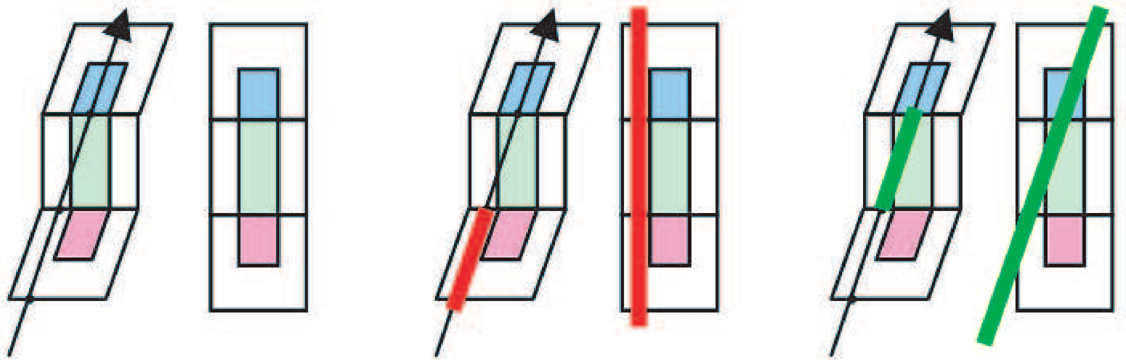
Figure 3.19: Rendering a view ray. The left pair of images show the deformation boxes in the deformed and undeformed space. A view ray, shown in black, crosses the layers. As the ray traverses the front layer (containing the pink object), it is deformed and tested for visibility (shown in the middle). In this case, the alpha is 0 and we proceed to the next layer. In the next layer (shown in green on the right), the view ray is deformed and tested for visibility. In this case the alpha is non-zero and its associated color is returned for this view-ray.

Figure 3.21 shows a few frames from an animation of a furry teddy bear. Using projectors, the bear is split into several deformation boxes to allow for independent arm, leg and head motion.

3.9 Summary

The first contribution of this thesis is light field deformation, a novel way to interact with light fields. The technique is an intuitive tool that lets animators deform light fields. We describe two key challenges in accomplishing deformation: maintaining consistent illumination and specifying a ray transformation. We show how to maintain consistent illumination through capturing a coaxial light field. We then introduce a novel ray transformation and analyze its properties, showing that it can perform affine and other non-projective transforms. Our implementation exploits texture-mapping on graphics hardware to facilitate interactive deformation.

Then, we show how to extend global deformation to local light field deformation by segmenting the light field into layers. Segmentation is accomplished using active

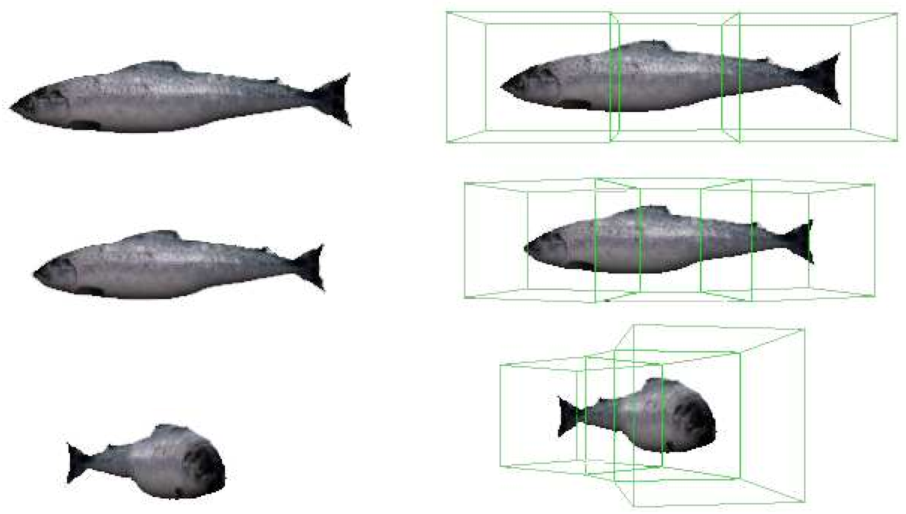

Figure 3.20: Deforming a fish with three independent deformations. The top-left image shows the original fish with deformation boxes shown in the top-right image. The middle-left image shows the deformed fish with corresponding control boxes in the middle-right image. The bottom-left image shows a different view. Notice that visibility changes are handled correctly by our algorithm, the fish head pixels are rendered in front of the tail pixels. This light field was created with 3D Studio Max.

illumination, as described in Appendix B. After deforming each layer, our novel rendering algorithm renders an image while preserving correct visibility between layers.

The technique has its limitations. Coaxial illumination is a limiting type of illumination. For example, shadows are not possible. One topic of future work is investigating the relationship between the types of ray-transformations and the illumination conditions that remain consistent under those transforms. A second limitation involves specifying the ray-transformation. The warp is specified by moving 8 control points in 3D. This means that there are 24 degrees of freedom. However, there are multiple configurations of control points that yield the same ray transform, so there is a redundancy in the specification. It would be useful to investigate other, more efficient ways to specify ray transformations, perhaps in ray-space.

Despite these limitations, the technique is shown to be useful for animators and can be extended to other deformation techniques (like skeleton-based deformation). In the second half of this thesis, we incorporate deformation as a tool in a host of tools for general manipulation of light fields.

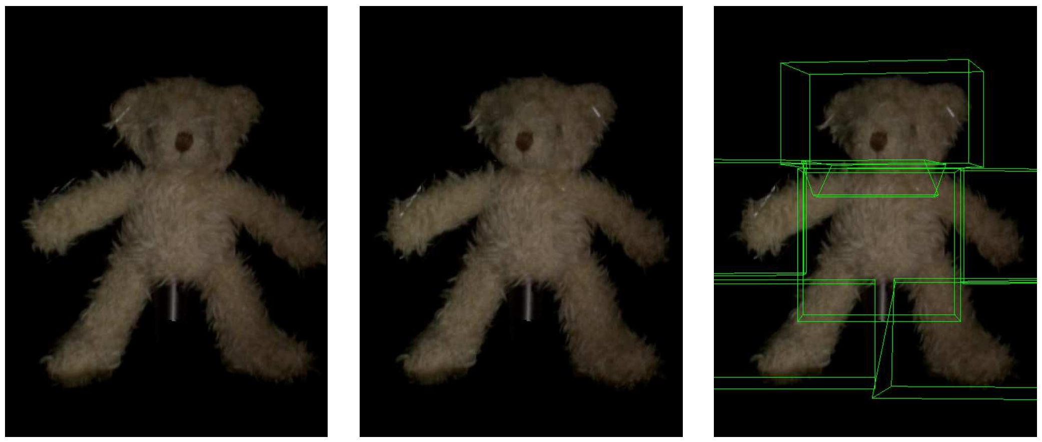
(a) (b) (c)

Figure 3.21: A deformation on a teddy bear. Image (a) shows a view of the original captured light field. In this case, the cameras were arranged in a ring, thus capturing a circular light field. Image (b) shows a deformation in which the head, arms and legs are all bended or twisted independently. Image (c) shows the deformation boxes used to specify the motion of the teddy bear.

Chapter 4

LightShop: A System for Manipulating Light Fields

4.1 Introduction

The first half of this dissertation introduced light field deformation. This tool, like those found in the literature, operates in a stand-alone application. In comparison, image manipulation applications, like Adobe Photoshop, allow a user to use and combine multiple tools. The ability to combine tools enables creative manipulation of images.

The second contribution of this dissertation is a system that provides a user with a mechanism to use and combine multiple tools for manipulating light fields. We call this system *LightShop*. A system that operates on multiple light fields faces two key challenges. First, operations can manipulate light fields in a variety of ways, so specifying an operation must be designed carefully. For example, some operations are sum over multiple pixels in each image (like focusing), or shift pixels across images (like deformation). Second, light fields are captured and parameterized differently, so one must design the system so that operations are independent of the light field representation.

Keeping these challenges in mind, we designed LightShop with the following goals:

1. Light field operations must be specified independent of the representation.
2. The system must be extendable to incorporate new operations.
3. The system must be amenable to graphics hardware.

The first design goal addresses the problem of multiple light field parameterizations. The second goal addresses the problem of specifying operations and combining them. The third goal enables interactive manipulation and editing. This also enables light fields to be easily integrated into video games.

Given these design goals, what are common operations that should be incorporated into LightShop? Table 4.1 lists five common operations on light fields and their applications. Ray transforms were demonstrated in the first half of this thesis for light field deformation. Compositing light fields is demonstrated in an application, called "pop-up light fields," to create ghost-free renderings from light fields. The idea is to segment a light field into multiple two-plane parameterizations (e.g. layers), where each ST-plane serves as a local geometric proxy to that part of the scene. The final image is rendered by compositing the samples from each layer of the light field. The third class of operations are the arithmetic operations on colors sampled from light fields. This has a use in relighting applications where several light fields of an object are captured under varying illumination. By taking linear combinations of samples from these light fields, relighting can be simulated. The fourth operation is focusing within a light field. Instead of creating a virtual view from a pinhole camera, one can simulate a camera with a finite-depth-of-field by summing over sampled colors in the light field. Researchers have demonstrate its use in seeing behind occluders and noise reduction. The final operation is perhaps the most fundamental: synthesizing a novel view. This involves sampling and interpolating from data in a light field to create an image from a novel viewpoint.

Given our design goals and a list of common operations on light fields, we can now introduce the system. To begin, we describe our conceptual model for manipulating and combining light fields. This conceptual model will drive LightShop's entire design.

Operation	**Application**
ray transformation	light field deformation [COSL05, ZWGS02]
compositing	pop-up light fields [SS04]
arithmetic	face relighting [DHT+00]
focusing	synthetic aperture photography [VWJL04, IMG00, LH96]
sampling	novel view interpolation [LH96, GGSC96, BBM+01]

Table 4.1: Common light field operations found in the literature.

4.2 LightShop's Conceptual Model

What does it mean to manipulate and combine light fields? To answer this question, we borrow from current modeling packages for mesh-based geometry. In particular, we study Pixar's RenderMan [Ups92] and OpenGL [BSW+05]. Both software packages are designed for modeling and manipulating 3D objects. We characterize their conceptual model as one that *models* a scene containing multiple objects, *manipulates* these objects, and *renders* an output image based on the modified scene. We then adapt this conceptual model for manipulating light fields.

In RenderMan, functions are exported to the user through the RenderMan Interface. These functions modify internal state that represents the scene and rendering contexts. Some functions enable the definition of polygons, surfaces, lights and shading properties: `RiPolygon, RiSurface, RiLightSource, ...`. These functions are part of the modeling process. Other functions modify previously defined objects: `RiDeformation, RiSolidBegin, ...`. These functions are part of the manipulation process. Finally, after a scene is modeled and modified it is rendered by the system. In RenderMan this rendering process is hidden from the user.

OpenGL also maintains similar internal state and exports a set of functions to model and manipulate the scene. However, instead of hiding the rendering process, OpenGL exposes two steps of the rendering pipeline to enable more control. The vertex shader enables a user to manipulate vertex information. The fragment shader allows for pixel-processing before frame-buffer operations. In other words, the fragment shader is a mechanism for the user to specify how an image is rendered from the scene.

Since both RenderMan and OpenGL are well-known modeling packages, we design LightShop with a similar 3-part conceptual model: model, manipulate, and render. For modeling a scene, LightShop exports functions for inserting two primitive types in a scene: light fields and viewing cameras. Appendix C lists the associated functions. Once a scene is composed, to manipulate it a user must specify operations on light fields. Recalling our design goals, these operation must be specified in a way that is independent of the light field representation, easily extendable, and amenable to graphics hardware.

The key insight to our design is that an operation on a light field can be realized by manipulating the viewing rays from the rendering camera. This is best explained by an example. Recall from Chapter 3 on deformation that rendering an image of a deformed light field can be performed in two ways: 1) transform all rays of the light field and interpolate a novel view or 2) apply the inverse ray-transform on all view-rays, and sample from the original light field. In the second approach, by manipulating the view-rays we can render deformed light fields. Figure 4.1 illustrates warping view-rays to simulate deformation. It turns out that all operations listed in Table 4.1 can be realized by manipulating view-rays in a straight-forward manner.

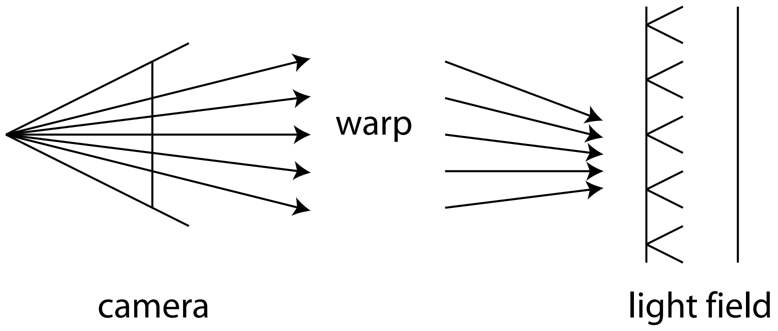

Figure 4.1: Warping view rays to simulate deformation. The rays emanating from the camera are transformed before sampling from the light field. This can simulate the effect of deforming the original light field.

This approach has three advantages over directly manipulating the light field. First, specifying an operation is in terms of the view-rays, which is independent of the parameterizations of the light field and optimized for changing only those rays needed for rendering a 2D image. Second, these view-ray operations can be combined, one after another. For example, one can first warp a view-ray, then sample from a light field, then composite it with the color from another light field. In fact, these operations are represented as functions in a language. We call a set of operations a *ray-shading program*. This is similar to Ken Perlin's Pixel Stream Editor [Per85]. The third advantage is that this language can be directly mapped to the fragment shader, so manipulating view-rays is amenable to graphics hardware. In fact, we the implement the ray-shading program as a fragment-shading program. The graphics rendering pipeline executes this program for every pixel, rendering an output image.

In summary, LightShop uses a conceptual model of 1) modeling a scene, 2) manipulating that scene and 3) rendering it to an output image. Modeling is performed by calling on LightShop's modeling API. The scene is both manipulated and rendered through the ray-shading program. The ray-shading program is a user-written program that specifies exactly how a view-ray should interact with light fields in the scene. The program is executed per output pixel and returns an RGBA color for that pixel. To demonstrate how a light field is manipulated, we present an example where render an image with shallow depth-of-field from a light field.

4.3 Example: Focusing within a Light Field

We now show an example that illustrates how a light field may be manipulated. Our example is creating an image focused at particular depth in the light field. Objects (represented by the light field) at the focused depth will be sharp, objects off this depth will be blurred. Figure 4.2 briefly summarizes how focusing occurs. Focusing is discussed in more detail in the graphics [LCV+04, WJV+05, IMG00, LH96] and vision [VWJL04] literature.

Assume during the modeling phase a scene is created containing a single light field and a single camera[1]. To manipulate the light field, a user writes a ray-shading program that describes how view-rays are manipulated as they travel through the light field. Figure 4.3 illustrates the ray-shading program for creating an image with

[1]Recall that a scene is modeled by LightShop's modeling API, described in Appendix C.

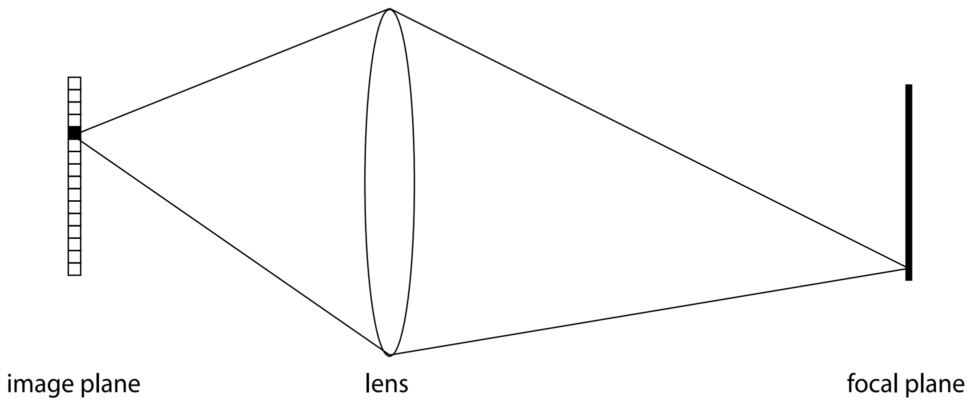

Figure 4.2: Focusing through a single lens. The radiance contributing to a single image pixel is a summation of light emitted from a point on the focal plane through the lens aperture. More specifically, the radiant exitance/emittance from a point on the focal plane is integrated as the irradiance on a image pixel. The radiant exitance of points off the focal plane is spread across multiple pixels (e.g. this point is “blurred”).

a shallow depth-of-field. The ray-shading program takes as input a 2D xy pixel location. It returns an RGBA color for this pixel location. The key component is the use of two for-loops and the summation operator to simulate light aggregation at the pixel location. To sample from the light field, the function, `LiSampleLF` is called. It takes a light field index and a ray, and returns a color sampled along that ray direction. Appendix C contains more details about this function, `LiSampleLF`.

The other operations listed in Table 4.1 are implemented as easily as focusing. They are discussed in Appendix C. Now that we have discussed the conceptual model behind LightShop and shown how to implement operations, we present the LightShop design in the following section.

4.4 LightShop’s Design

Figure 4.4 illustrates the overall design of LightShop. The system is designed to follow the model, manipulate, render conceptual model. It takes two inputs. The first is a series of function calls to model a scene. The second input is a ray-shading program that describes how a pixel should be colored, given the scene (e.g. the manipulating

```
LtColor main(LtVec2 pixelLocation) {
    LtColor sum = LtVec4(0,0,0,0);
    for(i=0; i < 1.0; i += 0.1) {
        for(j = 0; j < 1.0; j += 0.1) {
            LtRay ray = LiGetRay(0, pixelLocation, LtVec2(i,j));
            LtColor col = LiSampleLF(0,ray);
            sum += col;
        }
    }
    return sum;
}
```

Figure 4.3: Example ray-shading program for focusing. The core functionality that enables focusing is that two for-loops and a summation are used to simulate the aggregation at a pixel location, over the lens aperture. The two LightShop ray-shading functions, `LiGetRay` and `LiSampleLF` are discussed in more detail in Appendix C.

and rendering component). The output is a 2D image.

Following the arrows in Figure 4.4, the input modeling calls are evaluated by the modeler, which creates an internal representation of the scene. This scene representation is passed to the renderer, which takes the input ray-shading program and executes it over every output pixel location to produce a 2D image. To manipulate and combine light fields, a user modifies the ray-shading program. As the ray-shading program executes, it accesses the scene to retrieve data from the light fields. Recalling our three design goals, first note that the ray-shading program defines operations on rays, which is independent of the light field representation. Second, since the program utilizes a ray-shading language, new operations can be easily defined simply by writing new expressions. Third, the job of the renderer, which executes the ray-shading program at each ouput pixel location, can be directly mapped to a fragment shader. This makes LightShop amenable to graphics hardware.

Note that this design is independent of any implementation. LightShop can be thought of as a specification for manipulating and rendering light fields. In the following section we discuss one particular implementation of LightShop using OpenGL. Other implementations (using DirectX, for example) are also possible.

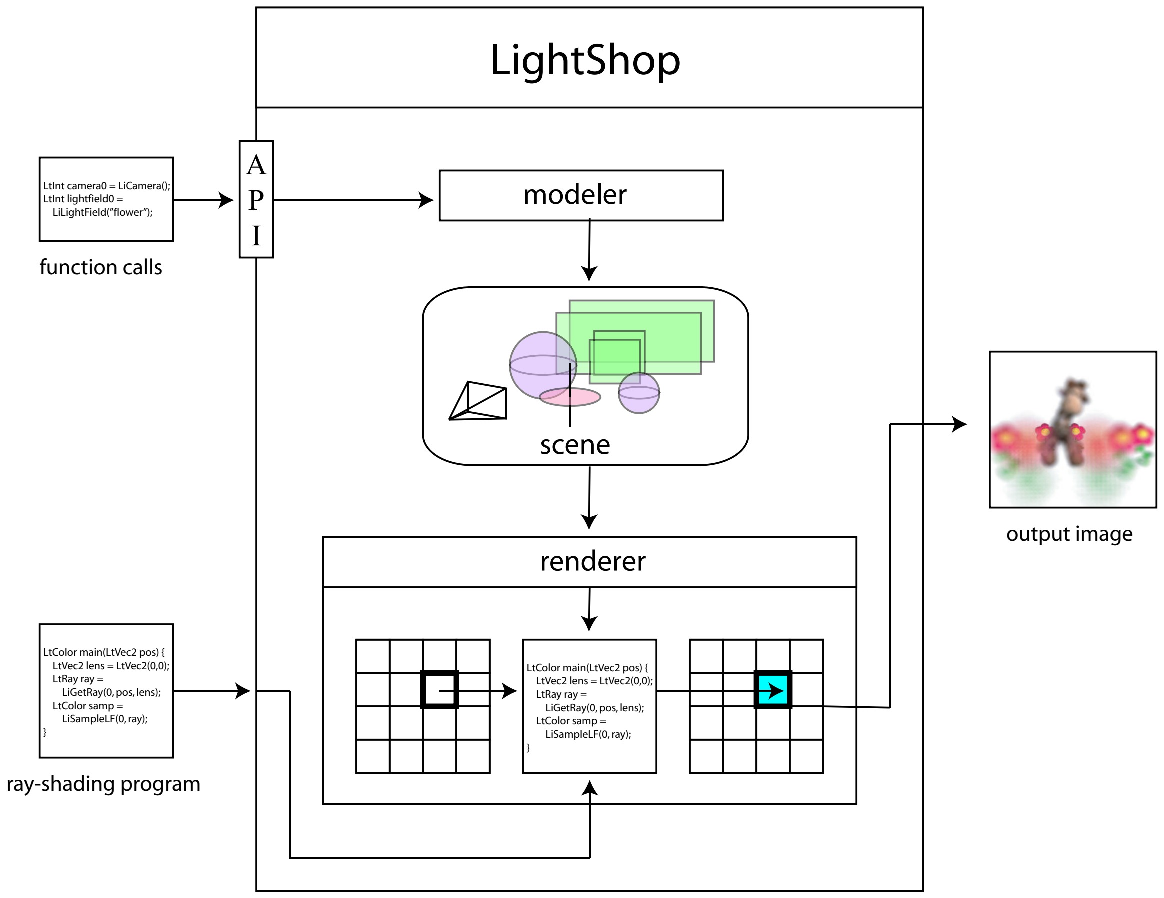

```
LtInt camera0 = LiCamera();
LtInt lightfield0 =
    LiLightField("flower");
```

```
LtColor main(LtVec2 pos) {
    LtVec2 lens = LtVec2(0,0);
    LtRay ray =
        LiGetRay(0, pos, lens);
    LtColor samp =
        LiSampleLF(0, ray);
}
```

```
LtColor main(LtVec2 pos) {
    LtVec2 lens = LtVec2(0,0);
    LtRay ray =
        LiGetRay(0, pos, lens);
    LtColor samp =
        LiSampleLF(0, ray);
}
```

Figure 4.4: Overview of LightShop. The user passes two inputs to the system. The first is a series of function calls that define a scene. The second is a ray-shading program denoting how a pixel should be colored, given the scene. The function calls are passed to the modeler which creates an internal representation of the scene. The scene is outputted to LightShop's renderer, which takes the user-defined ray-shading program and executes it per pixel of the output image. During computation, the ray-shading program accesses the scene. When the renderer has executed for every output pixel location, the output image is constructed and outputted.

4.5 The LightShop Implementation

Recall that LightShop is composed of three parts: the modeling interface, the ray-shading language, and the renderer. The modeling interface is implemented in C++; the ray-shading language and the renderer leverage the OpenGL programmable rendering pipeline. The goal of the system is to manipulate and render light fields. First, we describe our light field representation.

4.5.1 Light Field Representation

All light fields are represented by a set of images, regardless of parameterization and acquisition method. These images have a RGBA color per pixel[2]. The images are concatenated together into a single file[3]. The file is then compressed using S3 texture compression [INH99], yielding a 4:1 compression ratio. This compressed datafile represents the light field. The compression rate is modest, and few artifacts are visible. However, Figure 4.5 illustrates a case where the compression artifacts are evident. Other compression techniques exist for light fields: vector-quantization [LH96], predictive image coding [MG00], wavelet-based compression [Pe01], as well as model-based compression [MRG03]. However, S3 texture compression is supported natively on the graphics hardware; decompression is quick and invisible to LightShop.

All acquired data is converted to this internal representation. During the modeling phase, when a light field is inserted into the scene, the appropriate file is loaded from disk and stored into memory. The modeling implementation is described next.

4.5.2 LightShop's Modeling Implementation

LightShop's modeling interface is implemented in C++ and utilizes the OpenGL graphics state to pass information to the ray-shading component. The programmer uses the interface to load light fields and define cameras. When a procedure is called to insert a light field, LightShop loads the compressed file from disk to graphics memory in the form of a 3D texture. Similarly, when a user calls a function to insert a camera, data structures are allocated in graphics memory as *uniform* variables. Uniform variables are variables that are accessible by the fragment shader and are fixed when rendering a primitive in OpenGL[4]. In this way, when the ray-shading

[2]Alpha is obtained using active illumination (Appendix B) or focusing (Appendix D).

[3]For the two-plane parameterization, the images are first rectified to a common plane before being concatenated together. The rectification is performed by taking a light field of a planar calibration target [VWJL04].

[4]For more information on programmable graphics hardware, the reader is referred to [Ros04].

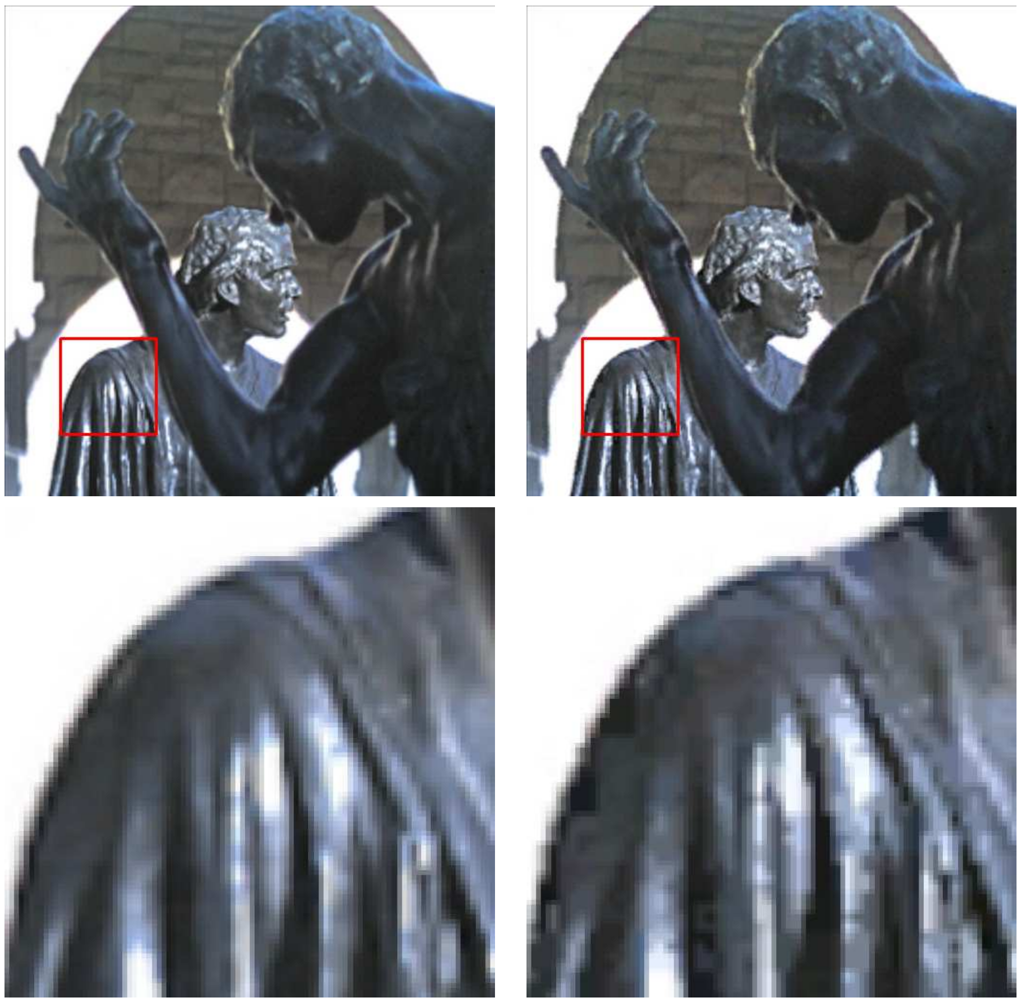

Figure 4.5: Comparing S3TC to uncompressed imagery. The top left is an image from an uncompressed version of the Burghers light field (see Appendix A). The top right is from a light field using S3TC compression. The bottom row of zoomed-in images show a comparison between the two images. Notice the triangular compression artifacts along the shoulder. The specular highlights are also corrupted by compression noise.

program executes (in the fragment shader), it has access to light field and camera data.

4.5.3 LightShop's Ray-shading Implementation

LightShop's ray-shading language is implemented using the OpenGL Shading Language (GLSL) [Ros04]. In other words, the ray-shading program is run through a preprocessor which performs variable name mangling, macro substitution and for-loop expansions to facilitate auxiliary state that LightShop needs in order to maintain a consistent graphics environment. The preprocessed ray-shading program is now valid GLSL code and is compiled by the graphics driver and linked into the rendering program for execution. The details are of the implementation are discussed in Appendix C.

Using GLSL is advantageous because it is designed for real-time rendering. This enables LightShop to be used as an interactive editing tool or as a library for games. Sampling from light fields is fast because GLSL takes advantage of texture memory coherence. Additionally, bilinear interpolation from one slice is computationally free so quadrilinear interpolation takes 4 computations as opposed to 16. A second advantage is that rendering an output image is taken care of by OpenGL. That is, the converted ray-shading program (e.g. fragment shader) is automatically executed for every output pixel and stored in the frame buffer. In fact, the LightShop's renderer implementation is exactly OpenGL's rendering pipeline.

Given this implementation, we now show results of using LightShop in digital photography and interactive games.

4.6 Results Using LightShop

The following results show applications of LightShop to digital photography and interactive games. All light fields and their properties are enumerated in Appendix A. Animation results are found on the website at
`http://graphics.stanford.edu/papers/bchen_thesis`.

4.6.1 Digital Photography

In this first demonstration, LightShop is used in two digital photography applications: 1) composing multiple light fields, similar to Photoshop for images, and 2) performing novel post-focusing for sports photography.

Composing Scenes

LightShop can be used as a compositing tool for light fields, the 4D analogy to image compositing with Adobe Photoshop. As a demonstration, LightShop is used to composite light fields of several actors into a light field of a wedding couple. Figure 4.6 shows one image from this wedding light field. This light field was captured using a hand-held light field camera [NLB+05].

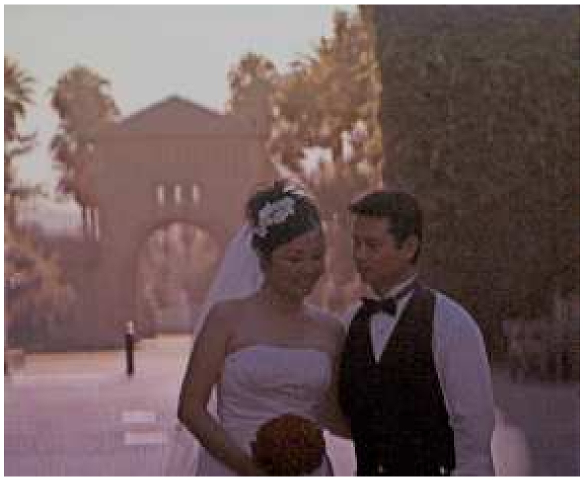

Figure 4.6: An image from a light field of a wedding couple.

Figure 4.7 shows images from three light fields of three actors. We will composite these actors into the wedding light field. The actors are captured using the camera array. Each actor is standing in front of a green screen to facilitate matte extraction [SB96]. Additionally, we acquire a light field of each actor under two lighting conditions: left light on and right light on. In order to acquire these multiple light fields, the actor must stand still for about 10 seconds. The purpose of acquiring light fields under different illumination is to enable coarse relighting. LightShop can simulate coarse relighting by taking linear combinations of the differently lit light fields. A sample ray-shading program that relights using two light fields is shown in Figure 4.8. Figure 4.9 shows the result of virtually relighting an actor by varying the linear combination weights. These light fields are listed as “mug shots” in Table A.1.

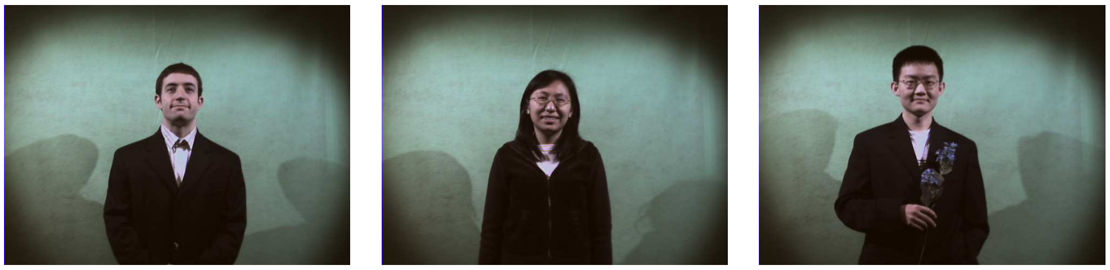

Figure 4.7: Images from three light fields of three individuals in front of a green screen, with two lights on.

```
LtColor main(LtVec2 loc) {
   LtRay ray = LiGetRay(0, loc, LtVec2(0,0))
   LtColor left = LiSampleLF(0, ray)
   LtColor right = LiSampleLF(1, ray)
   LtColor out = 0.25 * left + 0.75 * right;
   out.a = 1;
   return out;
}
```

Figure 4.8: Sample ray-shading code for relighting. Two light fields, “left” and “right” are sampled. The light fields correspond to left and right illumination, respectively.

In Figure 4.10a, the actors are relit to approximate the surrounding illumination and composited into the wedding scene. In Figure 4.10b, a deformation is inserted after relighting and before compositing into the scene. The rightmost actor’s pose has changed. Figure 4.11 shows the associated ray-shading program. Images such as Figure 4.10b are nearly impossible to create using conventional 2D editing tools. The pixels that form this image are selected from more than 436 images. In addition, since we are manipulating light fields multiple views can be rendered, each exhibiting the proper parallax. The images are rendered at 40 FPS.

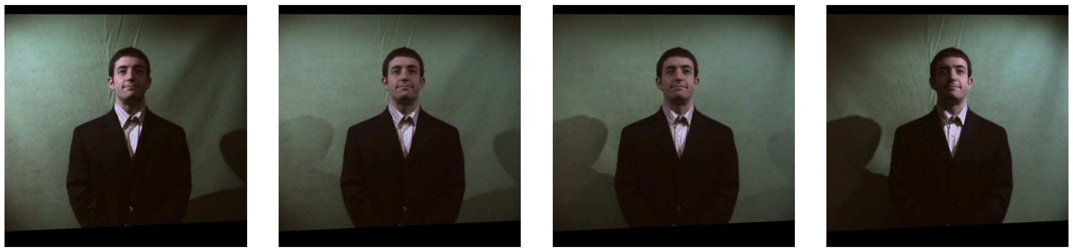

Figure 4.9: Virtually relighting an individual by taking linear combinations of colors of rays sampled from two light fields. The left- and right-most images are from the original light fields, lit from the left and right, respectively. The second image is sampled from a light field that takes 0.66 of the left light field and 0.33 of the right one. The third image uses the ratios 0.33 and 0.66 for the left and right light fields, respectively. Because the illumination is at only two positions, simulating a smoothly moving light source by blending will cause the shadows to incorrectly hop around.

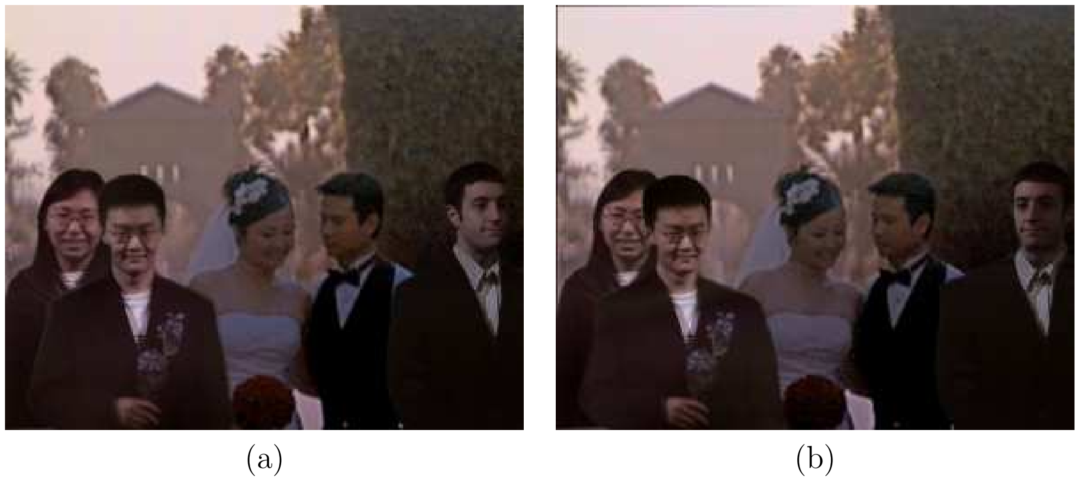

Figure 4.10: (a) An image from the composite light field. To approximate the illumination conditions in the wedding light field, we take linear combinations of the light fields of a given individual under different lighting conditions. The illumination does not match well because the lighting conditions were too sparse. (b) An image from the composite light field where we have turned a couple individuals' heads.

Manipulating Focus

The next demonstration uses LightShop as a post-focusing tool. However, unlike conventional focusing (see Section 4.3), which has a single plane of focus, LightShop

```
LtColor main(LtVec2 loc) {
   LtRay ray = LiGetRay(0, loc, LtVec2(0,0))
   // deform light fields
   ...
   // relight light fields
   ...
   // composite light fields together
   LtColor out = LiOver(woman, wedding);
   out = LiOver(right_man, out);
   out = LiOver(left_man, out);
   return out;
}
```

Figure 4.11: Ray-shading code for compositing the wedding scene.

allows a user to create an image with multiple planes of focus. This feature is useful in sports photography, where areas of interest may occur at multiple depths. A sports photographer would then want to focus only on these depths. For example, Figure 4.12 shows one image from a light field captured of several Stanford swimmers. We will show how to use LightShop to create an image where different swimmers are in focus.

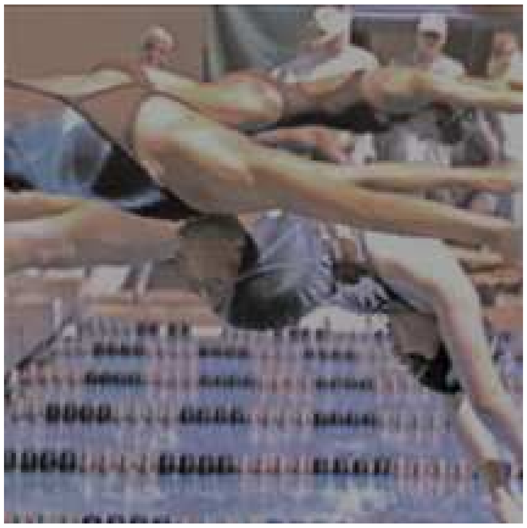

Figure 4.12: One image from the swimmers light field. Notice that are multiple planes of interest, corresponding to each swimmer.

The key idea is to combine the focusing and compositing operator using LightShop. We focus on different depths of the light field and composite these focused images together. In order to independently blur different depths of the light field, we segment it into layers. Recall from Section 3.6 that a layer is a subset of the original light field. In this case, instead of using projectors for light field segmentation, we use focus. Appendix D describes this focus-based segmentation technique in more detail. Treated as a black box, the algorithm takes a light field as input, and outputs separate layers (e.g. light fields).

Once the light field has been segmented into layers, a separate "focused image" can be computed from each layer. Each layer's sharpness is specified by its own camera and focal depth. In other words, if the light field is segmented into 3 layers, the user defines 3 cameras in the scene, one for each layer. The focal properties of each camera determine how light in the layer is integrated for a single pixel. Figure 4.13 illustrates how the integration occurs for a single pixel, through multiple layers.

One important aspect of this focusing process is the ordering in which compositing rays and focusing (e.g. integration) occurs. If one were to integrate rays from each layer of the light field and composite afterwards, this would produce an incorrect result. The physically correct result is to first composite individual rays (i.e. the black ray segments in Figure 4.13), then integrate the composited rays together. In addition, since each layer is a light field (and not an image), the refraction of the rays enables defocusing to see through occluders and around corners. This is impossible to perform correctly if the layers are only 2D images. Figure 4.14 shows the ray-shading program that accomplishes this compositing and focusing result.

In summary, in order to create a multi-focal plane image of the Stanford swimmers, first segment the light field into layers, one for each swimmer. Appendix D describes how the layers can be extracted from the swimmers light field. Second, insert each layer into the scene. For each layer, insert a lens camera. The cameras have the same attributes (i.e. image plane, lens aperture, lens position, etc.) except for the focal distance[5]. The focal distance controls the amount of blurring for that layer.

[5]If the four cameras had different poses and had pinhole apertures, one could also use LightShop to construct multi-perspective images like cross-slit images, panoramas, or general linear cameras [YM04].

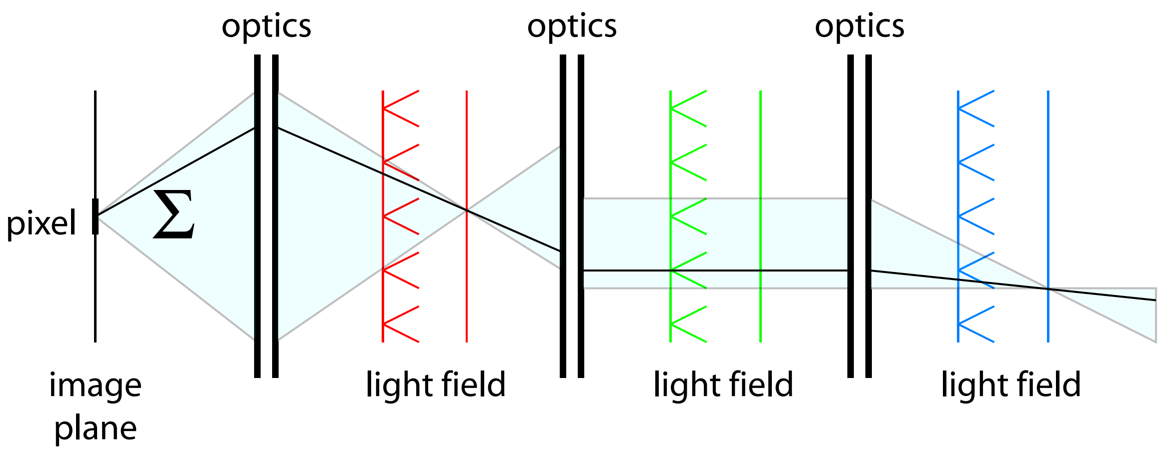

Figure 4.13: Illustration of how light is integrated for a single image pixel, over multiple layers. For a single pixel, light is integrated over different regions in each layer. The regions are shown as light-blue frusta. Specifying different cameras acts as optics to manipulate these frusta. Notice that these frusta need not be coincident at the optics interface, as the interface between the red and green light field shows. If we assume that the objects represented by these layers lie on the ST-plane in the two-plane parameterization, then the objects in the red and blue layer will be in focus, while the object within green light field will be blurred. This is because the radiant emittance of one point in the red and blue light fields is integrated as the irradiance at a single pixel (e.g. focused). The black line shows one ray as it travels through the deformed frusta.

Then execute the ray-shading program illustrated in Figure 4.14. This code correctly refracts, composites and integrates the rays to form the multi-focal plane image.

Figure 4.15a shows a conventional image with a single plane of focus. In Figure 4.15b the photographer has focused on the front and back swimmers, but left the middle one blurred. Alternatively, the photographer may want to focus on the middle, and back swimmers, but create a sharp focus transition to the front swimmer, as shown in Figure 4.15c.

4.6.2 Integrating Light Fields into Games

In the final application, LightShop is demonstrated as a tool for integrating light fields into interactive games. We successfully integrate a light field of a toy space-ship into a modern OpenGL space-flight simulator. In addition, we show how light fields can

```
LtColor main(LtVec2 currentPixel) {
   LtColor finalColor = LtVec4(0,0,0,0);
   LtColor sum = LtVec4(0,0,0,0);

   // iterate over the lens aperture
   for(float x=0.0;x<1.0;x+=1.0/16) {
      for(float y=0.0;y<1.0;y+=1.0/16) {
         LtColor composite_sample = LtVec4(0,0,0,0);

         // iterate over the 3 layers in the scene
         for(float i = 0; i < 3; i++) {
            LiVec2 lensSample = LtVec2(x,y);

            // form a ray from camera i's optical properties
            LtRay ray = LiGetRay(i, currentPixel, lensSample);

            // sample from light field i
            LtVec4 sample = LiSampleLF(i, ray);

            // composite the ray colors
            composite_sample = LiOver(sample, composite_sample);
         }

         // sum over the aperture
         sum += composite_sample;
      }
   }
   return finalColor;
}
```

Figure 4.14: Ray-shading code for multi-plane focusing. The first 2 for-loops iterate over the lens aperture. The inner for-loop iterates over the light field field layers. For each layer, the ray is transformed according to the optics of the associated camera. Then the appropriate light field is sampled, using this ray. The returned color value is composited with colors along previous ray segments. The final composited color is then summed with other rays in the aperture to produce the focusing effect.

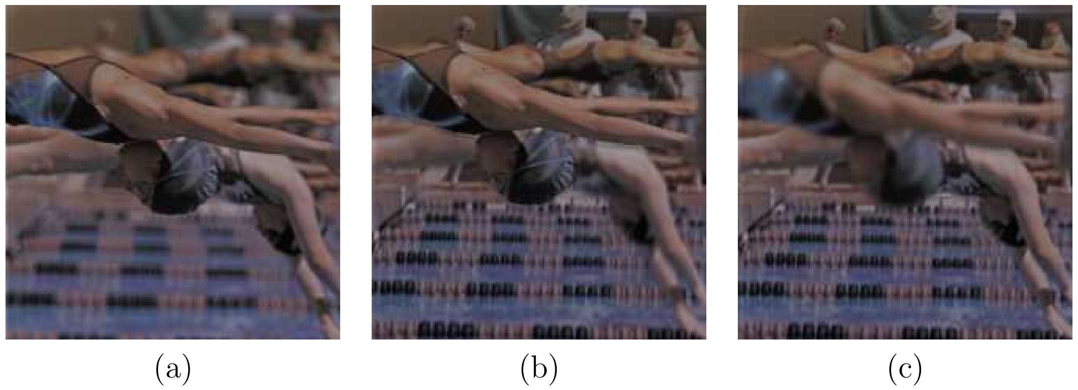

Figure 4.15: (a) Conventional focusing in a light field. The front swimmer lies on the focal plane. (b) A multi-focal plane image where the front and back swimmers are brought into focus for emphasis. The middle swimmer and the crowd are defocused. (c) The front swimmer is defocused, but a large depth of field exists over the depths of the middle and back swimmer. There is a sharp transition in focus between the front and mid swimmers, but the photograph still has a pleasing result.

be hacked, using LightShop, for producing refraction and shadowing effects. These effects are described in Appendix E.

Light Fields in Vega Strike

Because LightShop is implemented in OpenGL and GLSL, this makes it easy to integrate it into interactive games. Game programmers that utilize the programmable vertex and fragment shaders can use LightShop's functions to access light fields like any other texture. The vertex shader needs only to define a quad spanning the projected area of the light field and the fragment shader executes the LightShop's ray-shading program to color the quad. From the game programmer's point of view, LightShop provides an interface for a "3D billboard" [MBGN98, AMH02] [6].

To demonstrate LightShop's use in interactive games, it is integrated into *Vega Strike*, an open-source OpenGL-based space-ship game [Hor06]. Vega Strike is a popular spaceflight simulator with 1.3 million downloads since its inception in 2001. It is a medium-sized open source project with approximately 100,000 lines of code. The

[6]The billboard appears 3D since a 3D object appears to be inside it, but in fact the light field representation is in general 4D.

game is well supported by the community, with multiple user-contributed modules including Privateer, and Wing Commander. Figures 4.16 shows some screenshots of the game.

The light field that we wish to insert into Vega Strike represents a toy ship. The acquired light field is uniformly sampled [CLF98] around the toy ship. Figure 4.17 shows a view from this light field.

Figure 4.16: Images from Vega Strike.

In VegaStrike, each model has multiple meshes defining its geometry. Each mesh in turn has one associated 2D texture map. In the game loop, when a mesh is scheduled to be drawn at a particular location, the appropriate `MODELWVIEW` matrix is loaded into OpenGL and the associated texture is made active. The mesh vertices are then passed to OpenGL, along with the associated texture coordinates.

To integrate LightShop into VegaStrike, the game programmer defines a Texture4D sub-class that references the light field data. The mesh for a light field object is simply a quadrilateral spanning [-1, 1] x [-1, 1] x [-1, -1] in x, y, and z in normalized device coordinates. The vertex shader takes this quadrilateral and maps it to the correct screen coordinates, depending on the location of the view camera and the light field. The game programmer writes a simple ray-shading program (e.g. fragment program) that samples from the light field. This fragment shader is activated when the light field is ready to be drawn. Figure 4.18, shows the light fields of the toy ships integrated into the game.

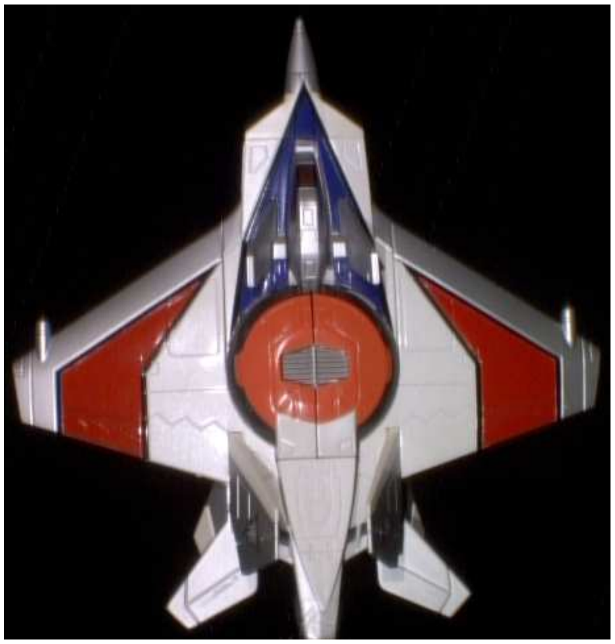

Figure 4.17: Image from a light field of a toy space ship.

The significance of this application is that through the use of LightShop, light fields can be integrated into the standard graphics pipeline. This means that one can take real-world objects and place them into games or other graphics applications. Another possibility is to use light fields from pre-rendered images of complex scenes. This effectively caches the images of a traditional 3D object, and LightShop is used to interactively render it. This level of facility in integrating light fields into interactive applications is unprecedented. Hopefully it will encourage the use of such image-based models in interactive games.

4.7 Summary

In summary, the second contribution of this thesis is LightShop, a system for general manipulation and rendering of light fields. It borrows from traditional modeling packages by using the *model, manipulate, render* conceptual model. The modeling component is represented by an API. Manipulating and rendering a light field is represented by manipulating view-rays as they emit from the virtual viewpoint. These

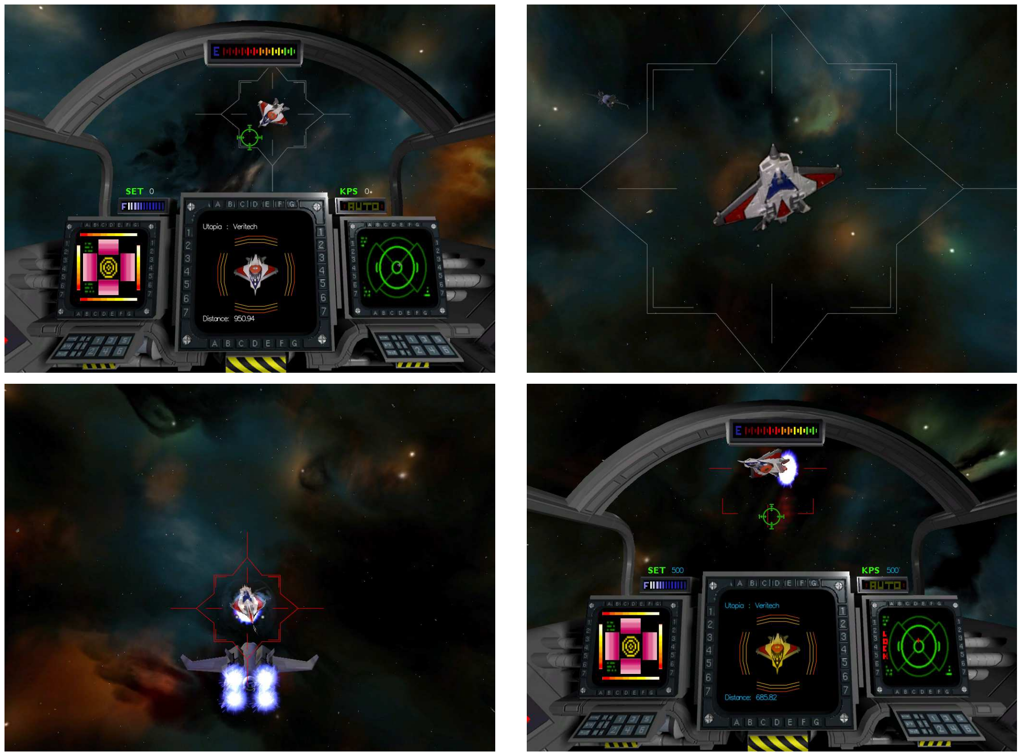

Figure 4.18: In-game screen captures of the light fields of the toy ships in Vega Strike. The game runs in real-time (30+ fps). In the top-left, the protagonist approaches an unidentified space-craft. Notice that the light field is integrated seamlessly into the surrounded 3D graphics. The top-right shows a closer view of the ship. Detailed geometry can be seen. Bottom-left shows an out-of-cockpit view where the protagonist has attacked the ship. The ship's shields light up around the light field. In the bottom-right the ship light field makes a pass by the cockpit. A particle system for the thrusters has been rendered with the light field.

manipulations are encapsulated in a ray-shading language that allows for novel definitions of operations and combining existing ones.

The system satisfies our initial design goals for building a light field manipulation system. The conceptual model of manipulating view-rays instead of light fields allows the user to abstract away the actual light field representation. The use of a ray-shading language enables for easily extending the system to new operations and combinations of operations. Finally, by mapping the ray-shading language to a fragment shader, the system is amenable to graphics hardware.

We show several compelling examples using LightShop in digital photography and interactive games. These demonstrations illustrate that LightShop can not only operate on a variety of light fields, but allows a user to creatively combine and manipulate them. It is our hope that LightShop can serve as a core component in any light field manipulation application. This thesis illustrates one step towards that direction.

Chapter 5

Conclusions and Future Work

This thesis presents two contributions towards light field manipulation. The first is an interactive technique for deforming a light field. We discuss the two key challenges to deformation: specifying a ray-transformation and maintaining consistent illumination. Our solutions are a modified free-form deformation and coaxial light fields. The second is a system, LightShop, that enables for general manipulation of a light field. We design the system to abstract away the light field parameterization, be easily extendable, and be amenable to graphics hardware. The system is designed having three-stages: model, manipulate, and render. We have demonstrated that deformations and LightShop have applications in photo-realistic animation, digital photography, and interactive games.

Above are just a few domains that could benefit from a system like LightShop. Other potential domains include opthalmology, surgical simulation, or rapid prototyping of scenes. In opthalmology, one important problem is the synthesis of scenes, as seen through human optical systems, for the analysis of corneal aberrations or diseases [Bar04]. LightShop can use Shack-Hartmann wavefront data to refract view-rays, and sample from light fields of real scenes. The images rendered using LightShop would contain optical aberrations consistent with human eye characteristics and also be rendered from imagery representing real scenes. Because LightShop allows a user to arbitrarily manipulate rays, there is a potential for designing optical systems to correct for such aberrations. In surgical simulation, LightShop can be used to simulate dynamic organ behavior by the use of light field deformation. The visual feedback of a realistic deforming organ may be useful for training purposes. In rapid-prototyping of scenes, film directors or game designers may want to quickly compose a photo-realistic scene, for pre-visualization purposes. Fundamentally, LightShop offers a simple mechanism for composing realistic scenes.

LightShop could be extended in a number of ways. First, one can find more uses for LightShop itself. For example, light field segmentation (either using active illumination or focus) could be better incorporated into the editing pipeline. Another novel use of LightShop is in combining multi-perspective imaging (i.e. panoramas) with focusing. One could produce panoramas that contain spatially-varying focus properties. This might be useful in blurring unwanted objects in street panoramas. A third use of LightShop is to modify a 3D modeling tool, like 3D Studio Max, to output function calls to drive LightShop. In this sense, LightShop acts as a light field renderer plugin for the modeling tool.

Other improvements extend LightShop's architecture. For example, in addition to RGBA per ray, one could incorporate depth, normal, or time as additional data. This would allow for more creative operations like painting, or new datasets like time-varying light fields. These extensions are incremental steps toward the ultimate editing tool: manipulation of reflectance fields. Since reflectance fields represent the exitant light field as function of incident lighting (it is 8 dimensional), it is a more comprehensive representation than a light field. In time, as data-acquisition becomes easier and compression techniques improve, one can imagine extending LightShop to ReflectShop, a general editing tool for reflectance fields. ReflectShop would enable not only changes in the shape of captured objects, but also changes in incident illumination. A scene composited in ReflectShop would encapsulate correct global illumination, i.e. shadows, inter-reflection, scattering, etc. This has the potential to allow directors to completely synthesize realistic actors, immerse gamers in a completely real environment, or enable doctors to train on photo-realistic simulation imagery. Hopefully, such editing tools will increase the use of image-based models in computer graphics.

Appendix A

Table of Light Fields and their Sizes

LF	Resolution	Width	Height	Size	Acquisition	Fig.
Buddha	128 x 128 x 32 x 32	4 RU	4 RU	16	ray-tracer	C.7
Burghers	256 x 256 x 16 x 16	37	37	10	LF camera	4.5
fish	320 x 240 x 180	360°	0	13	ray-tracer	3.20
flower	256 x 256 x 16 x 16	550	80	16	gantry	C.7
giraffe	256 x 256 x 16 x 16	550	80	16	gantry	E.2
glass ball (x2)	256 x 256 x 32 x 32	2 RU	2 RU	128	ray-tracer	E.1
highlight	256 x 256 x 32 x 32	2 RU	2 RU	64	ray-tracer	C.8
swimmers	292 x 292 x 16 x 16	37	37	10	LF camera	4.12
ship	256 x 256 x 31 x 61	360°	124°	130	sph. gantry	4.17
teddy bear	240 x 320 x 180	360°	0	13	sph. gantry	3.21
toy warrior	480 x 640 x 360	360°	0	52	turntable	3.1
twisted heads	512 x 512 x 12 x 5	1770	600	15	camera array	C.5
mug shots	512 x 512 x 12 x 5	1770	600	15	camera array	4.7
wedding	292 x 292 x 16 x 16	37	37	10	LF camera	4.6

Table A.1: Light fields, their sizes (in MB), and acquisition methods. The **Width** and **Height** denote maximum distance between cameras horizontally and vertically, in mm. When the light field uses a sphere-plane parameterization, "sph. gantry," width and height are specified in terms of degrees for θ and ϕ. "RU" stands for rendering units, which is in the coordinate system of the renderer. The "turntable" acquisition is acquired by placing the toy on a mechanical turntable and taking successive snapshots while rotating the table.

Appendix B

Projector-based Light Field Segmentation

In this appendix, we describe a technique to segment a light field into layers, using projector illumination. The definition of a layer is described in Section 3.6. To motivate the use of projectors to segment a light field into layers, consider the teddy bear shown in Figure 3.18. Suppose, before capturing a coaxial light field, we paint the bear. We paint his head red, his body blue, his left arm green, etc. Now, when capturing a light field of the painted teddy bear, the color of each pixel in this dataset denotes the layer in which that pixel belongs. For example, all reddish pixels in the light field correspond to rays which are incident to the teddy bear's head. This is one solution for segmenting a light field into layers: paint the individual regions then acquired this *colored light field*. Unfortunately, painting the object destroys the geometry and the appearance of the object. In other words, if we first paint the object and acquire a colored light field, then we cannot capture the object with its original appearance. If we first acquire a coaxial light field and then a colored light field, then the geometry will change between acquisitions from applying the paint.

For this reason, we use projectors to effectively "paint" the object. In other words, the image that is loaded into the projectors will color different regions of the object. This solution preserves the object's geometry. Afterwards, the projectors can be turned off, and a coaxial light field can be captured for light field deformation. The coaxial light field is then segmented into layers (e.g. light fields) by using the color information from the colored light field. For example, to segment the head layer from the coaxial light field, we examine all red-colored pixels in the colored light field and use their locations to copy from the coaxial light field to the head layer.

Figure B.1 illustrates the acquisition setup using the Stanford Spherical Gantry [Lev04b]. Two projectors throw colors onto the teddy bear. One projector illuminates the teddy bear's front, and the other his back. When capturing a light field with this projector illumination, which we call a colored light field, the color of each pixel in the light field denotes the layer.

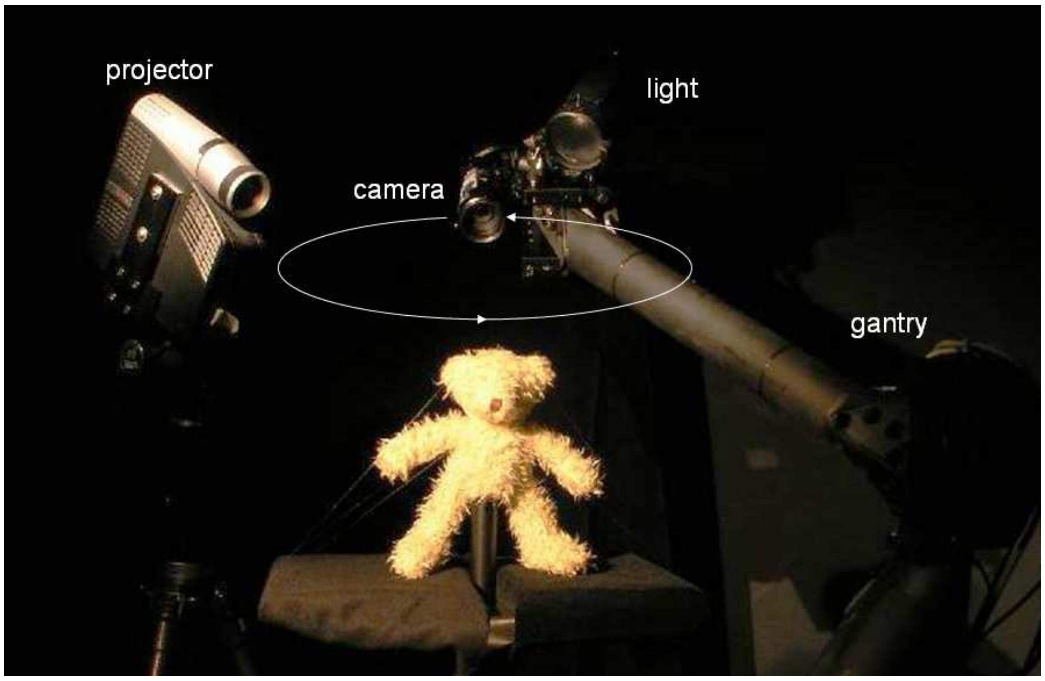

Figure B.1: The acquisition setup for capturing light fields. The camera is attached to the end effector of the Stanford spherical gantry and rotates in a circle around the object. Two projectors (one shown above) are placed above and outside of the gantry. The two projectors display a fixed pattern onto the front and back parts of the teddy bear. With the fixed pattern illuminated, the camera then proceeds to capture a colored light field of the object. After acquiring this colored light field, the projectors are turned off and the secondary light attached to the camera is turned on. With this new illumination, a separate, coaxial light field is captured. The colors in the colored light field are used to segment out layers from the coaxial light field.

So what images are displayed on the projectors while the camera captures images? In the case of the teddy bear, the images are color masks that coarsely segment the bear into regions. Note the difference between a region and a layer. A region is a physical region on the teddy bear (i.e. the head region). The corresponding layer is a light field in which all rays are in incident to that region. Figure B.2 shows an example mask for the front of the teddy bear. A similar mask is created for the projector aimed at the back of the teddy bear. The images are created by hand in an interactive process. A person sits at a computer that has two video outputs; the video outputs are exact clones of each other. One output is shown on a standard CRT monitor. The other output is displayed through a projector, aimed at the teddy bear. Using a drawing program displayed on the CRT monitor, the user paints colored regions which are displayed live onto the teddy bear, through the projector. Drawing the images that the projector emits takes less than 10 minutes because the images need only to segment the bear into layers, not to precisely illuminate fine geometry like its fur. After painting these colored regions (which are projected onto the teddy bear), a colored light field is captured under this new illumination. The middle image in Figure B.3 is an image from the colored light field captured with this projector illumination.

Notice in this image that within one color region there are still changes in color due to varying albedo or non-uniform illumination brightness. To solve this problem, we capture an additional light field, where the projectors are emitting a floodlit white pattern. The images from this floodlit light field are used to normalize the data from the colored light field, thus reducing non-uniformity artifacts. Normalization of each image of the colored light field is computed by the following equation:

$$B' = 256 * B/W \tag{B.1}$$

where W is a floodlit image (8 bits per channel), B is a colored image and B' is the normalized color image. Figure B.3 shows image B' for one camera's view of the teddy bear light field. Notice that the union of all colored regions in the normalized image is also a binary mask for an object's opacity. In other words, we may use the colored regions as an alpha mask for each image. In fact this mask is directly stored in the alpha channel for each layer.

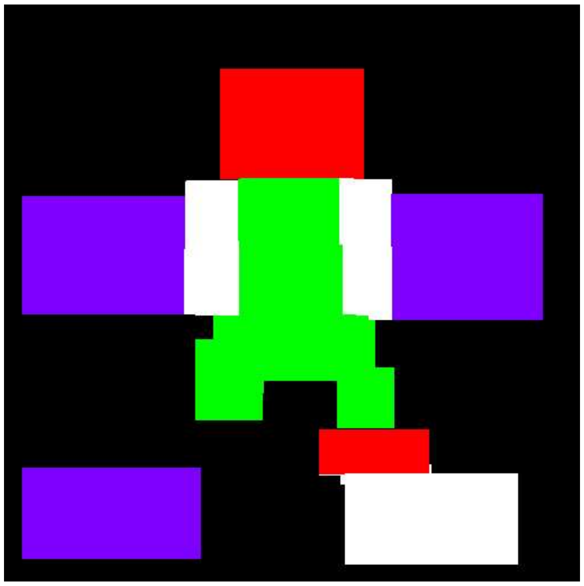

Figure B.2: A hand-drawn color mask is displayed on the front-facing projector to physically segment the teddy bear into colored regions. The user draws a coarse color mask. With this illumination pattern (and a corresponding back-facing pattern) turned on, a colored light field is captured.This light field is used to segment out layers from the coaxial light field.

In summary, to segment the teddy bear light field, we use projectors to effectively paint the bear when we acquire the data. This colored light field has the property that the colors of each pixel denote the layer to which that pixel belongs. Then, a separate coaxial light field is acquired. The colors in the colored light field are used to segment the coaxial light field into layers. Each layer has alpha per pixel, which describes an object's opacity. The output of this algorithm is a set of layers (e.g. light fields), each with alpha.

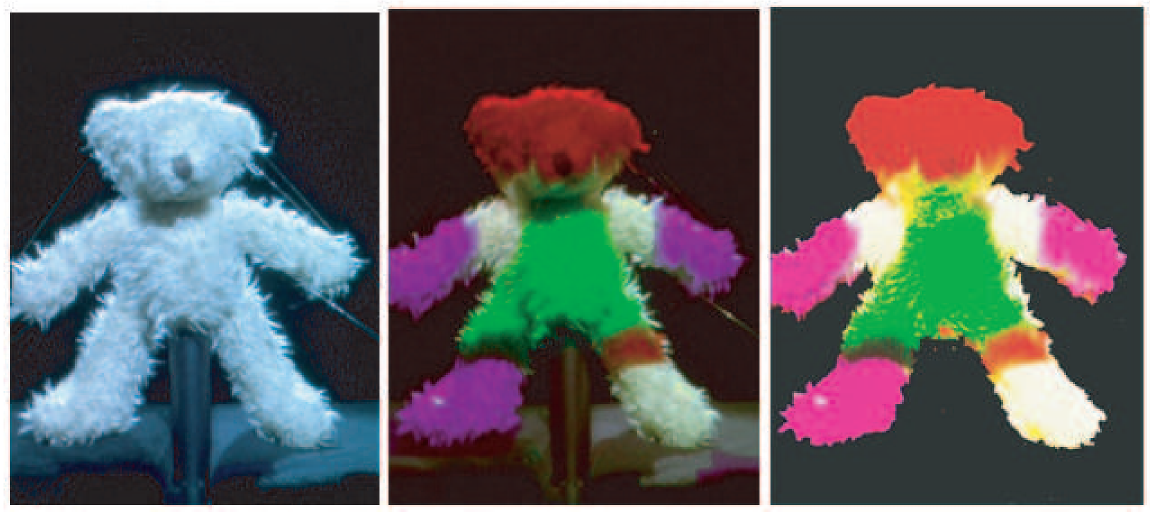

Figure B.3: Segmenting a teddy bear light field by using projector illumination. The left image is the bear under floodlit illumination. The middle image shows the same bear when projected with color masks. The colors designate layers for the head, torso, arms, legs and joints. Each color denotes the layer to which that pixel belongs. On the right is the same view after normalization. Notice that the union of the colored regions form an alpha mask for this image. We store this information in the alpha channel. These illumination conditions are captured for each camera position in the light field.

Appendix C

The LightShop API

This appendix describes the LightShop API and implementation details. The overall design and motivation for the system are described in Chapter 4.

C.1 Overview of the API

Recall that LightShop consists of a modeling interface, a ray-shading language and a rendering system. The modeling interface exports a set of functions that are used to define a scene containing light fields. The ray-shading language is used to describe how that scene should be rendered to a 2D image, i.e. how a view-ray is shaded, given multiple light fields in the scene. LightShop's renderer then executes the user-defined ray-shading program at each pixel of the output image. Each execution of the program shades a single pixel until the entire image is rendered. Figure 4.4 illustrates an overview of LightShop.

To use the interface, a programmer makes a series of procedure calls to setup a scene with light fields. These include positioning light fields and defining viewing cameras. To describe how an image is rendered from this scene, the programmer writes a ray-shading program that describes how a view ray from a selected camera is shaded as it interacts with the light fields. Figures C.1 and C.2 show a program containing procedure calls to setup a scene, and a ray-shading program that dictates how an image should be rendered.

First we describe LightShop's modeling interface. Then, we describe the ray-shading language that allows the programmer to specify how a 2D image should be rendered from the light fields in the scene.

C.2 LightShop's Modeling Interface

In LightShop, a scene is modeled with two primitive types: cameras with a single lens[1] and light fields. The programmer calls specific functions that insert these primitives into an internal representation of the scene. Each primitive stores its own related information: focal distance, sampling, etc. This information is called *LightShop attributes* or *attributes* for short. Table C.1 shows the supported LightShop primitives, and their associated attributes.

In LightShop, a camera with a lens (henceforth called a "lens camera" or "camera") follows the simple lens model. Figure C.3 illustrates the model. It has an image plane, a lens plane, and a focal plane. Intuitively, light emitted from a point on the focal plane passes through an aperture in the lens plane and is focused onto a point on the image plane. More specifically, on the image plane is a rectangular region defining the digital sensor or film area. The camera attributes "lower left," "up," and "right" define both the image plane and the sensor area. The lens plane is parallel to the image plane. The lens aperture is a rectangular region lying on the lens plane. The attributes "lens center," "lens width," and "lens height," define the location of this lens aperture. The focal plane is parallel to the lens plane and image plane. Its location is defined by the "focal distance" attribute, which is the distance between the focal and lens plane. Since diffraction is not modeled, a pinhole camera can be created by setting the "lens width" and "lens height" attributes to 0. As we will see in Section C.3.3, the `LiGetRay` ray-shading function makes use of the camera attributes to form a ray, given the 2D locations of the image pixel and a sample point on the lens.

[1]Although LightShop could include a more complex optical system, in practice a single lens model suffices for many applications. When more complexity is necessary, LightShop's ray-shading language allows for arbitrary ray refraction (see Section C.3).

```
// Initialize LightShop
LiBegin();

// insert the camera
LtInt camera0 = LiCamera();

// set camera0's attributes
LtDir lowerLeft= {-1, -1, -1};
LtDir up = {0, 2, 0};
LtDir right = {2, 0, 0};
LiDir lensCenter = {1,1,1};
LiFloat focalDistance = 10.0;
LiInt xRes = 512;
LiInt yRes = 512;

LiAttributeCam(camera0, ``x res'', &xRes);
LiAttributeCam(camera0, ``y res'', &yRes);
LiAttributeCam(camera0, ``lower left'', lowerLeft);
LiAttributeCam(camera0, ``up'', up);
LiAttributeCam(camera0, ``right'', right);
LiAttributeCam(camera0, ``lens center'', lensCenter);
LiAttributeCam(camera0, ``focal distance'', focalDistance);

// insert the light field
LtColor clear = {0, 0, 0, 0};
LtMatrix translate = {1, 0, 0, 0,   0, 1, 0, 0,  0, 0, 1, 0, 0, 0, -10, 1};
LtInt lightField1 = LiLightField(``lightfield.tlf'');
LiAttributeLF(lightField1, ``sampling'', ``quadralinear'');
LiAttributeLF(lightField1, ``wrapping'', clear);
LiAttributeLF(lightField1, ``transform'', translate);

// tell LightShop to clean up
LiEnd();
```

Figure C.1: A simple LightShop program that models a scene containing a lens camera and a light field.

```
LtColor main(LtVec2 currentPixel)
{
  LtColor col = LtVec4(0,0,0,0);

  // convert the current pixel location to a ray based on camera 0
  LtRay=LiGetRay(0, currentPixel, LtVec2(0, 0));\\

  // use the ray to sample from light field 0
  col = LiSampleLF(0, ray);

  // return the color sampled from the light field
  return col;
}
```

Figure C.2: A simple ray-shading program that takes the scene modeled in Figure C.1 and returns the color of a single pixel of the display image. LightShop's renderer executes the program over all pixels to compute a final image.

For light fields, we approximate the continuous 4D function with discrete samples that can be thought of as a 4D texture. Hence, light fields in LightShop have similar, texture-like attributes: sampling method (i.e. nearest-neighbor, or quadralinear, and wrapping behavior (i.e. repeat or clamp to a value). Nearest-neighbor sampling simply extracts the color of the ray "nearest" to the input ray. Quadralinear sampling [LH96] is the 4D equivalent to bilinear interpolation in 2D.

The third light field attribute, "transform", is an optional attribute that allows the programmer to pass implementation-specific parameters to LightShop. For example, in the implementation described in Section 4.5, LightShop supports the two-plane parameterization of light fields. The "transform" attribute is used to pass a 4x4 matrix that is applied to the vectors describing the UV- and ST-plane of the light field. This allows a programmer to position a light slab by providing an appropriate transform matrix. Other implementations may use this attribute for other applications.

Notice that LightShop does not specify a particular light field parameterization; the attributes are invariant to this and the implementor may support various types (i.e. UVST 2-plane, sphere-plane, circular, etc.) at her discretion.

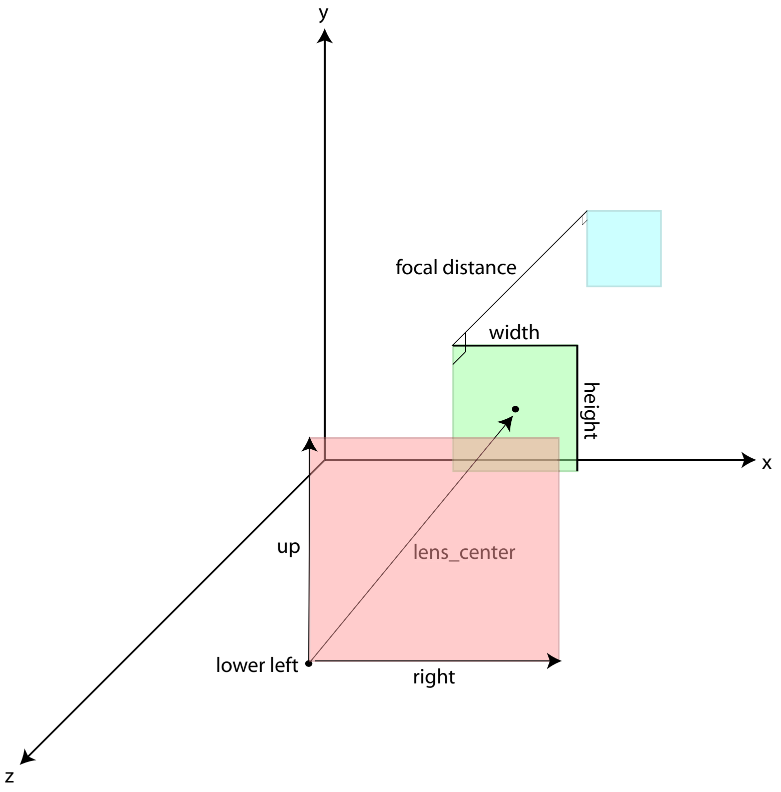

Figure C.3: The lens model used in LightShop. The pink, green and blue rectangles are the sensor area, lens aperture and focal plane, respectively. These camera attributes are used by the `LiGetRay` ray-shading function, described in Section C.3.3.

C.2.1 Graphics Environment (Scene)

Given the previously defined primitives, a programmer creates a scene by calling specific functions that modify an internal representation of the world. This internal representation is called the *graphics environment* or *scene*, which is invisible to the programmer and completely contained within LightShop. The graphics environment is simply a set of cameras and a set of light fields; it is shared between the modeling interface and the ray-shading language.

C.2.2 Modeling Functions Available to the Programmer

The goal of the LightShop functions is to provide an interface between the programmer and the graphics environment. The functions use specific data types defined by LightShop for arguments and return values. We first define these data types, then describe the procedures that use them. The data types are presented using a C-like syntax as an explanatory medium. However, note that LightShop can also be implemented in other high-level languages like Java or Python.

The name of each data type is prefixed with `Lt` (**L**ightShop **t**ype). Procedures and variables are prefixed with `Li` (**L**ightShop **i**nterface).

Scalar Types

```
typedef long LtInt;
typedef float LtFloat;
typedef char* LtString;
typedef void LtVoid;
typedef void* LtPointer;
```

LightShop supports the usual data types found in C.

Vector Types

```
class LtVector3;
class LtVector4;
class LtMatrix3;
class LtMatrix4;

typedef LtVector3 LtPoint;
typedef LtVector3 LtDir;
typedef LtVector4 LtColor;
```

The `Vector[34]` types are generic vectors used for variables containing 3D points, normals, homogeneous coordinates, etc. For convenience, LightShop also defines specific types for points, colors, and directions. The matrix types store transformations that can be applied to `LtVector[34]`s. Matrix elements are specified in *column-major order*, similar to OpenGL [BSW+05].

Functions

These functions allow the implementation to initialize any LightShop state and to ensure that this state is cleared when LightShop is done. They must be the first and last procedure calls to LightShop.

```
LtVoid LiBegin();
LtVoid LiEnd();
```

The following procedures insert and modify attributes of each of the primitives: cameras or light fields. Note that the functions take in an integer identifying the particular instance. The identifier is returned when the programmer calls the appropriate function to insert the primitive. The attribute names used in the function arguments are specified in Table C.1.

```
LtInt LiCamera();
LiAttributeCam(LiInt cameraID, LtString attributeName,
              LtPointer value);

LtInt LiLightField(LtString filename);
LtVoid LiAttributeLF(LtInt lightFieldID,
                     LtString attributeName,
                     LtPointer value);
```

C.3 LightShop's Ray-shading Language

After using the modeling interface to define a scene containing light fields, the programmer writes a ray-shading program that precisely defines how this scene should be rendered to a 2D image. An image is created by associating a ray to each output pixel, and deciding on how to shade this "view-ray". As the view-ray travels through the scene, its color (RGBA) or direction may change due to interaction with light fields. This is similar to ray-tracing except that objects are represented by light fields. LightShop's ray-shading language allows the programmer to precisely define how this view ray is affected by the light fields.

The ray-shading language executes in a manner similar to the Pixel Stream Editor [Per85]. It takes as input the xy location of a pixel of the 2D image, executes the ray-shading program at this pixel, and outputs a RGBA color. At any one pixel, the program has access to the graphics environment (i.e. the light fields and the cameras). It uses this environment to first form a ray from the given pixel position and then to shade the color of this ray. The pixel color is set to the computed ray color. LightShop's renderer executes the same ray-shading program at each pixel location to progressively construct the final image.

First we describe the language's data types, then flow control, then high-level functions available to the programmer. We use GLSL [Ros04] as the explanatory medium for data types and procedures. It has a C-like syntax and we build functionality on top of it in our implementation in Section 4.5. However, note that the ray-shading language could be implemented in other languages like C++, HLSL, or Cg.

C.3.1 Data Types and Scope

```
typedef void  LtVoid;
typedef int   LtInt;
typedef float LtFloat;

typedef vec2  LtVec2;   // A general 2-vector
typedef vec3  LtVec3;   // A general 3-vector
typedef vec4  LtVec4;   // A general 4-vector
typedef mat4  LtMat4;   // A general 4x4 matrix of floats
typedef vec4  LtColor;  // A RGBA color value
typedef vec3  LtPoint;  // A XYZ 3D point
typedef vec3  LtDir;    // A direction vector
typedef vec4  LtPlane;  // A plane equation Ax+By+Cz+D=0

struct LtRay {
  LtVec4 pos;
  LtDir dir;
};
```

The ray-shading language supports the standard C data types. The LtRay type describes a ray in 3-space. It is used for sampling from a light field to obtain a color in that ray direction. A ray in LightShop is represented by a point on the ray (in homogeneous coordinates) and a direction. Although a ray can be described by four parameters, the point-direction representation facilitates ray intersection calculations. The scope of variables is the same as in C++, i.e. local scope within the enclosing block and global scope otherwise.

C.3.2 Flow Control

The program starts execution in the main function. The same main function executes for every output pixel of the image. It takes as input the current pixel location and outputs a RGBA color. It can also access the global graphics environment.

Aside from a few different token names, the LightShop ray-shading language uses the same grammar as GLSL [Ros04]. Looping is accomplished using the same syntax and keywords as those in C++: `for`, `while`, and `do ... while`. Looping allows a programmer to map the colors of multiple rays in different light fields to a single pixel color. One useful application is for focusing, where a single pixel color is computed by integrating over the colors of multiple rays (see Section 4.6.1). Branches also use the same syntax as in C++: `if` and `if ... else`. This allows the program to have per-pixel variability. Functions are defined and called in the same way as in C++. A return type is followed by the name of the function, followed by a parameter list. The language allows for function overloading.

C.3.3 Light Field Manipulation Functions

On top of this language, LightShop offers the standard math functions (`sin, asin, pow`, etc.) and several high-level functions specifically for manipulating light fields.

The ray-utility function, `LiGetRay`, takes as input a 2D pixel location, a 2D position on the lens aperture and a camera primitive. It uses the camera attributes, defined in Section C.2, to produce a ray. First, `LiGetRay` forms an intermediate ray based on the pixel location and sample position on the lens. This ray is then refracted through the lens and returned as output. The amount of refraction is based on the simple lens model; rays emitted from one point on the image plane converge to a point on the focal plane defined by Gaussian optics. Recall that the focal plane and other camera attributes are specified during the modeling process, described in Section C.2. The LightShop function is the following:

```
LtRay LiGetRay(LiInt cameraID, LtVec2 currentPixel,
               LtVec2 lensSample)
```

For example, in the simple ray-shading program shown in Figure C.2, `LiGetRay` returns the refracted ray that started from the current pixel location, entered the lens center and refracted out. Section 4.3 demonstrates how focusing can be accomplished by summing the colors of rays that enter multiple positions on the lens aperture.

Once a ray has been formed, it can be passed as input to several high-level functions. These functions form a basis for a wide variety of light field manipulation operations. Additionally, these functions can be called in combination, which allows arbitrarily complex light field manipulations.

The following are the LightShop functions: **4D sampling**, which samples a RGBA color from a light field; **compositing**, which combines two RGBA colors into a single one; and **warping**, which maps rays to rays.

4D Sampling

The sampling procedure takes as input a ray and a light field and returns the color in that ray direction. Because light fields in LightShop are represented in a sampled form, any given ray direction may not have a color in the light field. Hence, the procedure utilizes the `sampling` light field attribute to determine how it should return a color for any given ray. The sampling procedure is most commonly used for novel view synthesis from light fields:

```
LtColor LiSampleLF(LtInt lightfieldID, LtRay ray)
```

For the two-plane parameterization, sampling the color along a ray direction is performed exactly in the same manner as described in Levoy and Hanrahan [LH96]. The color of a ray is a function of rays who have the nearest intersections (u, v, s, t) on the UV- and ST-plane. The `sampling` attribute determines whether to use nearest-neighbor or quadralinear interpolation.

The algorithm for sampling from sphere-plane light fields generalizes the technique used for rendering from concentric mosaics [SH99]. Assume that a view-ray r from a user-defined camera is sampling from a sphere-plane light field. The ray intersects the sphere and the plane defining the SLF. The farther intersection with the sphere is ignored. Recall, the plane is incident to the center of the sphere. Its normal is defined to be parallel to the vector from the camera center to the center of the sphere. In other words, the orientation of the plane is view-dependent. The sphere intersection locates nearest cameras. The plane intersection locates nearest pixels in those nearest cameras. Nearest-neighbor or quadralinear interpolation can be applied. Figure C.4 illustrates the sampling process. Ray r intersects the sphere at point m and the plane p at point x. m is used to select nearest cameras a and b. x is used to select nearest pixels a' and b'.

Compositing

Recall that a color sampled from a light field contains RGBA channels. RGB represent an approximation to the radiance along the ray direction in the light field. A, or alpha,

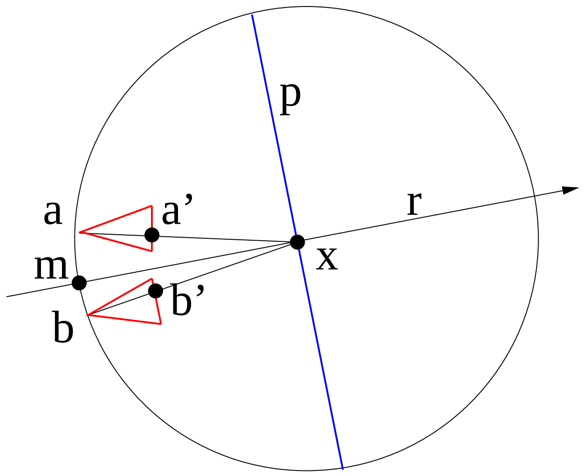

Figure C.4: Plan-view of rendering from a sphere-plane light field.

represents both opacity and coverage. Once a color has been sampled from a light field, it can be composited with samples from other light fields. Using the proper compositing operators and ordering allows a programmer to render an image of a scene of light fields.

The compositing operator allows for all twelve of Porter and Duff's [PD84] compositing operations. Similar to their formulation, LightShop assumes that the colors in the light field are premultiplied by the alpha channel. This is useful because compositing equations for RGB are the same as those for alpha.

The twelve compositing operations for two RGBA colors, A and B, can be expressed as a linear combination. More specifically, to compute the composited color, the programmer specifies weights, w_1, w_2 to the linear combination of A and B:

$$C = w_1 A + w_2 B \tag{C.1}$$

For particular choices of w_1 and w_2, the resulting color have familiar forms, as shown in Table C.2. The LightShop procedures in this table return a `LtColor` and take in two `LtColors` as argument. One example is shown below for the over compositing operator:

```
LtColor LiOver(LtColor A, LtColor B)
```

Also, for brevity the symmetric procedure for each operation has been omitted from the table (i.e. B over A, B in A, etc.).

Specific procedure names have been given to the common compositing operations. The LightShop procedure for general compositing is:

```
LtColor LiComposite(LtFloat w1, LtColor A, LtFloat w2, LtColor B)
```

Warping

LightShop's warping functions take a ray as input and return a new (i.e. warped) ray. Ray warping is commonly used to simulate deformation of a light field [COSL05], or refractive effects [HLCS99, YYM05].

LightShop provides two types of warps to the programmer: procedural warps and 4D table lookup. Procedural warps are commonly-used utility functions for warping rays. These are various functions that transform points. New rays can be formed by taking two points on the original ray, applying a transformation on them, and forming a vector from the two new points. Some of these functions are shown below:

```
LtPoint LiRotateX(LtPoint v, LtFloat theta)
LtPoint LiRotateY(LtPoint v, LtFloat theta)
LtPoint LiRotateZ(LtPoint v, LtFloat theta)
LtPoint LiRotateXAboutPt(LtPoint v, LtPoint org,
                         LtFloat theta)
LtPoint LiRotateYAboutPt(LtPoint v, LtPoint org,
                         LtFloat theta)
LtPoint LiRotateZAboutPt(LtPoint v, LtPoint org,
                         LtFloat theta)
```

Figure C.5 illustrates a twisting effect that can be accomplished using LightShop's warping functions. Figure C.6 shows several other views of this "twisted light field".

To accomplish the twisting effect for the left individual, two points on each view ray are selected and rotated about a vertical axis centered over the left person. The amount of rotation is a function of the height of each of the points. The higher a point is, the more rotation is applied. `LiRotateYAboutPt` is used to perform the rotation. The warped ray is formed from the rotated points. A similar warp is defined for twisting the right individual. To keep the left and right ray-warps from creating discontinuities in the image, the final ray warp is a linear combination of the left and right twists. The weight for each twist is inversely related to the ray's proximity to the left or right twist axes.

The warping functions that use a 4D lookup table represent the ray warp with discrete samples. The lookup table is treated in the same way as a light field, except that the value per ray is not an RGBA color, but a new ray. One can think of the light field as a *ray*-valued one as opposed to a *color*-valued one. The LightShop procedure that samples from the ray-valued light field is shown below. Notice that it returns a ray instead of a color.

```
LtRay LiWarpRayLookup(LtInt lightFieldID, LtRay ray)
```

The lookup table is treated in the same way as a light field, except that the value per ray is not an RGBA color, but information describing a warped ray. LightShop represents this ray information as two 3D points on the ray. Since each point takes 3 coordinates, xyz, the warped ray needs 6 coordinates. These 6 coordinates are stored separately in the 3 RGB channels of 2 light fields. The alpha channel of both light fields is used to indicate if a warp exists (1) or not (0) for that particular input ray. Using 6 coordinates to represent a ray wastes space, since a ray can be represented by 4 coordinates. However, the extra channel is used as a flag for when a ray warp is defined. Additionally, no extra information about the coordinate system of the parameterization needs to be known (i.e. the plane locations for a 2-plane parameterization). By convention, it is assumed that the two light fields have sequential identifiers, so that a ray warp lookup is performed by specifying the ray and the light field containing the first point on the warped ray.

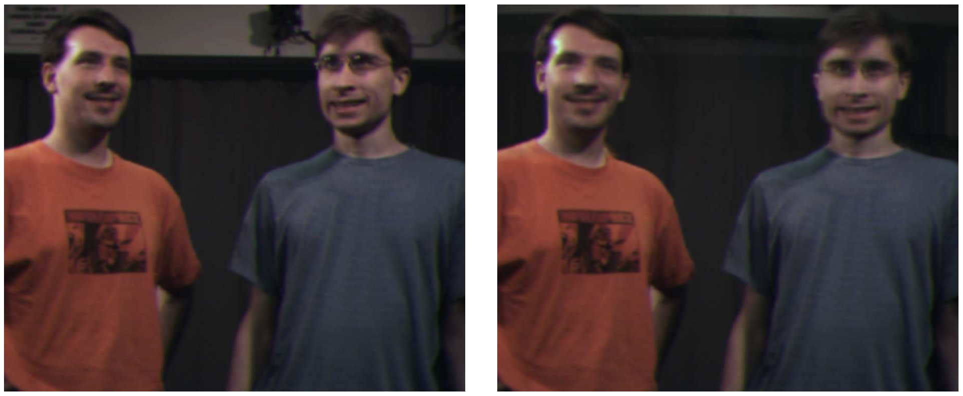

Figure C.5: On the left is an image from a light field of two people. Notice that their heads are not facing the same direction. On the right we apply a ray-warp to turn their heads.

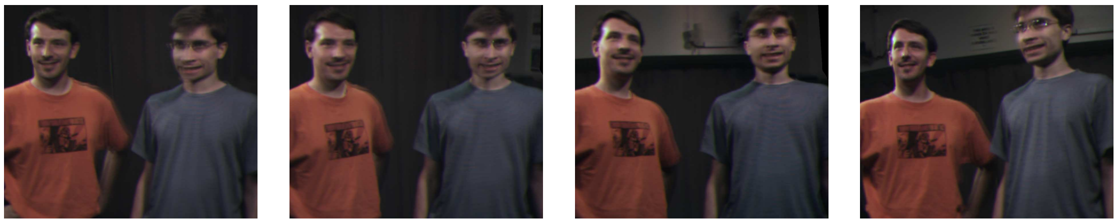

Figure C.6: Multiple views of the twisted light field. Notice that the actors appear to be looking in the same direction in all the images.

C.4 A Simple Example

Given our API, we conclude this appendix with a toy example that illustrates the expressive power of the LightShop system. LightShop is used to render an image from a scene of light fields, as shown in Figure C.7. Other views of this composited light field are shown in Figure C.8.

First, we describe the input to LightShop. The scene consists of 4 light fields. Two of them represent the Buddha and the flower. The third light field represents the ray warp that simulates the refraction effect of the glass ball. The fourth light field represents the specular highlight of the ball. The size of each light field is enumerated in Table A.1. All light fields in this example use the two-plane parameterization.

The light field that represents the 4D lookup table for warping a view ray is computed synthetically by ray-tracing through a sphere with glass material properties.

More specifically, in a ray-tracing program called yafray [yaf05], we create a scene consisting of a single sphere. We set the material properties of this sphere to mimic refractive glass with index of refraction 1.5. Then, for 32x32 camera positions, we ray-trace 256x256 rays into the scene containing the glass sphere. For each ray, the ray-tracer outputs a description of the refracted ray. We store this description in the RGBA components of the light field. This light field yields a mapping from any ray (from the 32x32x256x256 rays) to a ray refracted through the glass ball.

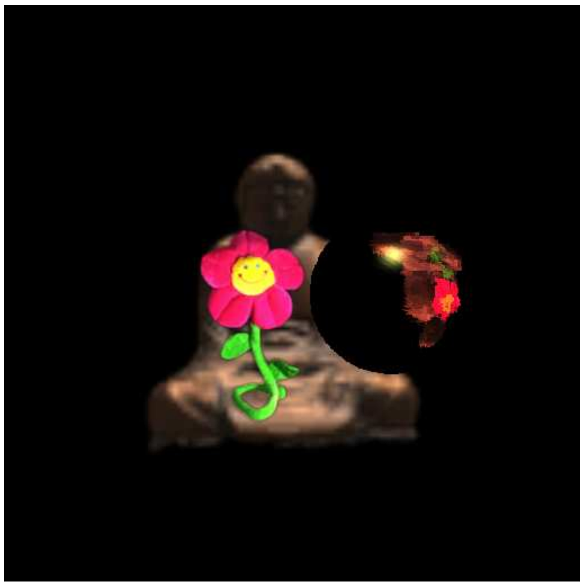

Figure C.7: A rendered image from a composite light field scene.

The procedure calls that model the scene are shown in Figure C.9. Referring to Figure C.9, the programmer first inserts a camera into the scene. It is a pinhole camera pointed at a specific location (namely, where we will position the light fields).

The next set of procedure calls insert light fields into the scene. The integer identifiers of each light field begin at 0 and increase sequentially (i.e. the Buddha light field is mapped to identifier 0). Light fields 0 and 1 are typical light fields that have RGBA as values per ray. Light field 2 is a 4D lookup table that warps rays as if the ray had gone through a glass ball. Light field 3 is an RGBA light field containing the specular highlight of the glass ball. Next, the programmer specifies various light field attributes that define their position.

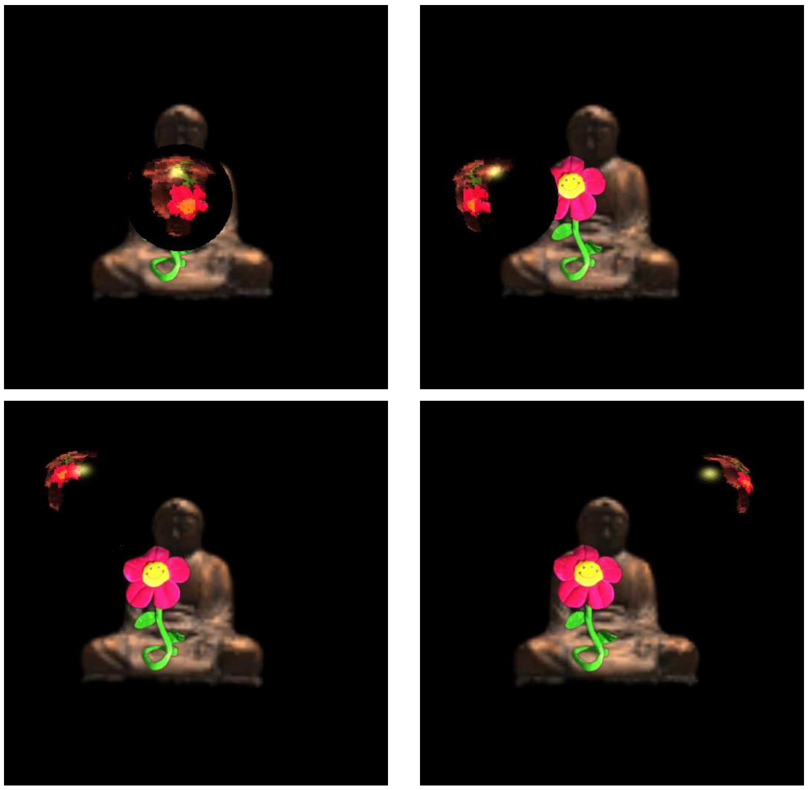
Figure C.8: Novel views of the scene of composited light fields.

Once the scene has been modeled, the programmer writes a ray-shading program that defines precisely how a 2D image is rendered from this scene. This is done by writing a program that executes per output pixel of the image to determine the color of each pixel, given the scene of light fields.

Figure C.10 shows the ray-shading program. We now proceed to describe each step of the program and show its effects on the current output image.

First, we convert the current pixel location into a ray and use this ray to sample from the Buddha light field. We set the background color to be black. Lines 5–13 produce Figure C.11.

Next, in line 17 we use the same ray to sample from the flower light field and composite that color over the Buddha sample, which produces Figure C.12.

Now, to create the spherical refraction effect, we warp the view ray as if the ray had gone through the glass ball. Recall that light field 2 maps an input ray to a warped ray. We use the `LiWarpRayLookup` procedure to acquire the warped ray. This warped ray is then used to sample from the Buddha and the flower light field to produce a refractive version. Figure C.13 shows the current image after lines 20–26.

Finally, in lines 44-46 we add a specular highlight to the scene by sampling from the light field containing the ball's specular highlight and adding this color to the final color. This produces the final image, as shown in Figure C.7, other views are shown in Figure C.8.

Primitive	**Attribute**	**Default**	**Description**
lens camera	lower left	[-1, -1, -1]	lower left of the image plane
	up	[0, 2, 0]	vector from the lower left to the upper left of the image plane
	right	[2, 0, 0]	vector from the lower left to the lower right of the image plane
	lens center	[1, 1, 1]	vector from the lower left to the center of the lens aperture
	lens width	2	width of the lens aperture
	lens height	2	height of the lens aperture
	focal distance	1	the perpendicular distance between the lens plane and the focal plane
	x res	512	horizontal resolution of the output image
	y res	512	vertical resolution of the output image
light field	sampling	quadralinear	sampling method: nearest-neighbor or quadralinear
	wrapping	[0, 0, 0, 0]	wrapping behavior when sampling outside the light field: “clamp”, “repeat”, or a RGBA user-defined color
	transform	4x4 identity	a transformation applied to the rays of the light field

Table C.1: Primitives and attributes that LightShop supports. Other image options, like bias, gain, pixel sampling rates, filter sizes, color quantization, etc., could also be supported by LightShop.

Operation	w_1	w_2	**Expression**	**Function**
A add B	1	1	$A + B$	$+$
A over B	1	$1 - \alpha_A$	$A + (1 - \alpha_A)B$	`LiOver`
A in B	α_B	0	$\alpha_B A$	`LiIn`
A out B	$1 - \alpha_B$	0	$(1 - \alpha_B)A$	`LiOut`
A atop B	α_B	$1 - \alpha_A$	$\alpha_B A + (1 - \alpha_A)B$	`LiAtop`
A xor B	$1 - \alpha_B$	$1 - \alpha_A$	$(1 - \alpha_B)A + (1 - \alpha_A)B$	`LiXor`

Table C.2: Common compositing operations that have special names in LightShop.

```
// Initialize LightShop
LiBegin();

// insert the camera
LtDir lowerLeft = {4.14, 4.00, 7.92};
LtDir up = {0.00, -8.00, 0.00};
LtDir right = {-7.99, 0.00, 0.15};
LtFloat lensWidth = 0;
LtInt camera0 = LiCamera();
LiAttributeCam(``lower left'', lowerLeft);
LiAttributeCam(``up'', up);
LiAttributeCam(``right'', right);
LiAttributeCam(``lens width'', lensWidth);
LiAttributeCam(``lens height'', lensHeight);

// insert the light fields
LtInt lightField0 = LiLightField(``buddha'');
LtInt lightField1 = LiLightField(``flower'');
LtInt lightField2 = LiLightField(``glass ball'');
LtInt lightField3 = LiLightField(``highlight'');

// set light field attributes
LtMatrix4 transform0 = {4,0,0,0,0,4,0,0,0,0,4,0,0,0,3.5,1};
LtMatrix4 transform1 = {.6,0,0,0,0,.6,0,0,0,0,.6,0,-1.25,0,4.0,1};
LtMatrix4 transform2 = {1,0,0,0,0,1,0,0,0,0,1,0,.5,0,0,1};

LiAttributeLF(lightField0, ``transform'', transform0);
LiAttributeLF(lightField1, ``transform'', transform1);
LiAttributeLF(lightField2, ``transform'', transform2);
LiAttributeLF(lightField3, ``transform'', transform2);

// tell LightShop to clean up
LiEnd();
```

Figure C.9: LightShop function calls that model the toy scene shown in Figure C.7.

```
LtColor main(LtVec2 currentPixel) {
  // the output color for this pixel
  LtColor col;

  // form a ray from the current pixel
  LtRay ray=LiGetRay(0,currentPixel,LtVec2(0,0));

  // set the background color to be black
  LtColor background = LtVec4(0,0,0,1);
  col = background;

  // sample from the Buddha light field
  // and composite over a black background
  col = LiOver(LiSampleLF(0, ray), col);

  // sample from the flower light field and
  // composite it over the buddha one
  col = LiOver(SampleLF(1, ray), col);

  // warp view ray to simulate the refraction effect
  LtRay warpedRay = LiWarpRayLookup(2, ray);

  if(warpedRay.dir != 0) {
     LtColor refractedBuddha = LiSampleLF(0, warpedRay);
     LtColor refractedFlower = LiSampleLF(1, warpedRay);
     LtColor refraction = LiOver(refractedFlower,
     LiOver(refractedBuddha, background));

     // tint the refracted ray color
     LtColor tint = LtVec4(1, .5, .5, 1);
     refraction = tint * refraction;

     // composite refracted color to output pixel color
     col = LiOver(refraction, col);
  }
  // obtain the specular highlight of
  // the glass ball and add it to the scene
  LtColor highlight = LiSampleLF(3, ray);
  col =  col + highlight;
  return col;
}
```

Figure C.10: A toy example ray-shading program. It renders the image shown in Figure C.7.

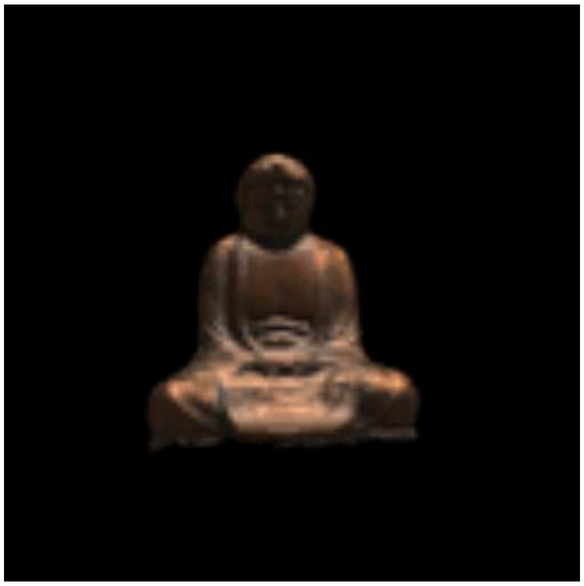

Figure C.11: The image after sampling from the Buddha light field.

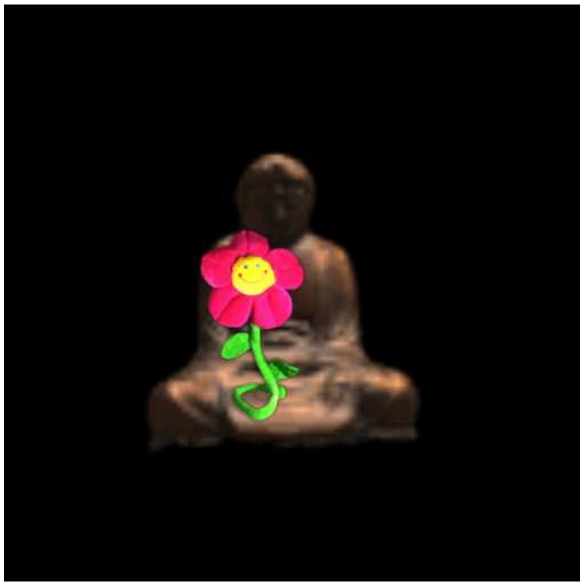

Figure C.12: The image after compositing the flower RGBA sample over the Buddha one.

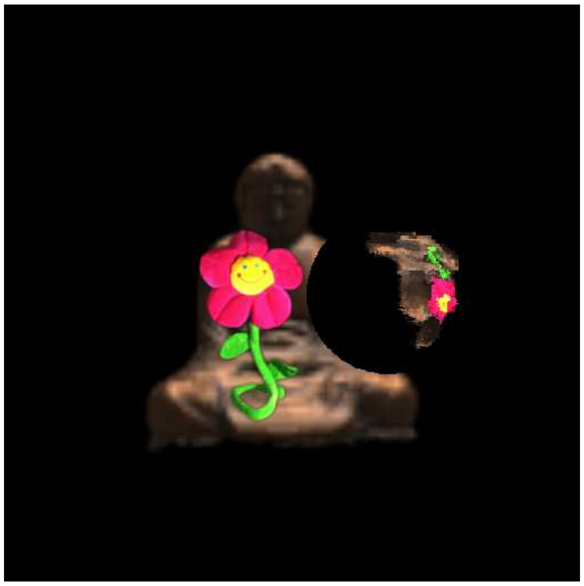

Figure C.13: The image after compositing the refracted Buddha and flower light fields. There are jaggy artifacts in the refraction due to the limited sampling rate of the ray warp. For simple geometric objects, this artifact can be remedied by providing a function characterizing the ray warp. For more complex objects, a higher sampling rate is necessary. LightShop can handle either solutions.

Appendix D

Focus-based Light Field Segmentation

In this appendix we describe how to segment a light into layers using focus. The dataset we use is the swimmers light field (see Section 4.6.1 and Appendix A). Segmenting this dataset for a given layer is equivalent to computing an alpha matte for each image of the light field. Thus the goal is to compute these alpha mattes.

To compute the alpha mattes for each layer, we process the layers in a front-to-back order. For the front swimmer, an implementation of intelligent scissors [MB95b] is used to segment it out in one of the images of the light field. Figure D.1a illustrates this contour and D.1b shows the binary mask. This binary mask needs to be propagated to all images, but in this case it turns out that the front swimmer lies on the ST plane, so the binary mask remains fixed to her silhouette in all images.

Next, a tri-map is created based on the binary mask to serve as an input to a Bayesian matte extraction algorithm [CCSS01]. The technique is similar to the one used by Zitnick et. al [ZKU$^+$04]. A tri-map consists of a foreground, background, and unknown region of the image. The foreground mask is computed by eroding the initial binary mask (shown in Figure D.1c). The background is computed by dilating the binary mask twice and taking the difference of the dilated masks (shown in Figure D.1d). The unknown region lies between the foreground and background masks. This tri-map is passed into the Bayesian matte extraction algorithm to produce the alpha matte in Figure D.1e. Figure D.1f shows the extracted front swimmer for this image. Since this swimmer lies on the ST plane, we can use the same alpha matte to extract her from all images.

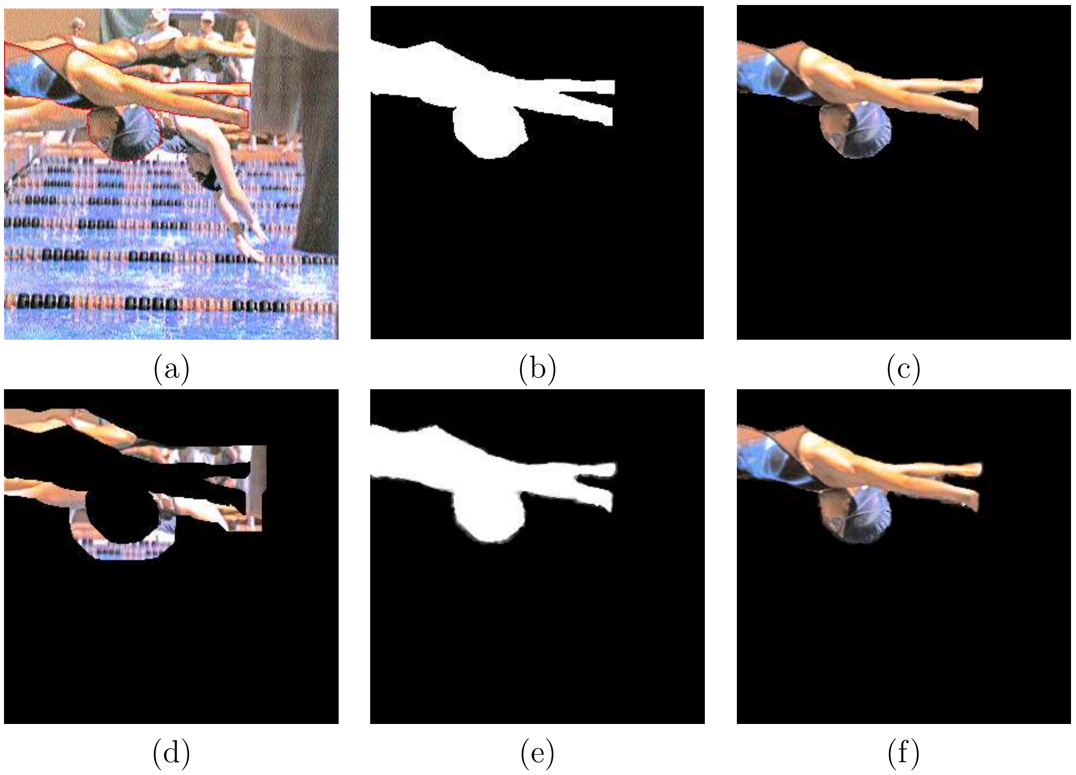

Figure D.1: Illustration of the alpha matte extraction pipeline. The user uses intelligent scissors to specify a binary mask in (a). The mask is shown in (b). The mask is then eroded by 3 pixels to form a foreground mask shown in (c). Dilating the mask by 2 and 30 pixels and taking their difference produces the background mask in (d). The output of the Bayesian matte extraction is shown in (e). A neighborhood size of 4 pixels was used. (f) shows the extracted front swimmer.

For the layers belonging to the middle and back swimmer, the binary mask in a single image will shift in the other images due to parallax. To handle this shift, we choose a plane approximating the depth of that layer. This plane is then used to project a binary mask in one image to all other images. In other words, the plane acts as a geometric proxy to propagate a binary mask in one image to all other images in the light field. How do we select the planar proxy depth? The solution is to use focus.

We use LightShop to create images where we focus on different depths in the swimmers light field. When a layer comes into focus, the corresponding depth is recorded. Given the depth of this plane, a binary mask in one image is projected to all other images by a homography induced by the plane [HZ00].

Now we quickly review how to compute a 3x3 homography matrix that is induced between two cameras and a plane. Using the notation presented in Hartley and Zisserman's book, two cameras are defined with projection parameters, $K[I|\mathbf{0}]$ and $K'[R|\mathbf{t}]$. The homography induced by a plane, $\mathbf{n}^{\mathrm{T}} + d = 0$, is given by:

$$H = K'(R - \mathbf{t}\mathbf{n}^{\mathbf{T}}/d)K^{-1} \tag{D.1}$$

Equation D.1 correctly computes the homography for general camera positions. However, for cameras in a two-plane parameterization, we can simplify the equation further. For camera images from a two-plane parameterization, each camera can be thought of as having an off-axis projection, with a common principle direction. This means that R maps to the identity matrix and the intrinsics and extrinsics only have a translation component that is a function of the relative camera locations in the UV-plane. Mathematically, Equation D.1 reduces to

$$H = K'(I - \mathbf{t}\mathbf{n}^{\mathbf{T}}/d)K^{-1} \tag{D.2}$$

where K', K have the form of

$$\begin{bmatrix} f & 0 & c_x \\ 0 & f & c_y \\ 0 & 0 & 1 \end{bmatrix} \tag{D.3}$$

and $\mathbf{t} = [-c_x - c_y - c_z]$. c_x, c_y, and c_z are the relative coordinates for the position of the second camera. In summary, Equations D.2 and D.3 provide a closed-form solution for computing homographies between cameras in a two-plane parameterized light field.

A similar technique is used for rendering ghost-free images from under-sampled light fields [SS04]. Instead of a plane, one could use image priors on the distribution of the foreground and alpha mask, like optical flow [CAC+02], image gradients [WFZ02], or continuity across images [AF04]. We found that using a plane was sufficient on the swimmers dataset.

The above technique works well when computing alpha values for an unoccluded layer. However, alpha mattes be occluded by foreground layers. For this reason, alpha mattes for each layer are computed in a front to back order. Then, the alpha values from the front layers are used to mask values in the current layer. This will account for occlusions, but what about disocclusions? Disocclusions in the alpha mask are handled by selecting the image in the light field that exposes the largest area of the swimmer in that layer. This image is used to compute the initial binary mask via intelligent scissors. This way, the mask in all other images can only undergo an occlusion[1].

In summary, this appendix has described a technique for using focus to segment a light field into layers. The input is a single light field and the output is a set of alpha masks, one set for each layer.

[1]For regions in a layer that undergo both occlusions and disocclusions, we manually segment those regions into only occlusion or disocclusion.

Appendix E

Other Light Field Manipulations

This appendix contains ways to manipulate light fields. They are not essential to LightShop, but were discovered in the process of using it to edit light fields. Perhaps these manipulations will inspire the reader towards other novel light field operations.

E.1 Refraction and Focusing

The first manipulation demonstrates combining refraction and focus. Appendix C.4 demonstrated refraction through a sphere. An interesting property of refracting a scene through a sphere is that the sphere acts as an optical lens, creating a real image of the scene in front of it. Then in Section 4.6.1 a method for focusing was presented. Focusing allows the user to focus at a depth, blurring out other parts of the scene. Combining refraction and focusing, we can effectively focus on the real image in the refraction by the sphere. Figure E.1a illustrates this concept. The camera is focused on this real image, so both the sphere and the background are out of focus. Changing the focal plane of the camera, one can focus on the background light field, and the sphere and the real image go out of focus. This is shown in Figure E.1b. The function calls for modeling the scene are similar to those shown in Figure C.9 for the toy example. The ray-shading program combines the double for-loop found in Figure 4.3 with the refraction and compositing code found in Figure C.10.

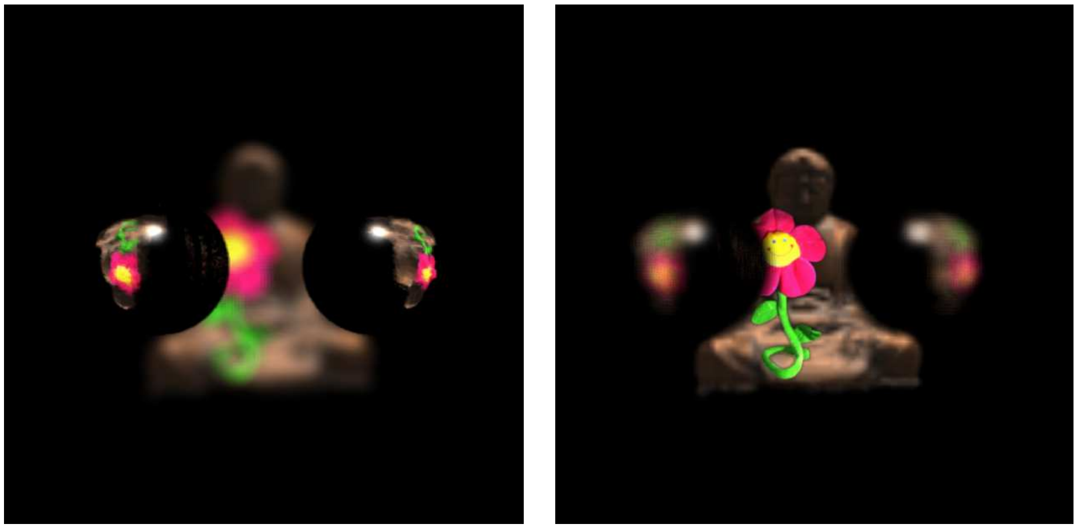
(a) (b)

Figure E.1: Combining focusing with refraction. In (a), the lens camera is focused on the real image created by the refracting sphere. Both the background and sphere are out of focus. In (b), the lens camera is focused on the background.

E.2 Shadows

The second manipulation enables light fields to cast shadows on one another. This is possible because LightShop's ray-shading language is general enough to act as a a ray-tracer for light fields. The idea is simple. Assume that an object represented by a light field is flat. In fact, the object lies on the ST-plane of a two-plane parameterized light field. Next, we assume each light field has alpha values per ray, representing coverage. Now, to determine if a part of a light field is in shadow, the ray is intersected with the ST-plane. From this depth, a "shadow ray" is shot to all light sources[1]. This shadow-ray samples from all other light fields to determine occlusion (based on alpha).

This process of computing shadows is easily encoded as a ray-shading program. In the following ray-shading code fragment, light field 0 casts a shadow onto light field 1. The user-defined function `Shadow` takes a light field and a 3D point. In this case, the 3D point is formed by intersecting the view ray with the ST plane of light field 1.

[1]While light primitives are currently not supported by LightShop, a user can still define light positions and pass them into ray-shading program via GLSL.

The `Shadow` function then forms a shadow ray from the 3D point to the point light source and uses this ray to sample from the argument light field (in this case, light field 0). It returns the RGBA color of sampling from light field 0, in the direction of the shadow ray. The resulting alpha is used to mask the color sampled from light field 1.

```
LiColor shadow = Shadow(0, IntersectST(1, ray));
LiColor col = LiOver(LiSampleLF(0, ray),
                     shadow.a * LiSampleLF(1,ray));
```

Figure E.2a and b illustrate shadows cast from the giraffe and flower light fields onto a ground plane (light field). The toy giraffe and flower are captured using the gantry, in front of a fixed-color background. Alpha mattes are extracted based on blue-screen matting [SB96]. The images are rendered at 10 FPS. Soft shadows are combined with focusing to produce Figure E.3. This image is rendered at 10 FPS.

This technique is obviously an over-simplification of shadows. The planar-depth assumption for a light field is a restrictive one. If actual depth is known per ray (from multi-baseline stereo, or range-finding, for example), this can be passed into LightShop as a *depth*-valued light field and utilized in the shadow computation. LightShop's framework is general enough to account for this extension.

Also, since the flower and giraffe light fields are captured under fixed illumination, their surface appearance will not match the user-specified illumination conditions. This limitation is the same for other image compositing/editing tools, like Adobe Photoshop. One solution is to capture the light fields of the object under different illumination conditions, and to use LightShop to add these light fields to better approximate the user-specified illumination. A similar technique was used in Section 4.6.1 when compositing several actors into a wedding light field. However, even with these simplifications, we demonstrate that shadows provide more realism to the scene.

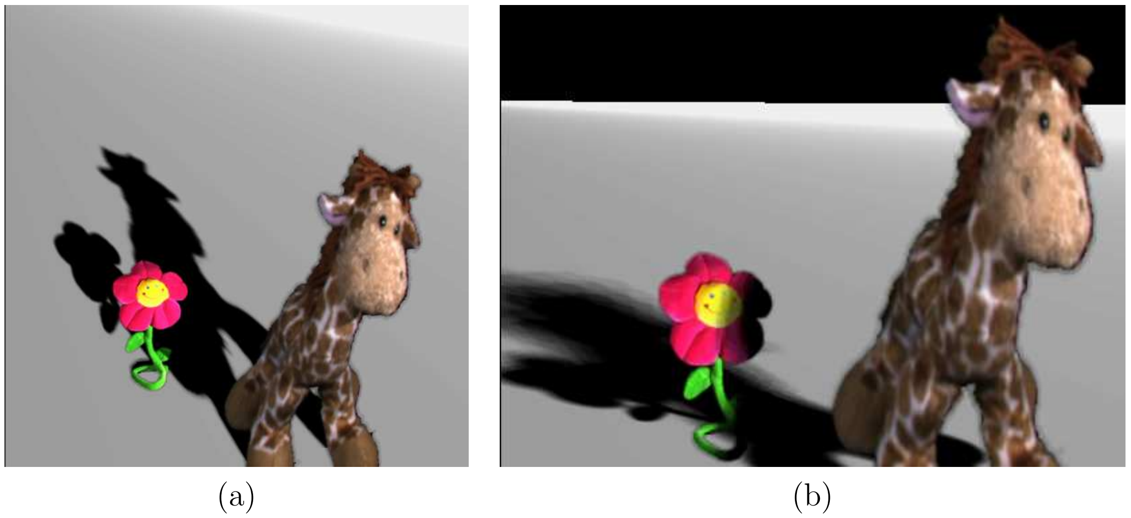

Figure E.2: Simulating shadows. In image (a), sharp shadows are being cast from the giraffe and flower light field. The shadow on the ground is computed by casting a shadow ray from a synthetic light field of a ground plane to a user-defined point light source. In image (b), we create multiple virtual light sources and sum their masks to approximate soft shadows. The shadow on the flower is computed by casting a shadow ray from the ST-plane of the flower light field to the point lights. Notice that the soft shadow interacts correctly with the flower light fields. More point light sources would lessen the aliasing in the soft shadows.

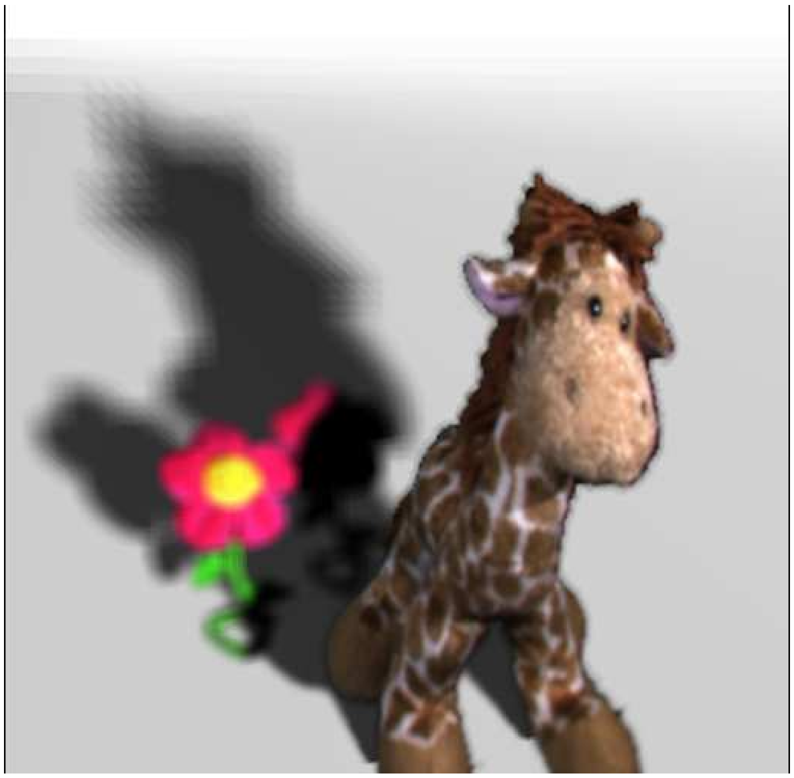

Figure E.3: Focusing combined with soft shadows. A lens camera with finite aperture is used to focus on the depth of the toy giraffe. Notice that the soft shadows and the toy flowers are out of focus.

Bibliography

[AB91] Edward H. Adelson and James R. Bergen. The plenoptic function and the elements of early vision. In *Computation Models of Visual Processing*, pages 3–20, 1991. 5, 6

[AF04] Nicholas Apostoloff and Andrew Fitzgibbon. Bayesian video matting using learnt image priors. In *Proceedings of Computer Vision and Pattern Recognition (CVPR)*, pages 407–414, 2004. 106

[AMH02] Tomas Akenine-Möller and Eric Haines. *Real-time Rendering*. A K Peters, 2002. 63

[Bar84] Alan Barr. Global and local deformations of solid primitives. In *Proceedings of SIGGRAPH*, pages 21–30, 1984. 35

[Bar04] Brian A. Barsky. Vision-realistic rendering: simulation of the scanned foveal image from wavefront data of human subjects. In *Proceedings of Symposium on Applied Perception in Graphics and Visualization (APGV)*, pages 73–81, New York, NY, USA, 2004. ACM Press. 69

[BBM$^+$01] Chris Buehler, Michael Bosse, Leonard McMillan, Steven J. Gortler, and Michael F. Cohen. Unstructured lumigraph rendering. In *Proceedings of SIGGRAPH*, pages 425–432, 2001. 10, 47

[BSW$^+$05] OpenGL Architecture Review Board, Dave Shreiner, Mason Woo, Jackie Neider, and Tom Davis. *OpenGL(R) Programming Guide : The Official Guide to Learning OpenGL(R), Version 2 (5th Edition)*. Addison-Wesley, 2005. 3, 47, 85

[CAC+02] Yung-Yu Chuang, Aseem Agarwala, Brian Curless, David H. Salesin, and Richard Szeliski. Video matting of complex scenes. In *Proceedings of Transactions on Graphics (SIGGRAPH)*, pages 243–248, 2002. 106

[CCSS01] Yung-Yu Chuang, Brian Curless, David H. Salesin, and Richard Szeliski. A bayesian approach to digital matting. In *Proceedings of Computer Vision and Pattern Recognition (CVPR)*, volume 2, pages 264–271. IEEE Computer Society, December 2001. 103

[CL05] Billy Chen and Hendrik P. A. Lensch. Light source interpolation for sparsely sampled reflectance fields. In *Proceedings of Workshop on Vision, Modeling and Visualization (VMV)*, pages 461–468, 2005. 1

[CLF98] Emilio Camahort, Apostolos Lerios, and Don Fussell. Uniformly sampled light fields. In *Proceedings of Eurographics Rendering Workshop*, pages 117–130, 1998. 9, 64

[COSL05] Billy Chen, Eyal Ofek, Heung-Yeung Shum, and Marc Levoy. Interactive deformation of light fields. In *Proceedings of Symposium on Interactive 3D Graphics and Games (I3D)*, pages 139–146, 2005. 1, 47, 91

[CTCS00] Jin-Xiang Chai, Xin Tong, Shing Chow Chan, and Heung-Yeung Shum. Plenoptic sampling. In *Proceedings of SIGGRAPH*, pages 307–318, 2000. 7

[CW93] Michael Cohen and John Wallace. *Radiosity and Realistic Image Synthesis*. Academic Press, 1993. 20

[DHT+00] Paul Debevec, Tim Hawkins, Chris Tchou, Haarm-Pieter Duiker, Westley Sarokin, and Mark Sagar. Acquiring the reflectance field of a human face. In *Proceedings of SIGGRAPH*, pages 145–156, 2000. 17, 47

[DTM96] Paul E. Debevec, Camillo J. Taylor, and Jitendra Malik. Modeling and rendering architecture from photographs: A hybrid geometry- and image-based approach. *Proceeedings of Computer Graphics*, 30(Annual Conference Series):11–20, 1996. 7

[EL99] Alexei A. Efros and Thomas K. Leung. Texture synthesis by non-parametric sampling. In *Proceedings of International Conference on Computer Vision (ICCV)*, pages 1033–1038, 1999. 41

[FvDFH97] James D. Foley, Andries van Dam, Steven K. Feiner, and John F. Hughes. *Computer Graphics: Principles and Practice*. Addison-Wesley, 1997. 6

[GGH03] Michael Goesele, Xavier Granier, Wolfgang Heidrich, and Hans-Peter Seidel 1. Accurate light source acquisition and rendering. In *Proceedings of Transactions on Graphics (SIGGRAPH)*, pages 621–630, 2003. 1

[GGSC96] Steven J. Gortler, Radek Grzeszczuk, Richard Szeliski, and Michael F. Cohen. The lumigraph. In *Proceedings of SIGGRAPH*, pages 43–54, 1996. 5, 10, 47

[GLL$^+$04] Michael Goesele, Hendrik P. A. Lensch, Jochen Lang, Christian Fuchs, and Hans-Peter Seidel. Disco – acquisition of translucent objects. In *Proceedings of Transactions on Graphics (SIGGRAPH)*, pages 835–844, 2004. 17

[GZN$^+$06] Todor Georgiev, Colin Zheng, Shree K. Nayar, David Salesin, Brian Curless, and Chintan Intwala. Spatio-angular resolution trade-offs in integral photography. In *Proceedings of Eurographics Symposium on Rendering*, pages 263–272, 2006. 11

[HLCS99] Wolfgang Heidrich, Hendrik Lensch, Michael F. Cohen, and Hans-Peter Seidel. Light field techniques for reflections and refractions. In *Proceedings of Eurographics Rendering Workshop*, pages 187–196, 1999. 91

[Hor06] Daniel Horn. Vega strike. *http://vegastrike.sourceforge.net*, 2006. 63

[HZ00] Richard Hartley and Andrew Zisserman. *Multiple View Geometry in computer vision*. Press Syndicate of the University of Cambridge, 2000. 28, 105

[HZ03] Richard Hartley and Andrew Zisserman. *Multiple View Geometry in Computer Vision (Second Edition)*. Press Syndicate of the University of Cambridge, 2003. 33

[IMG00] Aaron Isaksen, Leonard McMillan, and Steven J. Gortler. Dynamically reparameterized light fields. In *Proceedings of SIGGRAPH*, pages 297–306, 2000. 47, 49

[INH99] Konstantine Iourcha, Krishna Nayak, and Zhou Hong. System and method for fixed-rate block-based image compression with inferred pixel values. *US Patent 5,956,431*, 1999. 53

[Kaj86] James T. Kajiya. The rendering equation. In *Proceedings of SIGGRAPH*, pages 143–150. ACM Press / ACM SIGGRAPH, 1986. 6

[KS96] Sing Bing Kang and Rick Szeliski. 3-d scene data recovery using omnidirectional multibaseline stereo. In *Proceedings of Computer Vision and Pattern Recognition (CVPR)*, pages 167–183, 1996. 15

[LCV$^+$04] Marc Levoy, Billy Chen, Vaibhav Vaish, Mark Horowitz, Ian McDowall, and Mark Bolas. Synthetic aperture confocal imaging. In *Proceedings of Transactions on Graphics (SIGGRAPH)*, pages 825–834, 2004. 49

[Lev04a] Marc Levoy. The stanford large statue scanner. *http://graphics.stanford.edu/projects/mich/mgantry-in-lab/mgantry-in-lab.html*, 2004. 10

[Lev04b] Marc Levoy. Stanford spherical gantry. *http://graphics.stanford.edu/projects/gantry*, 2004. 10, 74

[LH96] Marc Levoy and Pat Hanrahan. Light field rendering. In *Proceedings of SIGGRAPH*, pages 31–42, 1996. 1, 2, 5, 7, 9, 10, 17, 47, 49, 53, 82, 89

[LPC$^+$00] Marc Levoy, Kari Pulli, Brian Curless, Szymon Rusinkiewicz, David Koller, Lucas Pereira, Matt Ginzton, Sean Anderson, James Davis, Jeremy Ginsberg, Jonathan Shade, and Duane Fulk. The digital michelangelo project: 3D scanning of large statues. In Kurt Akeley, editor, *Proceedings of SIGGRAPH*, pages 131–144. ACM Press / ACM SIGGRAPH / Addison Wesley Longman, 2000. 10

[Mag05] Marcus A. Magnor. *Video-based Rendering*. A K Peters, 2005. 7

[MB95a] Leonard McMillan and Gary Bishop. Plenoptic modeling: An image-based rendering system. *Proceedings of Computer Graphics*, 29(Annual Conference Series):39–46, 1995. 6

[MB95b] Eric N. Mortensen and William A. Barrett. Intelligent scissors for image composition. In *Proceedings of Computer graphics and Interactive Techniques*, pages 191–198, 1995. 103

[MBGN98] Tom McReynolds, David Blythe, Brad Grantham, and Scott Nelson. Programming with opengl: Advanced techniques. In *Course 17 notes at SIGGRAPH 98*, 1998. 63

[MG00] Marcus Magnor and Bernd Girod. Data compression for light field rendering. In *Proceedings of Transactions on Circuits and Systems for Video Technology*, number 3, pages 338–343, 2000. 53

[MPDW03] Vincent Masselus, Pieter Peers, Philip Dutre, and Yves D. Willems. Relighting with 4d incident light fields. In *Proceedings of Transactions on Graphics (SIGGRAPH)*, pages 613–620, 2003. 1

[MPN$^+$02] Wojciech Matusik, Hanspeter Pfister, Addy Ngan, Paul Beardsley, Remo Ziegler, and Leonard McMillan. Image-based 3d photography using opacity hulls. In *Proceedings of Transactions on Graphics (SIGGRAPH)*, pages 427–437, 2002. 1

[MRG03] Marcus Magnor, Prashant Ramanathan, and Bernd Girod. Multi-view coding for image-based rendering using 3-d scene geometry. In *IEEE*

Transactions on Circuits and Systems for Video Technology, pages 1092–1106, 2003. 53

[MSF02] D. Meneveaux, G. Subrenat, and A. Fournier. Reshading lightfields. Technical report, IRCOM/SIC, March 2002. No 2002-01. 15

[NLB$^+$05] Ren Ng, Marc Levoy, Mathieu Brédif, Gene Duval, Mark Horowitz, and Pat Hanrahan. Light field photography with a hand-held plenoptic camera. Technical report, Stanford University, 2005. 11, 56

[Oko76] Takanori Okoshi. *Three-Dimensional Imaging Techniques*. Academic Press, 1976. 11

[PD84] Thomas Porter and Tom Duff. Compositing digital images. In *Proceedings of Computer Graphics*, number 3, pages 253–259, 1984. 90

[Pe01] Ingmar Peter and Wolfgang Straßer. The wavelet stream: Interactive multi resolution light field rendering. In *Proceedings of Eurographics Rendering Workshop*, pages 262–273, 2001. 53

[Per85] Ken Perlin. An image synthesizer. In *Proceedings of SIGGRAPH*, pages 287–296. ACM Press / ACM SIGGRAPH, 1985. 49, 86

[RNK97] Peter Rander, PJ Narayanan, and Takeo Kanade. Virtualized reality: Constructing time-varying virtual worlds from real world events. In *IEEE Visualization 1997*, pages 277–284, 1997. 11

[Ros04] Randi J. Rost. *OpenGL Shading Language*. Addison-Wesley, 2004. 53, 55, 86, 87

[SB96] Alvy Ray Smith and James F. Blinn. Blue screen matting. In *Proceedings of Computer Graphics and Interactive Techniques*, pages 259–268, 1996. 56, 109

[SCG$^+$05] Pradeep Sen, Billy Chen, Gaurav Garg, Stephen R. Marschner, Mark Horowitz, Marc Levoy, and Hendrik P. A. Lensch. Dual photography. In

Proceedings of Transactions on Graphics (SIGGRAPH), pages 745–755, 2005. 1

[SH99] Heung-Yeung Shum and Li-Wei He. Rendering with concentric mosaics. In *Proceedings of SIGGRAPH*, pages 299–306, 1999. 89

[SK98] Steve Seitz and Kiriakos N. Kutulakos. Plenoptic image editing. In *Proceedings of International Conference on Computer Vision (ICCV)*, pages 17–24, 1998. 15

[SP86] Thomas W. Sederberg and Scott R. Parry. Free-form deformation of solid geometry models. In *Proceedings of SIGGRAPH*, pages 151–160, 1986. 2, 23, 24

[SS04] Heung-Yeung Shum and Jian Sun. Pop-up light field: An interactive image-based modeling and rendering system. In *Proceedings of Transactions on Graphics*, pages 143–162, 2004. 47, 105

[Ups92] Steve Upstill. *The RenderMan Companion: A Programmer's Guide to Realistic Computer Graphics*. Addison-Wesley, 1992. 3, 47

[VWJL04] Vaibhav Vaish, Bennett Wilburn, Neel Joshi, and Marc Levoy. Using plane + parallax for calibrating dense camera arrays. In *Proceedings of Computer Vision and Pattern Recognition (CVPR)*, pages 2–9, 2004. 2, 8, 47, 49, 53

[WAA$^+$00] Daniel N. Wood, Daniel I. Azuma, Ken Aldinger, Brian Curless, Tom Duchamp, David H. Salesin, and Werner Stuetzle. Surface light fields for 3d photography. In *Proceedings of SIGGRAPH*, pages 287–296, 2000. 7

[WFZ02] Yoni Wexler, Andrew Fitzgibbon, and Andrew Zisserman. Bayesian estimation of layers from multiple images. In *Proc. ECCV*, pages 487–501, 2002. 106

[WJV$^+$05] Bennett Wilburn, Neel Joshi, Vaibhav Vaish, Eino-Ville Talvala, Emilio Antunez, Adam Barth, Andrew Adams, Mark Horowitz, and Marc Levoy.

High performance imaging using large camera arrays. In *Proceedings of Transactions on Graphics (SIGGRAPH)*, pages 765–776, 2005. 11, 49

[WL01] Li-Yi Wei and Marc Levoy. Texture synthesis over arbitrary manifold surfaces. In *Proceedings of SIGGRAPH*, pages 355–360, 2001. 41

[WPG04] Tim Weyrich, Hanspeter Pfister, and Markus Gross. Rendering deformable surface reflectance fields. In *Proceedings of Transactions on Computer Graphics and Visualization*, pages 48–58, 2004. 15

[WSLH02] Bennett Wilburn, Michael Smulski, Hsiao-Heng Kelin Lee, and Mark Horowitz. The light field video camera. In *Proceedings of Media Processors 2002, SPIE Electronic Imaging*, 2002. 11

[yaf05] yafray. yafray. *http://www.yafray.org/*, 2005. 94

[YEBM02] Jason C. Yang, Matthew Everett, Chris Buehler, and Leonard McMillan. A real-time distributed light field camera. In *Proceedings of Eurographics Rendering Workshop*, pages 77–86, 2002. 11

[YM04] Jingyi Yu and Leonard McMillan. General linear cameras. In *Proceedings of European Conference on Computer Vision (ECCV)*, pages 14–27, 2004. 60

[YYM05] Jingyi Yu, Jason Yang, and Leonard McMillan. Real-time reflection mapping with parallax. In *Proceedings of Symposium on Interactive 3D Graphics and Games (I3D)*, pages 133–138, 2005. 91

[ZC04] Cha Zhang and Tsuhan Chen. A self-reconfigurable camera array. In *Proceedings of Eurographics Symposium on Rendering*, pages 243–254, 2004. 11

[ZKU$^+$04] C. Lawrence Zitnick, Sing Bing Kang, Matthew Uyttendaele, Simon Winder, and Richard Szeliski. High-quality video view interpolation using a layered representation. In *Proceedings of Transactions on Graphics (SIGGRAPH)*, pages 600–608, 2004. 103

[ZWGS02] Zhunping Zhang, Lifeng Wang, Baining Guo, and Heung-Yeung Shum. Feature-based light field morphing. In *Proceedings of Transactions on Graphics (SIGGRAPH)*, pages 457–464, 2002. 2, 15, 41, 47